VOL.VII No 2 AUGUST 2010

JMR

JOURNAL OF MARITIME RESEARCH

Spanish Society of Maritime Research

VOL. VII N.2
AUGUST 2010

JMR JOURNAL OF MARITIME RESEARCH

JMR
JOURNAL OF MARITIME RESEARCH

UNIVERSITY OF CANTABRIA

Escuela Técnica Superior de Náutica
c/ Gamazo nº1, 39004 SANTANDER
Telfno (942) 201362; Fax (942) 201303
e-mail: info.jmr@unican.es
http://www.jmr.unican.es

Layout: JMR

Printed bay: Gráficas Fisa, S.L.

ISSN: 1697-4840

D. Legal: SA-368-2004

CONTENTS

Journal of Maritime Research, Vol. VII. No. 2, pp. 3–20, 2010

ISSN: 1697-4840

MONITORING OF SOME MAJOR VOLATILE ORGANIC COMPOUNDS ON BOARD OF CHEMICAL TANKERS

W. Jacobs[1,4], D. Dubois[1,5], D. Aerts[1,6], P. Declerck[1,7], M. Stranger[2,8], A. Buczynska[2,9], A. Godoi[3] and R. Van Grieken[2,10]

Received 06 January 2010; in revised form 11 January 2010; accepted 04 June 2010

Abstract

Nowadays, chemical tankers are transporting a wide variety of chemical products. These products have different characteristics, and some are toxic. In literature several studies suggest an increased incidence of various forms of cancer for crew members on tankers. Most of these studies are based on medical statistics, rather than on effective measurements on board. The aim of this study is to monitor the average concentrations of toxic vapours on board of chemical tankers. Therefore we went on board of two chemical tankers for a 14-day trip and performed measurements during the normal operation of the vessel, in order to find out whether cargo vapours are traceable in the atmosphere in and around the vessel. The concentrations measured clearly show that there is a relationship between the cargoes transported and the concentration of the cargo vapour in the atmosphere in and around the vessel. The results further show an elevated concentration of the analyzed substances in the engine room and an important influence of the relative wind direction. Tank vents situated in the gas-safe zone influenced the results as well.

Keywords: shipboard conditions, diffusive monitoring, occupational health, BTEX.

[1] Antwerp Maritime Academy, Noordkasteel-Oost 6, B-02030 Antwerp, Belgium. [2] Department of Chemistry, Micro and Trace Analysis Center, University of Antwerp, Universiteitsplein 1, B-2610 Antwerp, Belgium. [3] Professor, Federal University of Parana (ana.godoi@unicenp.edu.br), Rua Francisco H. dos Santos, Curitiba, Brazil. [4] Captain,(werner.jacobs@hzs.be). [5] Professor (dirk.dubois@hzs.be). [6] Lecturer, (diane.aerts@hzs.be) [7] Officer (patrick.declerck@hotmail.com). [8] Doctor (m.stranger@ha.be). [9] PhD student (anna.buczynska@ua.ac.be). [10] Professor (rene.vangrieken@ua.ac.be).

INTRODUCTION

Numerous gas and chemical tankers transport a wide variety of chemicals to feed the economy. It is inevitable that during common operations toxic cargo vapours are released into the atmosphere. But no recent data on their concentration in the atmosphere in and around ships are available.

In the literature there are several studies suggesting a causal relation between sailing as a crew member on tankers and the incidence of various forms of cancer (e.g. *Nilsson et al., 1998; Saarni et al., 2002).* Most of these studies are based on medical statistics. Only a few researchers went effectively on board to perform sampling and to identify the possible cause. The study of *Moen et al. (1995a)* was based on measurements of benzene performed on board. One can only hope that the high concentrations measured at that time have generally decreased thanks to improved operation procedures. Examples are closed gauging, loading with high velocity valves or, even better, with the use of a vapour return. In the case of high velocity valves, however, the released vapours are still present in the atmosphere nearby the ship. Our interest is whether we could find any traces of these vapours back on board. Especially the study published in the *International Safety Guide for Oil Terminals and Tankers, ISGOTT (ICS, OCIMF and IAPH (2006))* concerning air dispersion, may create some doubts. This study shows the air circulation around the ship's superstructure. It might be possible that parts of the cargo vapours released ahead of the superstructure are transported behind it by natural air circulation. The inlets of the ventilation for the accommodation (AC) and the engine room (ER) are situated at the aft end of the superstructure. One can assume that parts of these toxic vapours are being sucked by the ventilation intake. Also the flue gasses from the ship's engines as well as the vents of the different bunker tanks can be considered as a possible source of toxic vapours. To test this assumption was the main drive for our investigation.

Another item that can be questioned is whether the segregation between the gas-dangerous (gdz) and the gas-safe zone (gsz) is as well defined as mentioned in the international bulk chemical code (IBC)(*IMO, (2007)*). This subdivision is illustrated in Figure 1.

The aim of this study is to give a general overview of the concentrations of the toxic vapours at different locations on board, in various situations. In a later cam-

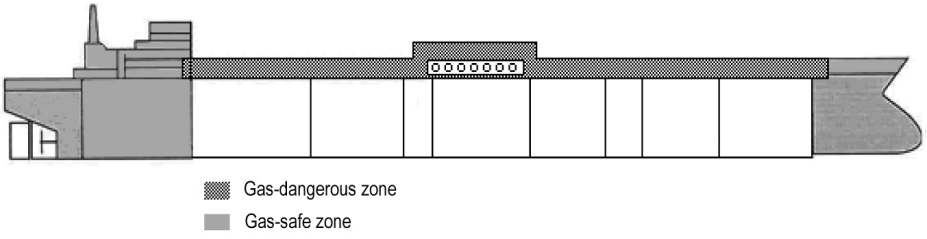

Figure 1: Gas-dangero s and gas-safe zones according to the IBC code

paign, we intend to study more in detail the concentrations in some specific spaces or zones that have been found interesting, based on the results of this campaign.

METHODS

Sampling and analytical methods

Diffusive sampling is particularly suited to determine time-weighted average volatile organic compound (VOC) concentration in occupational hygiene and environmental air monitoring *(Oury et al., 2006; Pennequin-Cardinal et al., 2005)*. Moreover it has as main advantages its simplicity and its cost effectiveness. Traditional diffusive sampling is characterized by low sampling rates and requires long sampling times. However, Radiello diffusive samplers are characterized by high and constant sampling rate values, high sensitivity and relatively short exposure times (Radiello Users Manual). The sampling rate is invariant towards humidity in the range 15-90% and wind speeds between 0.1 and 10 $m.s^{-1}$ (Radiello Users Manual). This method is also suitable for multipoint and simultaneous measurements. The used Radiello diffusive samplers consist of an adsorbing cartridge (530 mg of activated charcoal) inserted in a microporous polyethylene membrane. The diffusive sampler is exposed to air for a measured time period. The rate of sampling for a specific compound is determined by prior exposure in a standard atmosphere. VOCs migrate into the sampler by diffusion and are collected on the activated charcoal. In the laboratory, the collected material is desorbed by carbon disulfide. The solution is analyzed by gas chromatography coupled to mass spectrometry (GC-MS), according to a previously developed method *(Joos et al. 2003; Stranger, 2005)*.

A validation of this technique has been organized previously by our research group. Here all samples were collected in triplicate, with an extra annular denuder system nearby. The coefficients of variance, all having values below 10%, indicate the sufficient reproducibility for the collection of benzene, toluene, ethylbenzene and xylenes (BTEX) by means of Radiello passive samplers. The highest coefficients of variance, 12.2%, were calculated for the m+p-xylene determinations. However, all average BTEX concentrations agreed very well with the fixed monitor's results, as the ratios Radiello/denuder system were all close to one *(Stranger, 2005)*.

Also three blank cartridges were carried along with each vessel. They were kept sealed and stored near the cartridges that have been used. Later analysis showed that the readings of these blank samplers were all below the detection limits and so no correction had to be made on the obtained results.

To monitor all of the VOC compounds in air quantitatively is very time consuming and expensive. We have chosen 8 aromatic hydrocarbons based upon their presence in gasoline. As most cargoes are related to gasoline or are distillates from gasoline, and since gasoline is also used in the engine, we expected to find higher concentrations of these compounds on board. The compounds we analyzed the cartridges for

were benzene, toluene, ethylbenzene, m+p-xylene, o-xylene, 1,3,5-trimethylbenzene (1,3,5-TMB) and 1,2,4- trimethylbenzene (1,2,4 -TMB). Acute (short-term) exposure to gasoline and its components benzene, toluene and xylenes has been associated with skin and sensory irritation, central nervous system (CNS) problems (tiredness, dizziness, headache, loss of coordination), effects on the respiratory system and eye and nose irritation. On top of skin, sensory and CNS problems, prolonged exposure to these compounds can also affect the kidney, liver and blood systems *(Agency for Toxic Substances and Disease Registry, 2004, 2007; Calabrese and Kenyon, 1991)*. These effects are also a justification for the choice of the 8 analyzed compounds.

The ships

We had access to two chemical tankers, sister ships, with a length of 112 m, equipped with 17 cargo tanks and an overall capacity of just less than 10,000 m^3. Both ships were trading between Rotterdam and the Baltic Sea area. The sampling places, chosen after a visit to the ships, are shown in Figure 2. These are the shelter on the maindeck, the manifold, the facing, the ventilation intake of the engine room (ER), the ventilation intake of the accommodation (AC), two different levels in the ER and two in the AC. In order to get an image as complete as possible of the concentrations, we took 63 samples per ship.

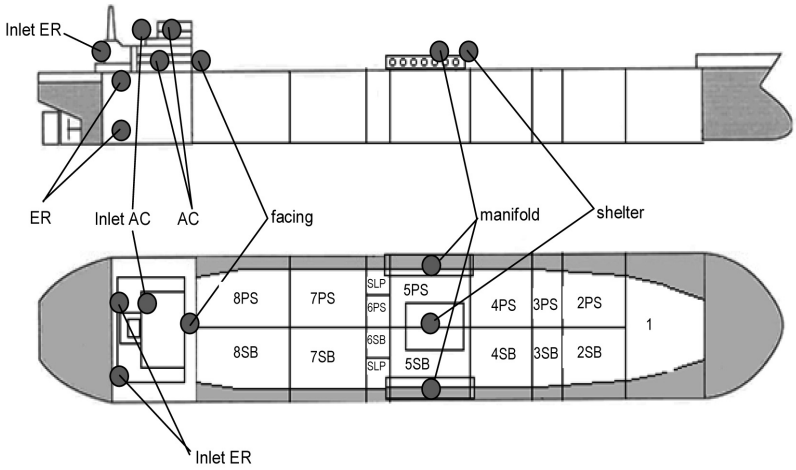

Figure 2: The location of the diffusive samplers on board.

PS = portside, looking from aft to forward the left side of the vessel.
SB = starboardside, looking from aft to forward the right side of the vessel

We made a logbook and a diary to keep records of the location of the tubes, the prevailing wind, weather conditions, voyage data, cargo operations, products on board, exposure time, etc. The temperature was automatically logged every 15 minutes.

Study protocol

We changed the Radiello® adsorbing cartridges every time the pilot came on board on arrival in port, and every time the pilot disembarked on departure from a port. This way of working resulted in separate measurements for the time in port and the time at sea. We expected the results for the time spent at sea to be different from the results for the time spent in port. Possible reasons for this difference might be the use of the main engine, influence from pollution sources ashore, influences from other vessels and the influence of cargo related operations. For vessel A we have data from 2 sea voyages and 3 ports, for vessel B data are available from 3 sea voyages and 3 ports.

For further classification of the results we divided a ship into four different areas. The first subdivision was in an indoor and outdoor area. Secondly indoor was split into AC and ER, outdoor in a gdz and a gsz. Indoor space was split into AC and ER, as the first one has to be considered as a living environment, the second one as a workplace. Outdoor was subdivided as specified in the IBC code, the international code for the construction and equipment of ships carrying dangerous chemicals in bulk (*IMO, 2007*). The gdz, being the area from forward to 3-5 m aft of the end of the superstructure facing the cargo area, and the gsz being the area from aft to 3-5 m aft of the end of

Table 1: Cargo handling during the measurement period.

Ship	Cargo	Tanks	Loading port to
Ship A	toluene	8PS	Antwerp to Rauma
	xylene	7PS	Rotterdam to Rauma
	ethanol	2PS, 4SB, 5PS, 5SB	Rotterdam to Rauma
	isopropyl alcohol IPA	6PS	Antwerp to Rauma
	butyl acrylate	3PS, 7SB	Rotterdam to Hamina
	monopropylene glycol	2SB	Rotterdam to Rauma
	varsol 40 (a)	3SB	Antwerp to Rauma
	exxsol D60 (b)	4PS	Antwerp to Rauma
	solvesso 150 (c)	6SB	Antwerp to Rauma
	solvesso 100 (c)	8SB	Antwerp to Rauma
Ship B	phenol	4PS, 4SB	Kotka to Rotterdam
	isoprene	1, 2PS	Kotka to Rotterdam
	paraffin C14-C17 (d)	3SB, 6SB, 7PS, 8PS, 8SB	Kotka to Rotterdam
	NPE-9 (e)	7SB	Kotka to Rotterdam
	NPE-10 (f)	5PS, 5SB	Kotka to Rotterdam
	NaOH	2PS, 2SB, 4PS, 4SB, 5PS	Wilhelmshaven to Kotka

(a): hydrocarbon aliphatic fluid, 16-20 wt % aromatic content, 41 $mg.kg^{-1}$ benzene content
(b): a complex mixture of aliphatic, cycloparaffinic hydrocarbons
(c): a highly refined lubricating mineral base oil, hydrocarbon fluid, with 34% weight 1,2,4-TMB
(d): heavy alkanes C14-C17
(e): nonylphenol + 9 EO polyethoxylate C9H19C6H4-O-(OCH2CH2)n-H (n=9)
(f): nonylphenol + 10 EO polyethoxylate C9H19C6H4-O-(OCH2CH2)n-H (n=10)

the superstructure facing the cargo area, are shown in Figure 1. In order to reduce the number of results, we often used average values for one zone or space.

Table 1 gives an overview of the different products carried by the two vessels during our campaign, with their respective stowage on board and loading and discharging port.

RESULTS

Port

In order to make clear which port has been called by which vessel, we will indicate (A) or (B) after each port and after each seavoyage. The results of the measurements in port are shown in Table 2.

Table 2: Concentrations in port in $\mu g.m^{-3}$.{exposure time in hours}.

IN PORT	Zone	Port of Wilhelmshaven (B) {15 h}	Port of Kotka (B) {108 h}	Port of Rotterdam (B) {11 h}	Port of Rotterdam (A) {24 h}	Port of Rauma (A) {33 h}	Port of Hamina (A) {52 h}
benzene	AC	5.01	2.06	62.1	–	–	–
	ER	3.10	16.5	75.4	–	–	–
	Gsz	6.88	1.92	76.4	–	–	–
	Gdz	2.45	1.50	58.9	–	–	–
toluene	AC	16.1	7.49	14.2	99.3	75.6	–
	ER	13.4	55.1	20.9	277	69.1	25.6
	Gsz	22.4	6.99	14.7	101	78.7	–
	Gdz	39.0	159	86.2	935	80.3	–
m+p-xylene	AC	15.8	7.37	10.5	85.7	70.0	18.6
	ER	15.2	76.0	22.7	324	1550	78.7
	Gsz	24.5	7.59	10.8	104	56.8	15.3
	Gdz	6.46	46.2	2.93	932	73.2	–
o-xylene	AC	6.28	1.87	4.41	55.4	23.8	–
	ER	5.86	23.6	9.56	275	314	13.6
	Gsz	9.63	1.73	4.58	57.8	18.5	–
	Gdz	2.58	1.13	1.53	418	25.4	–
ethylbenzene	AC	12.2	2.43	7.55	17.9	23.5	–
	ER	11.3	51.8	17.2	173	309	22.7
	Gsz	19.1	2.41	9.41	38.3	20.6	–
	Gdz	5.10	1.19	2.54	811	31.6	–
1,3,5-TMB	AC	3.98	0.857	2.55	–	–	–
	ER	3.69	16.0	6.12	68.5	45.6	20.0
	Gsz	6.22	0.736	2.41	12.8	–	–
	Gdz	1.13	0.247	0.376	270	6.86	–
1,2,4-TMB	AC	12.6	2.89	8.41	77.7	38.5	18.9
	ER	12.2	52.0	20.0	435	293	123
	Gsz	19.6	2.45	7.10	47.8	21.9	9.51
	Gdz	2.90	0.767	1.11	1794	53.0	–

(– = below the detection limit)

The benzene concentrations for ship A were all found to be below the detection limit.

Sea voyage

The results of the measurements at sea are displayed in Table 3. The benzene concentrations for ship A were all found below the detection limit except for two measurements in the AC at sea, location AC 0. Although some of the transported products might contain a small amount of benzene, its vapour is not detectable in our measurements.

Table 3: Concentrations at sea in $\mu g.m^{-3}$ {exposure time in hours}.

AT SEA	Zone	Seavoyage Rotterdam Wilhelmshaven (B) {19h}	Seavoyage Wilhelmshaven Kotka (B) {76h}	Seavoyage Kotka Rotterdam (B) {93h}	Seavoyage Rotterdam Rauma (A) {93h}	Seavoyage Rauma Hamina (A) {33h}
Benzene	AC	2.21	3.27	2.10	3.27	1.65
	ER	2.52	22.1	9.72	–	–
	Gsz	1.59	1.94	1.49	–	–
	Gdz	–	1.18	1.26	–	–
toluene	AC	7.75	7.85	4.71	16.9	291
	ER	10.3	41.7	33.0	11.3	608
	Gsz	6.81	6.80	6.31	13.5	471
	Gdz	74.4	338	343	58.4	385
m+p-xylene	AC	6.49	12.7	3.56	44.8	86.9
	ER	9.99	38.1	40.2	109	261
	Gsz	5.92	4.34	3.88	39.5	141
	Gdz	3.11	7.80	6.26	531	157
o-xylene	AC	2.62	7.70	2.31	4.36	1.30
	ER	3.77	11.9	13.3	23.9	49.8
	Gsz	2.18	1.64	1.39	12.2	34.5
	Gdz	1.28	2.34	1.43	178	32.9
ethylbenzene	AC	3.47	5.83	1.88	7.51	22.8
	ER	6.78	33.4	23.4	22.5	56.7
	Gsz	3.29	2.92	2.29	15.4	27.3
	Gdz	0.211	2.65	1.99	191	43.2
1,3,5-TMB	AC	1.05	2.84	0.970	3.55	15.3
	ER	2.15	6.56	9.18	11.5	37.9
	Gsz	0.944	1.02	0.926	3.55	16.7
	Gdz	–	0.301	0.369	30.8	20.0
1,2,4-TMB	AC	3.49	8.53	3.28	21.8	85.4
	ER	7.55	20.0	29.5	72.5	250
	Gsz	3.06	3.27	3.05	16.9	103

(– = below the detection limit)

The results for benzene on ship B reflect a concentration below or near to the detection limit. Two exceptions are the ER during the voyage from Wilhelmshaven to Kotka (B) and from Kotka to Rotterdam (B).

DISCUSSION

During normal cargo operations some cargo vapours are released into the atmosphere. These vapours should be traceable in the gdz. What we wanted to

investigate is whether traces of these cargo vapours can also be found in other areas on board of the vessel. The first zone that has been evaluated is the gsz.

A comparison between the gsz and the gdz

In order to compare both zones, the (gdz/gsz) ratio will be used. We will first discuss the results ship by ship, and draw up a conclusion later by comparing both results.

Ship A

Ship A transported cargoes whereof the vapours had a direct influence on our measurements, namely toluene, xylene, solvesso 100 (34 wt% 1,2,4-TMB). As a general result for this vessel, we found that the concentration in the gdz exceeded the concentration in the gsz. Exceptions to this rule are the port of Hamina and the toluene and o-xylene concentration between Rauma and Hamina. This is shown in Table 4.

Table 4: Concentration ratios for the gdz to the gsz for ship A

Ratio gdz/gsz	Benzene	Toluene	m+p-Xylene	o-Xylene	Ethyl - benzene	1,3,5-TMB	1,2,4-TMB
Port of R'dam (A)	*	9.2	9.0	7.2	21	21	37
Sea voyage R'dam-Rauma (A)	*	4.3	13	15	12	8.6	13
Port of Rauma (A)	*	1.0	1.3	1.4	1.5	*	2.4
Sea voyage Rauma-Hamina (A)	*	0.8	1.1	0.9	1.5	1.1	1.2
Port of Hamina (A)	*	*	0.0	*	*	*	0.0

* indicates that the concentration in the gsz equals 0

From table 4 we learn that in Rotterdam and during the voyage from Rotterdam to Rauma the gdz/gsz ratio was situated well above unity, while in Rauma and during the voyage from Rauma to Hamina the same ratio was close to one, or even smaller than one. For both ports, the relative wind direction was the same, abeam from starboard, and therefore this parameter cannot be responsible for the difference. The major reason is the fact that during loading operations a considerable amount of cargo vapours are released on deck (gdz > gsz), while during discharging operations this is considerably less or even nil (gdz ≅ gsz). When loading, the ship's tank is filled up, and consequently the pressure inside the tank will rise. At a preset pressure the relief valve will evacuate the tank vapours at a speed of 30 $m.s^{-1}$ into the atmosphere of the gdz. Thanks to the true wind coming in from the starboard side, most of the vapours were evacuated to the portside, and not into the gsz. This resulted in Rotterdam in an important difference in concentrations between the gdz and the gsz. When discharging, the ship's tank is emptied, and a negative pressure is created inside the tank. The vacuum valve will at a preset negative pressure open, and allow air into the tank to partially fill up the vacuum. During this operation no cargo

vapours will escape from the tank and therefore the influence of the cargo on our measurements in Rauma is rather small.

Comparing both sea voyages is more difficult. The voyage from Rotterdam to Rauma was a laden voyage. Due to ship movements small amounts of toluene, xylene and 1,2,4-TMB vapours were released in the gdz. We noticed that only fractions from these concentrations were measured in the other zones. This is illustrated in Figure 3.

The voyage from Rauma to Hamina was a voyage with extensive tank cleaning and tank ventilation. Considerable amounts of toluene, xylene and 1,2,4-TMB vapours have been ventilated into the gdz. We expected here also a greater value in the gdz compared to the gsz. But the results in Figure 4 clearly show that the concentration in both zones is almost equal or even a little bit higher in the gsz. As we definitely know that the main sources here are the tanks, we conclude that the ventilated cargo vapours entered the gsz, and even show a tendency to accumulate there. Accordingly the concentration in the 3 other zones is remarkably higher than during the previous voyage.

Another exception is the port of Hamina. As can be found in Table 2, all values from both zones are close to the detection limit, reducing the significance of the gdz/gsz ratio. The reason why the concentrations here are situated near the detection limit can be explained by the fact that all cargoes with a direct influence on the measurements have been discharged and cleaned earlier and the fact that there is only little industrial activity in Hamina.

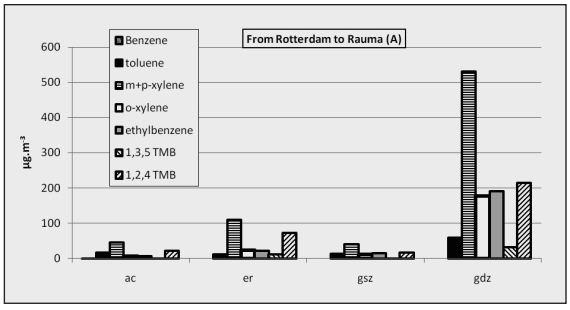

Figure 3: Concentrations in µg.m^{-3} for the different zones from Rotterdam to Rauma, ship A.

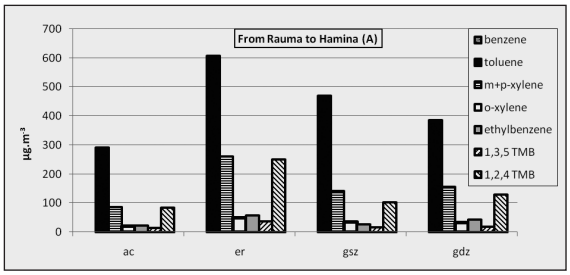

Figure 4: Concentrations in µg.mm^{-3} for the different zones from Rauma to Hamina, ship A.

Ship B

For ship B none of the transported cargoes did have a direct influence on the measurements. While on ship A in general gdz concentrations exceeded the gsz ones, we found on ship B the opposite. Exceptions were the toluene and the m+p-xylene concentrations in Kotka. These results are shown in Table 5. Also for the o-xylene concentrations for Wilhelmshaven to Kotka and for Kotka to Rotterdam, the gdz value exceed

those of the gsz. But since the absolute concentrations are very low, varying from 1.39 to 2.34 μg.m^{-3} (see Table 2), we found this less relevant.

Table 5: Concentration ratios for the gdz to the gsz for ship B

Ratio gdz/gsz	Benzene	Toluene	m+p-Xylene	o-Xylene	Ethyl - benzene	1,3,5-TMB	1,2,4-TMB
Seavoyage R'dam-W'haven(B)	0.0	10.9	0.5	0.6	0.1	0.0	0.1
Port of W'haven(B)	0.4	1.7	0.3	0.3	0.3	0.2	0.1
Seavoyage W'haven-Kotka(B)	0.6	49.7	1.8	1.4	0.9	0.3	0.3
Port of Kotka(B)	0.8	22.8	6.1	0.7	0.5	0.3	0.3
Seavoyage Kotka-R'dam(B)	0.8	54.3	1.6	1.0	0.9	0.4	0.4
Port of R'dam(B)	0.8	5.8	0.3	0.3	0.3	0.2	0.2

The ratio clearly shows a toluene pollution source situated in the gdz. Unlike ship A, no toluene cargo was on board of this ship. However we found an intermediate bulk container (IBC) on deck, containing approximately 1 m^3 of toluene. This toluene is sometimes used for tank cleaning purposes. An inspection of this IBC taught us that the container was not gastight closed as the cap was broken. In this way toluene vapours were released continuously, explaining the relatively high concentrations for toluene in the gdz. The IBC was situated within 10 meter distance from our sampler. This situation looks very similar to the laden voyage of ship A, where only the sampler near the facing showed an increased concentration for the products transported. The higher m+p-xylene ratio in Kotka was due to an increased gdz value. An explanation for this increment has not been found.

In contrast with ship A, the gdz/gsz ratio on ship B is in general below 1. And although the absolute concentrations for ship B are lower, it is a contradiction that the gdz shows lower concentrations than the gsz. This was definitely not the intention of the IBC code. The ratio indicates that the major source is closer to or situated in the gsz.

Evaluation of the ER

The results found on ship B in the gsz were expected to be lower compared to the gdz. However, the concentrations in the ER of ship B are the highest of all four zones on the exception of toluene in the gdz. May we consider the ER as the major voc source on board of ship B? In order to confirm this statement, we calculated the indoor/outdoor (I/O) ratio for the ER. This ratio is shown in Table 6.

In most cases the ratio is well above 1 in spite of the powerful mechanical ventilation present in the ER. The I/O ratio is in most cases above unit, indicating that the engine room itself is the major source and the ventilation here is insufficient or inefficient. The I/O ratio is only in two locations below unit, namely in Wilhelmshaven and for benzene in Rotterdam. The results in Wilhelmshaven are appar-

Table 6: Indoor/outdoor ratio in the ER for ship B.

I/O ER	Benzene	Toluene	Ethyl - benzene	m+p-Xylene	o-Xylene	1,3,5-TMB	1,2,4-TMB
R'dam/W'haven	1.6	1.6	2.2	2.0	2.0	2.7	3.1
W'haven	0.3	0.5	0.4	0.5	0.5	0.5	0.5
W'haven/Kotka	11.3	4.9	11	7.4	6.3	6.3	6.0
Kotka	11	9.0	50	16	19	467	42
Kotka/R'dam	4.8	3.1	6.1	6.3	5.9	5.8	5.7
R'dam	0.8	2.3	2.7	3.6	3.2	4.9	5.3

ently influenced by pollution from outside since the main engine is not running. The toluene/benzene ratio in Table 7 confirms that both compounds are coming from the same source, except of course for the facing where the sampler has been influenced by the small amounts of toluene escaping from the IBC. The presence of the coal driven power plant nearby might be the main cause for this outdoor pollution.

Table 7: Toluene - benzene ratio in Wilhelmshaven

AC 0	AC bridge	inlet AC	inlet ER	Facing
3.3	3.1	3.2	3.2	16

In Rotterdam we measured unexpectedly high benzene concentrations at all samplers, indicating that the whole ship was "covered" by a same level of benzene vapours. As there was no benzene cargo on board, and as never before such high concentrations of benzene have been measured on board, it seems obvious that this pollution came from shore.

Besides these two cases where the atmosphere around the vessel has been under influence of shore pollution, we find on ship B an I/O ratio for the ER (well) above 1. Regretfully we could not make the same comparison for ship A as the results for inlet ER ship A were disturbed by an excessive air flow from the ER ventilation.

Based on the results of ship B we conclude that in the ER important pollution sources are present. Further detailed research in the ER is necessary in order to identify these sources.

Positioning of the ventilation inlets

As we measured quite a difference in absolute concentrations between the ventilation inlet of the AC and the ventilation inlet of the ER, we tried to determine which of both inlets was located best. Both concentrations are only available for ship B, as the concentrations near the inlet ER on ship A were rejected due to a too high ventilation speed. The results for ship B are shown in Table 8.

Both ventilation intakes are somewhat 20 meters apart. But more important is the fact that the AC intake is situated about 8 meters higher than the ER intake. The latter is situated 4 m more aft and on the starboard side. This is the side where we placed our sampler and it is the intake which is most frequently used. The AC

Table 8: Ratio inlet AC/inlet ER for the different compounds and different measuring periods with the corresponding wind direction and wind force on board of ship B.

Position	Benzene	Toluene	Ethyl-benzene	m+p-Xylene	o-Xylene	1,3,5-TMB	1,2,4-TMB	Rel. wind direction	Rel. wind force
Kotka	1.5	1.3	3.7	2.2	1.7	3.2	3.0	110 SB	2
R'dam	0.7	2.3	1.9	2.5	2.1	2.9	2.8	160 PS	3
W'haven	0.5	0.5	0.5	0.6	0.6	0.6	0.6	60 SB	3
Kotka/ R'dam	0.5	0.2	0.2	0.2	0.2	0.2	0.2	25 PS	4
R'dam/W'haven	1.0	1.1	1.1	1.4	1.3	1.4	1.5	155 PS	4
W'haven/Kotka	1.0	0.6	0.9	0.7	0.7	0.9	1.0	20 SB	3

intake is situated on the portside. From Table 8 we learn that there is a direct relation between the ratio inlet AC/inlet ER and the relative wind direction. When this relative wind is forward of the beam or ahead, we noticed that the ratio is smaller than 1. If on the other hand, the relative wind is coming in from a direction abaft the beam or from astern, the ratio is found to be above 1. We have seen before that the influence of the cargo on our measurements on board of this vessel is rather small. The exhaust gases from the main engine and the auxiliaries together with possible shore pollution in port can be considered as the major sources. This is in agreement with the relative position of both inlets compared to the position of the funnel. In terms of percentage, a wind from forward of the beam has a higher frequency of occurrence than a wind from abaft the beam, due to the ship's speed. Therefore we may conclude that the position of the AC inlet is a better choice, although not ideal in all circumstances. One exception on the above described relation is the benzene concentration in Rotterdam. This is a confirmation of a previous conclusion, namely that in Rotterdam a shore benzene pollution influenced our measurements. The concentrations near the AC inlet were clearly lower than near the ER room inlet. In view of the difference in height, the relative vapour density of benzene (2.7) is a possible explanation. So the result in Wilhelmshaven where also shore pollution was considered could be explained by this same reason.

Evaluation of the AC

An interesting space to discuss more in detail is the AC. The result of the samplers placed inside the AC, one at level 0, and one at the bridge level, should give an answer to the question whether cargo vapours are traceable in the ER.

As shown in Table 9, there is a good correlation between the results of level 0 and the bridge level concentrations on ship A. This correlation is somewhat lower for m+p-xylene, although both locations have the same ventilation inlet. Moreover the absolute concentrations at level 0 were always found to be greater than the bridge level concentrations. Opening and closing of doors for deck access at level 1 is a possibility for an increased concentration.

Table 9: Pearson correlation between samplers at AC level 0 and bridge level on board of ship A.

Toluene	Ethylbenzene	M+p-Xylene	o- Xylene	1,3,5-TMB	1,2,4-TMB
0.995	0.950	0.821	0.973	0.991	0.984

Table 10: Indoor/outdoor ratio for AC on board of ship A.

I/O AC	Benzene	Toluene	Ethyl - benzene	m+p-Xylene	o-Xylene	1,3,5-TMB	1,2,4-TMB
R'dam		1.0	0.9	0.8	1.0	0.0	1.6
R'dam/Rauma		2.5	1.0	1.1	1.1	1.0	1.3
Rauma		1.0	1.1	1.2	1.3	*	1.7
Rauma/Hamina		0.6	0.8	0.6	0.6	0.9	0.8
Hamina		*	*	1.2	*	*	2.0

*outdoor concentration equals 0

The presence of cargo vapours in the AC is visible in the indoor/outdoor ratios of Table 10. As expected, the indoor/outdoor ratio in Rotterdam is below unit, due to the local pollution outside. However an exception is 1,2,4-TMB. But when we keep in mind that Solvesso 100 has been loaded in Antwerp only 14 hours ago, it is possible that remnants of this operation are still present inside the AC, resulting in a relatively high ratio. Once at sea, we would expect lower concentrations outside and thus a ratio above unit. This is particularly the case for the cargo related vapours, toluene, xylene and 1,2,4-TMB. This is another indication that cargo vapours entered the AC during the stay in Rotterdam. In Rauma the concentrations at the AC inlet hardly differ from the inlet concentrations at sea, except for toluene. This means that the air quality in Rauma is almost as good as at sea, resulting in an indoor/outdoor ratio equal to or above unity. When we started cleaning and venting the tanks on the way to Hamina, the ratios decreased below one. As can be concluded from Table 10, particularly the vapours related to the transported cargoes show a lower ratio, proving that cargo vapours arrived at the ventilation inlet of the AC . Finally we arrived in Hamina with all toluene, xylene and Solvesso 100 tanks cleaned and made gas free. And as the industrial activity in Hamina is rather low, the ratios became again above unity, at least for these results where the measured concentrations were above the detection limit.

The results of the bridge sampler and the level 0 sampler on ship B are strongly correlated as shown in Table 11. Both have the same ventilation intake, and we do not expect different sources for both spaces. The indoor/outdoor ratio shown in Table 12 teaches us that in general on ship B this ratio is below unity in port, above unity at sea. This is an understandable result, as we may consider the air at sea to be less polluted compared to the air in port. This statement is somewhat less evident for the benzene concentration indicating the presence of a benzene source or accumulation inside. The relatively high percentage of smoking crewmembers might be responsible for that result.

Table 11: Pearson correlation between the samplers at AC level 0 and at the bridge level on ship B.

correlation AC-bridge	Benzene	Toluene	Ethyl - benzene	m+p-Xylene	o-Xylene	1,3,5-TMB	1,2,4-TMB
	1.000	0.978	0.991	0.974	0.993	0.981	0.957

Table 12: Indoor/outdoor ratio for AC on board of ship B.

I/O AC	Benzene	Toluene	Ethyl - benzene	m+p-Xylene	o-Xylene	1,3,5-TMB	1,2,4-TMB
R'dam/W'haven	1.3	1.1	1.0	0.9	0.9	0.9	0.9
W'haven	1.1	1.1	0.9	0.8	0.8	0.8	0.8
W'haven/Kotka	1.7	1.5	2.0	3.6	3.1	2.9	2.7
Kotka	0.9	0.9	0.6	0.7	0.8	0.8	0.8
Kotka/R'dam	1.7	2.4	2.5	2.5	2.4	3.5	3.4
R'dam	1.0	0.7	0.6	0.7	0.7	0.7	0.8

From the AC indoor/outdoor ratio on ship A and ship B we learned that in some particular cases, cargo vapours do enter the AC, that generally spoken in port the concentration indoor is below outdoor concentration, and that at sea it is just the other way around. Particularly cleaning and venting of cargo tanks leads to increased outdoor concentrations, and as a consequence also to increased indoor concentrations. The ideal would be if we could fully isolate the AC from all toxic vapours outside. This is of course hypothetical as the crew needs access to the deck part. Naval architects have thought about a solution to have access to deck without vapours from outside entering the AC. This is called the 'crew changing room'. It is a small compartment situated at level 1 on the starboard side, with a door on one side giving access to the AC, on the other side a door giving access to the main deck. This compartment acts as an air lock. According to the ventilation plan, this room has a ventilation capacity of $400 m^3.h^{-1}$ resulting in 27 air changes per hour. Another use of this compartment is that the crew changes their workclothes used outside, with clothes for indoor use and leaves the used clothes also in this compartment in order to bring them later to the laundry. As it is realistic that in this space higher concentrations could occur, we placed on ship B an extra sampler and the results are shown in Figure 5. Some peak values can be found in this figure. Especially the sea voyages Wilhelmshaven to Kotka and Kotka to Rotter-

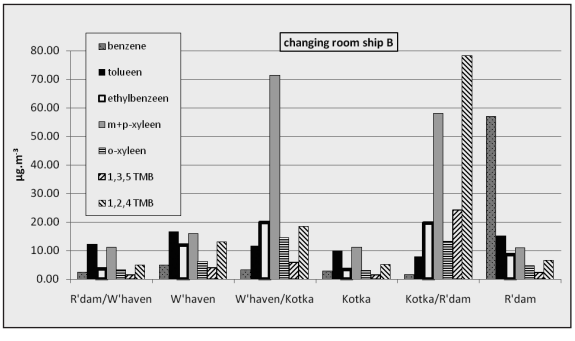

Figure 5: Concentrations in the changing room of ship B.

dam draw our attention. The ethylbenzene, xylenes and 1,2,4-TMB concentrations were significantly higher. In an attempt to find out whether all compounds are originating from the same source, Table 13 shows ratios between the analyzed compounds and respectively toluene and benzene. Toluene and benzene concentrations are related to another source, at least for the two above mentioned voyages.

Although the ventilation in the changing room is completely separated from the ventilation in the AC, we will compare both concentrations. The sampler placed in the AC on level 0 is located somewhat 8 meters away from the changing room. Any differences in concentrations between the two samplers are most probably in relation with the quality of the supplied air. The correlation between both concentrations over the whole measuring campaign is shown in Table 14. This correlation confirms the conclusion from Table 13. For benzene and toluene there is a good to even perfect correlation.

For the other compounds there is no correlation at all, confirming that these results were influenced by a different source. When we compare the absolute concentrations of the AC level 0 and the absolute concentration in the changing room for those compounds that do not show any correlation, the changing room concentrations are during 2 seavoyages definitely higher, namely from Wilhelmshaven to Kotka and from Kotka to Rotterdam. During these two voyages the ratio changing room over AC level 0 varies between 1.8 and 18. There is a source of ethylbenzene, xylenes and trimethylbenzene present in the changing room. As none of these products were related to the cargo, the source must be different. A first possibility is cigarette smoke from the duty mess nearby. But a further study of the ventilation plan showed a very surpris-

Table 13: Ratios for the measured compounds to toluene and benzene in the changing room on ship B.

Compound ratios in changing room	Benzene/ toluene	Ethyl-benzene/ toluene	m+p-Xylene/ toluene	o-Xylene/ toluene	1,3,5-TMB/ toluene	1,2,4-TMB/ toluene	Ethyl-benzene/ benzene	m+p-Xylene/ benzene	o-Xylene/ benzene	1,3,5-TMB/ benzene	1,2,4-TMB/ benzene
R'dam/W'haven	0.2	0.3	0.9	0.3	0.1	0.4	1.5	4.6	1.3	0.6	2.0
W'haven	0.3	0.7	1.0	0.4	0.2	0.8	2.4	3.3	1.3	0.8	2.6
W'haven/Kotka	0.3	1.7	6.2	1.2	0.5	1.6	6.0	21.9	4.4	1.8	5.6
Kotka	0.3	0.3	1.1	0.3	0.2	0.5	1.2	4.0	1.1	0.6	1.9
Kotka/R'dam	0.2	2.5	7.4	1.7	3.1	9.9	12	37	8.4	15	49
R'dam	3.7	0.6	0.7	0.3	0.1	0.4	0.2	0.2	0.1	0.0	0.1

Table 14: Pearson correlation between the concentrations measured in the AC and in the changing room on ship B.

Correlation between the AC and changing room	Benzene	Toluene	Ethyl - benzene	m+p-Xylene	o-Xylene	1,3,5-TMB	1,2,4-TMB
	1.000	0.979	0.102	-0.090	-0.007	-0.246	-0.255

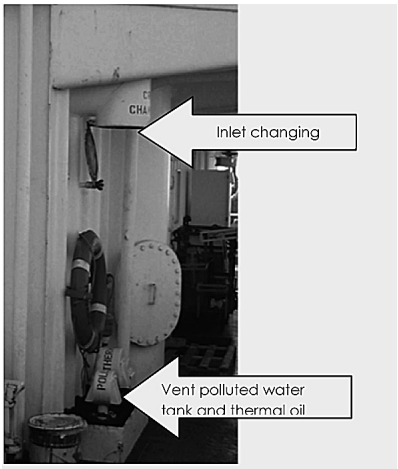

Figure 6: Positioning of inlet changing room relative to vent polluted water tank and thermal oil tank.

ing result. The intake of the supply of the changing room is situated just above the vents of the polluted water tank and thermal oil tank, as shown in Figure 6. The polluted water tank contains a mix of water and all kinds of other liquids that cannot be discharged directly because of ecological reasons. These liquids are temporarily stored in the polluted water tank for decantation. Examples of other liquids are bilges water or liquids from any leak in the ER. It is not uncommon that these liquids contain hydrocarbons. In order to accelerate the segregation/decantation with water, this tank is kept at a temperature between 50°C and 70°C. Therefore it is not surprising that different compounds do have a higher concentration in the changing room. We would therefore advice the crew not to use the supply for the changing room, but only the extraction fan. Our results show that the air in the gdz is cleaner than the air near the polluted water tank vent. This error in the configuration of the ventilation raises some doubts whether naval architects are really concerned about the seafarers' health.

CONCLUSIONS

Comparing ship A with ship B shows that the cargo has a very important influence on the absolute concentrations. During most of the cargo handling the influence of cargo vapours is restricted to the gdz, but when loading and especially during cleaning and ventilating the tanks, the cargo vapours can be found all over the vessel. A second important pollution source is the ER. Although the absolute concentrations found are well below these of the cargo, the results clearly show that there is a problem in the ER despite the mechanical ventilation. A third pollution source, depending on the location, is the shore. The loading and discharging operations mostly take place in an industrial area, and sometimes really close to the production or treatment plant. The example given of the crew changing room ventilation arises the doubt whether naval architects are sufficiently concerned about the seafarers' health. Our conclusion is that the actual ventilation configuration can be improved.

ACKNOWLEDGEMENTS

The authors would like to thank Ahlers Maritime Services Antwerp, for the hospitality and the cooperation on board. The authors also would like to thank the Flemish Institute for the Sea (VLIZ), for providing measuring apparatus.

REFERENCES

Agency for Toxic Substances and Disease Registry (ATSDR). (2007). *Toxicological profile for benzene.* Atlanta, Georgia: U.S. Department of Health and Human Services, Public Health Service.

Agency for Toxic Substances and Disease Registry (ATSDR). (2004). *Interaction profile for benzene, toluene, ethylbenzene and xylene (BTEX)*. Atlanta, Georgia: U.S. Department of Health and Human Services, Public Health Service.

Agency for Toxic Substances and Disease Registry (ATSDR). (2007). *Toxicological profile for ethylbenzene.* Atlanta, Georgia: U.S. Department of Health and Human Services, Public Health Service.

Calabrese EJ, Kenyon EM. (1991) *Air Toxics and Risk Assessment*. Lewis Publishers, Chelsea, MI. ISBN 0873711653.

ICS, OCIMF, IAPH. (2006) ISGOTT 5th ed. *International Safety Guide for Oil Tankers & Terminals.* Witherby Marine Publishing, London.

IMO. (2007) *International code for the construction and equipment of ships carrying dangerous chemicals in bulk (IBC Code)*. IMO publications, London.

Joos PE, Godoi AFL, De Jong R, de Zeeuw J, Van Grieken R. (2003) Trace analysis of benzene, toluene, ethylbenzene and xylene isomers in environmental samples by low-pressure gas chromatography–ion trap mass spectrometry. *Journal of Chromatography* A; 985, 191-196.

Moen BE, Hollund BE, Berntsen M, Flo R, Kyvik KR, Riise T. (1995a). Exposure of the deck crew to carcinogenic agents on oil product tankers. *The Annals of Occupational Hygiene*; 39 347-361.

Moen BE, Bjorg E, Hollund BE, Berntsen M, Flo R, KyvikK R, and Rilse T. (1995b). Occupational exposure of deck crews to carcinogenic agents on crude oil tankers. *American Journal of Industrial Medicine*; 27 555-564.

Nilsson RI, Nordlinder R, Hörte LG, Järvholm B. (1998). Leukaemia, lymphoma, and multiple myeloma in seamen on tankers. *Occupational Environment Medicine*; 55 517-521.

Oury B, Lhuillier F, Protois J-C, Moréle Y. (2006). Behavior of the GABIE, 3M 3500, PerkinElmer Tenax TA, and Radiello 145 diffusive samplers exposed over a long time to a low concentration of VOCs. *Journal of Occupational and Environmental Hygiene*; 10 547-57.

Pennequin-Cardinal A, Plaisance H, Locoge N, Ramalho O, Kirchner S, Galloo J.(2005). Performances of the Radiello diffusive sampler for BTEX measurements: Influence of environmental conditions and determination of modelled sampling rates. *Atmospheric Environment*; 39 2535-2544.

Saarni H, Pentti J, Pukkala E. (2002). Cancer at sea: a case-control study among male Finnish seafarers. *International Archives of Occupational and Environmental Health*; 59 613-619

Stranger M. (2005). *Characterisation of health related particulate and gasphase compounds in multiple indoor and outdoor sites in Flanders*. Thesis (PhD), University of Antwerp, Belgium.

Victorin K. (1993). Health effects of urban air pollutants guideline values and conditions in Sweden. *Chemosphere*; 27 1691–1706.

Journal of Maritime Research, Vol. VII. No. 2, pp. 21-36, 2010

ISSN: 1697-4840

EVALUATION OF THE ENERGETIC POTENTIAL OF SWELL FOR THE CANARY ISLES

J. Perera [1,3], G. Arencibia [1,4], F. Garcia[2] and E. Melón[1,5]

Received 20 May 2009; in revised form 23 May 2009; accepted 11 June 2010

Abstrac

A summary of the methodology and calculations on the Canary Isles tidal power potential.

The background data have been provided by the Spanish State Ports *(Puertos del Estado),* an institution dependent on the Spanish Ministry for Public Works (Ministerio de Fomento).

Swell data have been obtained from WANA points and by means of the different beacons placed along the Canary Isles coasts which measure the height and period of swell.

In the event of dealing with real swelling, the swell analysis will be done statistically, assuming that swelling is a stochastic process nearly – stationary. This condition forces the interruption of swell registers at time intervals relatively short, but long enough to be statistically reliable. These time intervals in which swelling registers are divided for analysis are called sea states. The statistical analysis of sea states constitutes what is called short term wave analysis. At present, the State Ports controlled Average Wave Network, divides wave registers in 1 hour time sea states.

WAM is a third generation model which solves the transportation equation without any limitations in the energy spectrum shape. To this effect, a customization of the non-linear transference function and the specification of the dissipation functions were necessary.

Keywords: Energetic; Swell; Wave

[1] Dpto. de Ciencias y Tecnicas de la Navegacion, ULL, Fax. (+34) 922 319 835, Avda. Francisco La Roche s/n, 38001 S.C. de Tenerife (Spain). [2]Professor Dpto. de Ingeniería Marítima, ULL, E-mail address: fgarcia@ull.es, Fax. 922 319 835, Avda. Francisco La Roche s/n, 38001 S.C. Tenerife (Spain). [3]Professor. Corresponding author: E-mail address jperera@ull.es. [4]E-mail address: gerardoarencibia@hotmail.com, [5]Professor. E-mail address: emelon@ull.es.

ENERGETIC POTENTIAL OF SWELL

A summary of the methodology and calculations on the Canary Isles tidal power potential are presented on this section.

The background data have been provided by the Spanish State Ports (Puertos del Estado), an institution dependent on the Spanish Ministry for Public Works (Ministerio de Fomento).

Swell data have been obtained from WANA points and by means of the different beacons placed along the Canary Isles coasts which measure the height and period of swell.

Calculation of the estimated wave power potential

For a given set of waves with an H (m) height and a T (s) period, the average energy per horizontal area unit, E (W), is obtained by means of the expression:

$$E = \frac{1}{8} \cdot \rho \cdot g \cdot H^2 \tag{1}$$

Where ρ is the water density (Kg/m^3) and g is the acceleration of gravity (m/s^2).

In order to know the magnitude of this energy, it is worth determining the average power of swell per width unit Pw (W/m), which crosses a vertical plane perpendicular to the wave propagation direction. For regular swelling, such average flow of energy can be determined by means of the expression:

$$Pw = E \cdot C_g \tag{2}$$

where Cg is the group swiftness or the energy carrying speed. Such a speed is given by:

$$C_g = \frac{c}{2} \cdot \left(1 + \frac{2 \cdot k \cdot h}{sen\,(2 \cdot k \cdot h)} \right) \tag{3}$$

where $c = \frac{L}{T}$ is the wave swiftness, $k = \frac{2 \cdot \pi}{L}$ is the wave number, h is the water depth and L is the wavelength, that can be obtained from the period and depth by solving the dispersion equation:

$$L = \frac{g \cdot T^2}{2 \cdot \pi} \cdot \tan(2 \cdot k \cdot h) \tag{4}$$

At undefined depths, when h/L > 0.5, the equations (3) and (4) are simplified to:

$$C_g = \frac{c}{2} \tag{5}$$

$$L = L_0 = \frac{g \cdot T^2}{2 \cdot \pi} \tag{6}$$

and the average power (2) is simplified to:

$$Pw = \frac{1}{32\pi} \rho g^2 H^2 T \approx 981 H^2 T \quad (W/m) \tag{7}$$

As seen, average power has a linear growth alongside the period, and a square growth in relation to the wave height.

In the event of dealing with real swelling, the swell analysis will be done statistically, assuming that swelling is a stochastic process nearly – stationary. This condition forces the interruption of swell registers at time intervals relatively short, but long enough to be statistically reliable. These time intervals in which swelling registers are divided for analysis are called sea states. The statistical analysis of sea states constitutes what is called short term wave analysis. At present, the State Ports controlled Average Wave Network, divides wave registers in 1 hour time sea states.

Short term statistical analysis of wave registers is customarily done on the frequency domain, by obtaining the function that represents the distribution of energy in angular frequencies, $\omega = 2 \cdot \pi / T$ and directions, θ, called directional spectral density function, $S(\omega, \theta)$ on the free surface of the ocean, which represents an average of the total energy in the existing time on every frequency interval $\Delta\omega_i$ and on every direction interval $\Delta\theta_j$. If swell component "i, j" is defined as the waves contained in the frequency $\Delta\omega_i$, $\Delta\theta_j$, such component will be assigned a height H_{ij} and its average energy per area unit (W/m^2) will be:

$$E_{i,j} = \frac{1}{8} \cdot \rho \cdot g \cdot H_{i,j}^2 \tag{8}$$

The total average energy per swell unit area in a sea state is to be obtained as the sum of all energy corresponding to all components:

$$E = \frac{1}{8} \cdot \rho \cdot g \cdot \sum_{\Delta\omega_i} \sum_{\Delta\theta_j} \frac{1}{2} H_{i,j}^2 = \rho \cdot g \cdot \int_{-\pi}^{\pi} \int_{0}^{\infty} S(\omega, \theta) \cdot d\omega \cdot d\theta \tag{9}$$

The average wave power will be obtained as the sum of energy flows of all the components, according to the expression:

$$Pw = \frac{1}{8} \cdot \rho \cdot g \cdot \sum_{\Delta\omega_i} \sum_{\Delta\theta_j} H_{i,j}^2 \cdot C_{gi,j} = \rho \cdot g \cdot \int_{-\pi}^{\pi} \int_{0}^{\infty} S(\omega,\theta) \cdot C_{gi,j} \cdot d\omega \cdot d\theta \quad (10)$$

In the event of being at undefined depths, h/L > 0.5, the expression (10) will be simplified to:

$$Pw = \frac{1}{32} \cdot \rho \cdot g^2 \cdot \sum_{\Delta\omega_i} \sum_{\Delta\theta_j} H_{i,j}^2 \cdot T_{i,j} = \frac{1}{2} \cdot \rho \cdot g^2 \cdot \int_{-\pi}^{\pi} \int_{0}^{\infty} \omega^{-1} \cdot S(\omega,\theta) \cdot d\omega \cdot d\theta \quad (11)$$

If we integrate the directional spectral density function on all the direction spectrum, a scalar spectral density function on the free surface of the ocean, S(ω) is obtained:

$$S(\omega) = \int_{-\pi}^{\pi} S(\omega, \theta) \cdot d\theta \quad (12)$$

In order to be able to obtain the directional spectral density function, the register and analysis of temporary series of several swell parameters (free surface, speed, etc.) is required. Whereas to obtain the scalar spectral density function for the free surface of the ocean the register and analysis of only one parameter is required. Therefore, equipments for directional swelling measures are more expensive than those for scalar measures. Nowadays, most of the existing instrumental information belongs to scalar buoys.

The frequency where the maximum of spectral density function is found is called peak frequency, ω_p and its associate period, peak period, T_p. The direction where the maximum spectrum is found it is called peak direction, θ_p or main propagation direction.

From the spectral density function a series of parameters is obtained which provides condensed information about the characteristics of the analysed register. Among these parameters it is worth mentioning the spectral moments and the sea state parameters derived thereof.

The order moment, n, on the scalar spectral density function is defined as:

$$m_n = \int_0^{\infty} \omega^n S(\omega)\, d\omega \quad ; n = 0, 1, 2, ... \quad (13)$$

The zero order moment, m_0, or the area under the spectrum, matches the square root of the average quadratic movement, ηρms of the free sea state surface and is proportional to the energy per sea state unit area (9). From the zero order moment it is defined the height of the sea state zero moment order, H_{m0}, by means of:

$$H_{m0} = 4.004\sqrt{m_0} \tag{14}$$

Where the process is narrow band and the wave height distribution is Rayleigh, it may be demonstrated that:

$$H_{m0} = 4.004 \cdot \eta_{rms} = H_s \tag{15}$$

Where H_s is the height of a significant wave, or average height of the N/3 highest waves on a free surface register made up of N waves.

The first two moments are especially relevant, as they are used to define the average frequency, $\overline{\omega}$, the average period, $\overline{T}$ and the average period for the rising passage through zero, Tz:

$$\overline{\omega} = \frac{m_1}{m_0}; \quad \overline{T} = 2\pi\frac{m_0}{m_1}; \quad \overline{T_z} = 2\pi\sqrt{\frac{m_0}{m_2}} \tag{16}$$

A parameter that facilitates a measure of the energy concentration round the spectrum peak is the dimensionless spectral width, ν, given by:

$$\nu^2 = \frac{m_0 m_2}{m_1^2} - 1 \tag{17}$$

Parameter ν facilitates a measure of the spectral width and has been theoretically proved that is inversely proportional to the average number of waves in a group. Equation (17) indicates that when all energy is concentrated on a single frequency, $\omega = \overline{\omega}$, then $\nu_2 \to 0$. When energy is scattered in many frequencies, then ν is incremented. A typical value in gales is ν = 0.3.

The average propagation direction is determined from this directional spectrum through the expression:

$$\theta_m = \arctan\left(\frac{\int_0^{2\pi}\int_0^{\infty}\sin\theta \cdot S(\omega,\theta)\cdot d\omega \cdot d\theta}{\int_0^{2\pi}\int_0^{\infty}\cos\theta \cdot S(\omega,\theta)\cdot d\omega \cdot d\theta}\right) \tag{18}$$

Once the scalar spectral density function of the free surface on a sea state is obtained, and after some hypothesis, the theoretical distribution functions of the different wave register parameters can be formulated, such as the height of wave, the period and the direction. These distribution parameters are expressed according to the spectral moments.

Average wave power, as a general rule given through the spectral density function by means of the expression (10), can be simply approached if the distribution of wave heights and their periods are known. A single approach to the energy flow at undefined depths can be obtained by making a scan with the sea states formula (11) with an average JONSWAP spectrum and H_s, T_z and A variables. Variable A will oscillate in 0.34 and 0.57 depending on the wave spectrum to be evaluated.

Adjusting the energy flows to a (7) type function which to the effects of data analysis is used as Pw per kW/m is obtained:

$$Pw = A H_s^2 T_z \quad (kW/m) \tag{19}$$

Methodology used for the calculation of estimated swell power potential and results obtained

In order to evaluate the average wave power existing in the Canary Isles, formula (19) has been used as well as Tables for height-period from years 2002 to 2007 from the Swell database, Banco de Datos Oceanográficos de Puertos del Estado [State Ports Oceanographic Data Bank], an institution depending on the Spanish Ministry for Public Works (Ministerio de Fomento). To this effect, the following approximation $T_e \approx 0.8572 \times T_p$ will take place, where H_s and T_p. are the evaluated data.

Pw (kW/m)		Tp (s) 1	2	3	4	5	6	7	8	9	10	12
Hs (m)	0											
	0,5		0,080	0,133	0,186	0,239	0,292	0,346	0,399	0,452	0,505	0,585
	1,0	---	0,399	0,665	0,931	1,197	1,462	1,728	1,994	2,260	2,526	2,925
	1,5	---	1,037	1,728	2,420	3,111	3,802	4,494	5,185	5,877	6,568	7,605
	2,0	---	1,994	3,324	4,653	5,983	7,312	8,642	9,971	11,301	12,630	14,625
	2,5	---	3,271	5,451	7,631	9,812	11,992	14,173	16,353	18,534	20,714	23,985
	3,0	---	4,866	8,110	11,354	14,598	17,842	21,086	24,330	27,574	30,818	35,684
	3,5	---	6,781	11,301	15,821	20,342	24,862	29,383	33,903	38,423	42,944	49,724
	4,0	---	9,014	15,024	21,033	27,043	33,052	39,061	45,071	51,080	57,090	66,104
	4,5	---	11,567	19,278	26,989	34,701	42,412	50,123	57,834	65,546	73,257	84,824
	5,0	---	14,439	24,064	33,690	43,316	52,942	62,567	72,193	81,819	91,445	105,883
	7	---	23,612	39,354	55,096	70,837	86,579	102,320	118,062	133,803	149,545	173,157

Source: http://www.puertosdetenerife.es

Table 1. General data table from year 2004 used in the calculations of the average wave power.

To calculate the wave energy, formula (19) will be used with a conversion for Mw h year/m:

Energy (Mw h year/m) = Probability x Pw x 8760/1000/100

WAM Model and WANA simulation Points on the Canary Isles

WAM is a third generation model which solves the transportation equation without any limitations in the energy spectrum shape. To this effect, a customization of the non-linear transference function and the specification of the dissipation functions (Ozger *et al*, 2004) were necessary. WAM is formulated for spherical coordinates and uses an implicit method of integration.

This method tends to make spectrums wider than if more rigorous methods were used (Curran, Whittaker and Stewart, 1998). When numerically solving the source terms, on the whole, the solution is not stable. Therefore, a restrictor in the growth of wave energy is used according to frequency and timing. Hersbach and Janssen (1999) found that the original WAM restrictor is not suitable for high geographical resolutions. Therefore, they suggested a restrictor depending on the speed of friction and high-frequency cut-off (Falcão and Rodrigues, 2002).

In WAM it is assumed that waves are generated in the same direction as wind, and an empirical growth coefficient (restrictor) is used. Although helpful in high seas, in shore areas these considerations may not be valid (Falcão and Rodrigues, 2002; Falcão, 2002; Setoguchi *et al*, 2001). Therefore, tests were performed with a WAM adapted for its use on high spatial resolutions, mainly on shore areas, where modifications for propagation, inclusion of the effect of currents, bed friction and bed breaking were carried out. The authors concluded that when using a small timing, WAM is numerically stable in cases of growth with limited fetch. Therefore, problems become more numerical than physical. In spite of this, the growth restrictor (Falcão and Rodrigues, 2002; Sen, 2000) was also implemented.

WAM has been adopted by centres from all over the World for their operational use, including The National Center for Environmental Prediction (NCEP), United Kingdom Meteorological Office (UKMO), The European Centre for Medium-Range Weather Forecasts (ECMWF), and the U.S. Naval Oceanographic Office (NAVOCEANO). With experience, some model tendencies were found; for instance, the subforecasts of storm peaks and swelling events.

Some comparisons have shown that the influence in using either superficial winds, or superficial strength, is not significant.

WAM, as compared to buoy data (Tucker, 2001), provided good results, although there is evidence about its slow answering to variable conditions, possible due to the low resolution of wind fields. Impact on the assimilation of data in the prediction of swelling has been very limited. Furthermore, the assimilation effect disappeared in one hour after the testing time.

WAM model, although in use at different parts of the world by researchers and climate prediction centres, however, it has not been sufficiently analysed in terms of its validity for limited seas such as the Mediterranean. One of the few works carried out is the implementation by Cavaleri et al. (1991), Dell'Osso et al. (1992), where model tests with measures showed that, in order to obtain reliable predictions, it is necessary to have horizontal resolutions, with a cell size of, at least, 40 km.

WANA Simulation Points

The following Figure shows the location of all the evaluated WANA points in order to determine the energetic wave power potential of the Canary Isles.

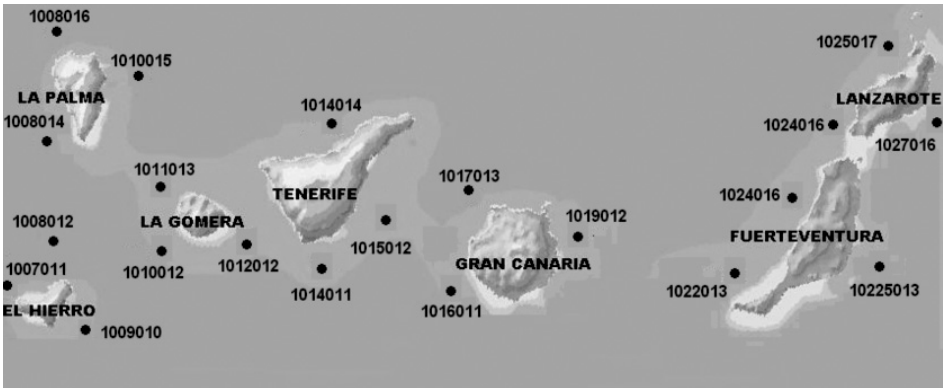

Source: Own elaboration, 2008.

Figure 1. Representation of the WANA points location on the Canary Isles.

Results obtained from the analysis of monthly maximums for significant wave height (Hs) and period (Ts)

Below are shown the results obtained from the analysis of monthly maximums for significant wave height (H_s) and period (T_s). In order to summarise the swell climate on every WANA point studied, Tables for maximum height and period per month and per year are obtained. Average values of the analysed parameters are shown.

El Hierro WANA Point 1009010

Year	Hs (m)		Tp (s)	
	Summer	Winter	Summer	Winter
2002	1,92	3,27	8,32	19,97
2003	1,85	3,62	5,85	16,82
2004	1,37	2,92	8,6	13,07
2005	1,17	2,77	9,42	14,97
2006	1,77	3,47	6,2	12,55
2007	2,07	3,12	6,41	11,52
Prom.	1,690	3,270	7,460	13,810

WANA Point 1008012

Year	Hs (m)		Tp (s)	
	Summer	Winter	Summer	Winter
2002	2,15	4,75	8,17	16,45
2003	2,02	4,82	7,5	17,22
2004	1,5	3,55	11,3	15,27
2005	1,32	3,52	3,97	14,7
2006	2,22	4,32	9,15	14,2
2007	2,75	3,95	10,17	12,75
Prom.	1,990	4,150	9,340	15,090

WANA Point 1007011

Year	Hs (m)		Tp (s)	
	Summer	Winter	Summer	Winter
2002	2,15	5,32	9,95	14,95
2003	2,07	5,2	11,4	17,6
2004	1,75	3,87	10,67	14,9
2005	1,55	3,92	11,1	14,82
2006	1,97	4,55	11,65	14,2
2007	2,15	4,02	13,52	14,65
Prom.	1,940	4,480	11,382	15,187

Source: Own elaboration, 2008.

Table 3. Summary of the H_s and T_p seasonal maximums for El Hierro.

La Gomera WANA Point 1012012

Year	Hs (m)		Tp (s)	
	Summer	Winter	Summer	Winter
2002	1,72	3,42	9,5	15,4
2003	1,7	3,35	8,17	16,87
2004	1,57	2,8	11,65	15,42
2005	1,35	2,52	9,97	12,72
2006	1,57	2,67	10,47	13,37
2007	1,62	2,62	11,72	13,3
Prom.	1,588	3,897	10,247	14,513

WANA Point 1010012

Year	Hs (m)		Tp (s)	
	Summer	Winter	Summer	Winter
2002	2,1	4,05	9,47	15,02
2003	1,92	3,9	7,65	17,06
2004	1,6	3,07	9,62	14,9
2005	1,42	3,2	8,55	14,27
2006	2	3,75	8,55	14,27
2007	2,35	3,4	8,75	13,9
Prom.	1,898	3,562	8,765	14,993

WANA Point 1011013

Year	Hs (m)		Tp (s)	
	Summer	Winter	Summer	Winter
2002	2,15	4,15	10,02	15,4
2003	1,95	3,92	8,27	16,87
2004	1,95	3,32	11,6	14,72
2005	1,37	3,2	10,15	15,02
2006	2,12	3,72	9,15	16
2007	2,45	3,15	10,72	15,27
Prom.	1,998	3,577	9,985	15,547

Source: Own elaboration, 2008.

Table 4. Summary of the H_s and T_p seasonal maximums for La Gomera

La Palma WANA Point 1010015

Year	Hs (m)		Tp (s)	
	Summer	Winter	Summer	Winter
2002	2,32	4,3	9,45	14,45
2003	2,27	4,15	6,92	15,45
2004	2,2	3,6	8,27	14,67
2005	1,82	3,3	10,75	11,32
2006	2,5	3,65	10,57	15,1
2007	1,62	2,62	11,72	13,3
Prom.	2,227	3,750	9,260	14,193

WANA Point 1008014

Year	Hs (m)		Tp (s)	
	Summer	Winter	Summer	Winter
2002	1,5	3,95	9,05	15,09
2003	1,4	3,85	8,4	17,22
2004	0,92	3,07	12,6	13,62
2005	0,92	2,92	9,35	14,55
2006	1,5	3,65	11,67	14,25
2007	1,72	3,65	12,7	14,47
Prom.	1,327	3,515	10,628	15,002

WANA Point 1008016

Year	Hs (m)		Tp (s)	
	Summer	Winter	Summer	Winter
2002	2,42	5,67	9,65	16,82
2003	2,32	5,4	9,6	17,22
2004	3,2	4,22	11,37	15,37
2005	2	4,3	9,55	14,87
2006	2,3	4,87	10,67	14,17
2007	2,55	4,12	10,07	13,72
Prom.	2,315	4,763	10,257	15,362

Source: Own elaboration, 2008.

Table 5. Summary of the H_s and T_p seasonal maximums for La Palma

Tenerife WANA Point 1015012

Year	Hs (m)		Tp (s)	
	Summer	Winter	Summer	Winter
2002	1,22	1,95	4,79	6,27
2003	1,25	1,37	4,95	6,37
2004	0,9	1,22	5,5	6,45
2005	0,72	1,05	5,07	5,6
2006	2	3,2	6,67	8,05
2007	2,47	2,05	7,57	7,8
Prom.	1,427	1,882	5,788	6,757

WANA Point 1014014

Year	Hs (m)		Tp (s)	
	Summer	Winter	Summer	Winter
2002	2,12	5,17	11,65	16,82
2003	2,07	4,95	11,35	16,87
2004	2,02	3,62	11,6	15,6
2005	1,72	3,62	11,1	14,8
2006	2,05	3,8	10,5	14,32
2007	2,05	3,5	11,45	15,7
Prom.	2,005	4,110	11,108	15,685

WANA Point 1014011

Year	Hs (m)		Tp (s)	
	Summer	Winter	Summer	Winter
2002	1,32	2,6	5,07	8,4
2003	1,27	1,9	5,07	14,15
2004	0,9	1,82	4.22	9,72
2005	0,75	1,55	4,35	9,6
2006	1,9	2,15	6,27	12,15
2007	2,37	2,75	6,95	11,55
Prom.	1,418	2,128	5,322	10,928

Source: Own elaboration, 2008.

Tables 6. Summary of the H_s and T_p seasonal maximums for Tenerife

Lanzarote WANA Point 1025017

Year	Hs (m)		Tp (s)	
	Summer	Winter	Summer	Winter
2002	3,02	4,36	9,82	16,82
2003	2,8	5,62	9,27	16,87
2004	2,5	4,1	10,52	16,02
2005	2,02	4,42	9,52	14,85
2006	2,42	4,07	9,52	14,07
2007	2,9	3,97	9,97	16,95
Prom.	2,61	4,42	9,77	16,03

WANA Point 1027016

Year	Hs (m)		Tp (s)	
	Summer	Winter	Summer	Winter
2002	3,17	4,4	8,22	11,25
2003	3,05	4,4	8	3,47
2004	2,6	3,52	8,47	12,15
2005	2,07	3	7,12	13,15
2006	2,37	3,1	9,45	11.7
2007	2,87	3,52	8,3	14,02
Prom.	2,68	3,65	8,27	12,62

WANA Point 1024016

Year	Hs (m)		Tp (s)	
	Summer	Winter	Summer	Winter
2002	2,09	5,72	9,82	16,82
2003	2,72	5,57	9,27	16,87
2004	2,37	4	10,5	15,82
2005	1,97	4,32	9,57	15,07
2006	2,35	4,07	9,75	14,55
2007	2,77	3,87	11,42	17,12
Prom.	2.51	4,59	10,05	16,04

Source: Own elaboration, 2008.

Tables 7. Summary of the H_s and T_p seasonal maximums for Lanzarote

Fuerteventura WANA Point 1023014

Year	Hs (m)		Tp (s)	
	Summer	Winter	Summer	Winter
2002	2,77	5,5	9,65	16,82
2003	2,52	5,35	10,75	17,32
2004	2,17	3,8	11,25	15,72
2005	1,87	4,05	9,27	15,05
2006	2,22	3,87	9,7	14,34
2007	2,52	3,85	12,42	15,05
Prom.	2,34	4,40	10,50	15,75

WANA Point 1025013

Year	Hs (m)		Tp (s)	
	Summer	Winter	Summer	Winter
2002	2,57	3,15	7,47	8,02
2003	2,3	2,85	7,3	9,02
2004	1,77	2,2	8,2	8,22
2005	1,47	1,65	6,87	6,57
2006	2,55	2,02	6,8	6,92
2007	2,25	2,62	8,1	8,27
Prom.	2,20	2,41	7,79	7,83

WANA Point 1022013

Year	Hs (m)		Tp (s)	
	Summer	Winter	Summer	Winter
2002	2,77	5,22	9,65	16,82
2003	2,57	5,12	9,27	16,87
2004	2,22	4,22	10,35	15,75
2005	1,9	3,82	9,25	15,22
2006	2,3	3,65	9,52	13,65
2007	2,67	3,92	11,12	13,8
Prom.	2,40	4,33	9,86	15,35

Source: Own elaboration, 2008.

Table 8. Summary of the H_s and T_p seasonal maximums for Fuerteventura

Gran Canaria WANA Point 1017013

Year	Hs (m)		Tp (s)	
	Summer	Winter	Summer	Winter
2002	2,35	3,52	7,32	11,87
2003	2,3	3,65	7,62	15,45
2004	2,25	3,2	8,27	12,8
2005	1,8	2,97	7,82	12,75
2006	2,22	2,8	8,9	10,87
2007	2,47	3,3	9,22	15,3
Prom.	2,23	3,24	8,19	13,17

WANA Point 1016011

Year	Hs (m)		Tp (s)	
	Summer	Winter	Summer	Winter
2002	1,55	2,52	5,35	8,32
2003	1,47	1,82	5,2	8,02
2004	1,25	1,67	4,75	9,92
2005	1	1,65	4,4	5,87
2006	1,97	2,02	6,25	6,8
2007	2,5	2,5	7,15	13,25
Prom.	1,62	2,03	5,51	8,69

WANA Point 1019012

Year	Hs (m)		Tp (s)	
	Summer	Winter	Summer	Winter
2002	2,45	3,82	7,3	9,87
2003	2,4	4	7,62	15,62
2004	2,25	4,82	10,4	15,17
2005	1,87	3,12	9,35	13,77
2006	2,15	2,9	7,25	9,65
2007	2,5	3,22	7,7	12,65
Prom.	2,27	3,64	8,27	12,78

Source: Own elaboration, 2008.

Table 9. Summary of the H_s and T_p seasonal maximums for Gran Canaria

Ocean waves are classified according to its period. Summer season waves are to be classified within wind swell (which corresponds to waves of every size and wave longitude, which propagates in different directions) and those from winter season within ground swell (perfect sinusoidal waves, regular, parallel and of great length and width).

Available wave power in the Canary Isles

Below are shown the results obtained after having studied the different WANA simulation points data for every one of the islands in the Canary Isles archipelago and for a period of time between the years 2002 and 2007.

Suitable Area: that is the area that shows enough power to implement energetic Systems. A minimum power of 15 Kw/m has been considered for this area.

Intermediate Area: that area which presents an intermediate power, and, where more detailed Studies (such as gathering data on the spot by means of buoys) should be done, in order to definitely accept or reject such location. For this area, a range oscillating between 13-15 Kw/m has been taken into account.

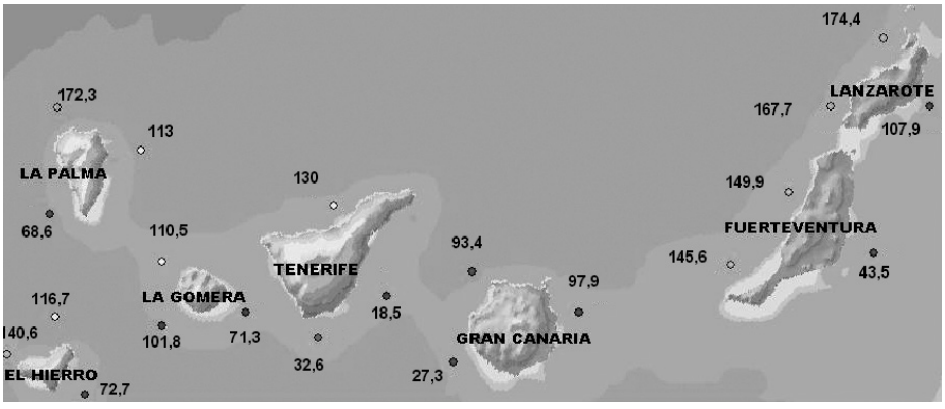

Source: Own elaboration, 2008.

Figure 10.1. Representation of the average wave power energy (Gwhyear/m) on the Canary Isles archipelago.

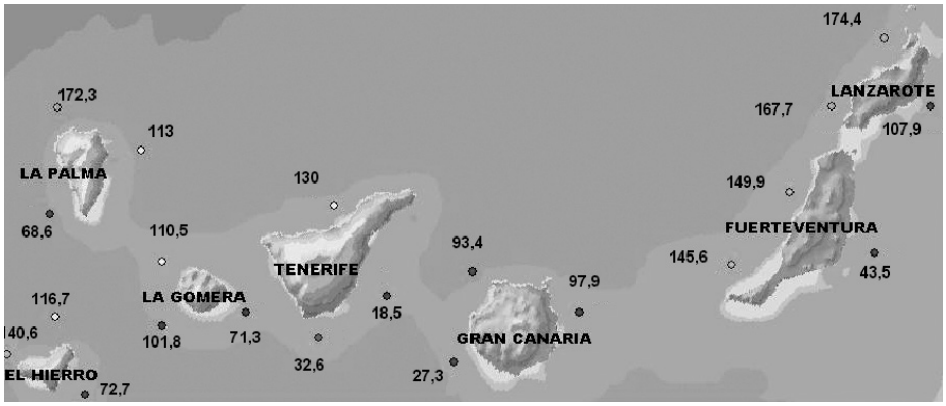

Source: Own elaboration, 2008.

Figure 10.2. Representation of average Powers (Kw/m) on the Canary Isles archipelago.

Exclusion Area: those areas that do not reach the necessary minimum power (15 Kw/m) so that, with current energetic systems, the resource exploitation might be profitable. All points showing a power within the 0-13 Kw/m power will be included in this area.

CONCLUSIONS

A fact that corroborates the obtained results is that ports are built in those places which offer a better shelter against the action of swelling and wind. Taking into account the location of the aforesaid ports on every isle of the archipelago, and when comparing them with the Figure where the average Powers are represented, one may see that all ports are located at exclusion areas.

One of the circumstances that will explain the results obtained is the given proximity between some isles, as well as, their steep orography –with big mountains and pronounced cliffs– that will emphasize even more the well-known "shadow effect".

If we focus on the most western isles (Lanzarote and Fuerteventura), we will appreciate that those are the isles that show the highest amount of energy of the entire archipelago. This is due to their being first affected by the trade winds, and therefore those winds will transfer a great part of their kinetic energy to the water surface, giving rise to waves with a higher amount of energy in comparison with other points in the archipelago. As may be seen on the Figure, both isles have suitable areas for the implementation of wave power capturer systems.

On the analysed WANA points for the isle of Lanzarote, we observe a marked seasonal variation that may come beyond the 2 m in significant wave height and the 6 s of period between summer and winter months.

The isle of Fuerteventura shows seasonal variations of more than 2 m in significant wave height and of 5 s periods, in two out of the three studied points. On the third

one (WANA Point 1025013), located east of the island, seasonal variation is minimal. This is due to the fact that this point is more protected from the action of the trade winds, due to the "shadow effect" provoked by the island of Lanzarote, which gives rise to the difference between the summer and winter times being virtually non-existent.

Apart from everything that has been said before, as may be seen on the types of swelling Figure, the Canary Isles are affected by a Westerly swelling. Therefore, it stands to reason that main Powers may be located on every island's north-west areas, whilst on those waters located to their east, lower energetic potentials may be found, as they are more sheltered against the action of this kind of swelling.

When focusing on the isle of Gran Canaria, we may see that it does not have either suitable or intermediate areas, just exclusion areas. On the whole, it shows the lowest energetic potentials in the whole archipelago. This fact might have an explanation, as it is more than likely that both the isle of Lanzarote and that of Fuerteventura may provoke some "shadow effect" over Gran Canaria, so that the trade winds may not completely affect the island.

The same might happen with a westward swell, as western isles will give rise to a screening that will diminish this area's potential.

Some seasonal variations exist at the tested points, but these are little when compared to those on the other isles.

Taking into account all of this, one may say that the isle of Gran Canaria is the one which finds itself better protected from the action of the trade winds and swell. Therefore, it represents the lowest energetic potentials. Thus, the implementation of ocean energetic Systems is quite complicated as it does not have enough resources.

With regards to the western isles, the only one that shows a well defined suitable area is La Palma. This island is quite exposed to the action of the trade winds, the north part being the first to get them. In addition, it is also quite affected by a westerly swell. This isle would be totally capable of implementing wave power capturers.

The isle of El Hierro has a suitable area, located north of the island. It also presents an intermediate area, which, as said before, deals with areas where the no-implementation of these systems cannot be absolutely discarded. A more detailed study would be needed, with on the spot data gathering by means of using sensing buoys and a much longer sampling period in order to obtain data closer to reality.

The isle of La Gomera may be expected to be exerting some kind of "shadow effect" over the isle of El Hierro. But, in short, it is well exposed to the trade winds and a westward swell.

When paying attention to the isle of La Gomera, some intermediate areas are observed to the north (exposure to the trade winds action in May), whilst other locations on the isle are exclusion areas, mainly originated from the lack of potential, due to the proximity of the isle of Tenerife, giving rise to a clear "shadow effect".

Lastly, the isle of Tenerife counts on intermediate areas in the north, whilst in other locations potentials are practically reduced to a minimum. The proximity of

the isle of de Gran Canaria is more than likely responsible for this situation, as well as the geography of the isle, as the Anaga massif –to the north–, is going to slow down the advance of the trade winds, preventing their way out to the south.

On the other hand, due to the proximity to the isle of La Gomera, it is probable that it may be less affected by the westward swell.

REFERENCES

Curran, R.; Whittaker, T J. T. and Stewart, T. (1998). Aerodynamic conversion of power from wave to wire. *J. Energy Convers. Mgmt.*, 39, 1919–1929

Falcão AF. (2002). Control of an oscillating-water-column wave power plant for maximum energy production. *Appl Ocean Res* 24:73–82.

Falcão AFO, Rodrigues RJA. (2002). Stochastic modelling of OWC wave power plant performance. *Applied. Ocean Research*, (24):59-71,

Özger, M.; Altunkaynak, A. and Şen, Z., (2004). Stochastic wave energy calculation formulation, *Renewable Energy*, 29(10), 1747-1756.

Sen, Z. (2000). Stochastic wind energy calculation formulation. *Journal of Wind Engineering & Industrial Aerodynamics* 84: 227–34.

Setoguchi, T.; Santhakumar, S.; Maeda, H.; Takao, M. and Kaneko, K. (2001). A review of impulse turbines for wave energy conversion. *Renew Energy* 23:261–92.

Tucker, MJ. and Pitt. EG. (2001) Waves in ocean engineering. Elsevier.New York.

LF. Dell'Osso, J. Van der Steen, RM. Steinman and H. Collewijn (1992). Foveation dynamics in congenital nystagmus I: Fixation, *Doc Ophthalmol*, vol. 79, pp. 1-23.

Cavaleri, L., L. Bertotti, and P. Lionello (1991). Wind Wave Cast in the Mediterranean Sea, *J. Geophys. Res.*, 96(C6), 10739–10764

POTENCIAL ENERGÉTICO DEL OLEAJE

Resumen

El presente apartado se presenta un resumen con la metodología y calculo del potencial mareomotriz del archipiélago canario.

Los datos base han sido suministrados por Puertos del Estado, organismo dependiente del Ministerio de Fomento español.

Los datos de oleaje han sido obtenidos a partir de puntos WANA y por las diferentes boyas situadas en las costas de canarias que realizan mediciones de altura y período del oleaje.

Cálculo del potencial estimado de energía del oleaje

Para un conjunto de ondas de altura H (m) y período T (s), la energía media por unidad de área horizontal, E (W), se obtiene mediante la expresión:

$$E = \frac{1}{8} \cdot \rho \cdot g \cdot H^2$$

donde ρ es la densidad del agua (Kg/m^3) y g es la aceleración de la gravedad (m/s^2).

Para conocer la magnitud de esta energía, interesa determinar la potencia media del oleaje por unidad de anchura Pw (W/m), que atraviesa un plano vertical perpendicular a la dirección de propagación de la onda. Para un oleaje regular, dicho flujo medio de energía se puede determinar mediante la expresión:

$$Pw = E \cdot C_g$$

donde Cg es la celeridad de grupo o la velocidad con que se transporta la energía.

En el caso de tratarse de oleaje real, el análisis del oleaje se realiza de forma estadística, asumiendo que el oleaje es un proceso estocástico cuasi - estacionario. Esta condición obliga a cortar los registros de oleaje en intervalos de tiempo relativamente cortos, pero con suficiente duración como para dar fiabilidad a la estadística. Estos intervalos de tiempo en los que se dividen los registros de oleaje para su análisis se denominan estados de mar y el análisis estadístico de estados de mar constituye lo que se denomina análisis del oleaje a corto plazo. En la actualidad, la Red de Medida de Oleaje controlada por Puertos del Estado, divide los registros de oleaje en estados de mar de 1 hora de duración.

El análisis estadístico a corto plazo de los registros de oleaje se realiza habitualmente en el dominio de la frecuencia, obteniéndose la función que representa la dis-

tribución de energía por frecuencias angulares, $\omega = 2 \cdot \pi / T$ y direcciones, θ, denominada función de densidad espectral direccional, S(ω, θ) de la superficie libre del mar, la cual representa la energía total promediada en el tiempo existente en cada intervalo de frecuencia $\Delta\omega_i$ y en cada intervalo de dirección $\Delta\theta_j$. Si se define la componente "i,j" del oleaje como a las ondas contenidas en el intervalo de frecuencias $\Delta\omega_i$, $\Delta\theta_j$, a dicha componente le corresponderá una altura H_{ij} y su energía media por unidad de área (W/m^2) será:

$$E_{i,j} = \frac{1}{8} \cdot \rho \cdot g \cdot H_{i,j}^2$$

Metodología utilizada para el cálculo del potencial estimado de energía del oleaje y resultados obtenidos

Para evaluar la potencia media del oleaje existente en las Islas Canarias se ha utilizado la formula (19) y las Tablas alturas-periodo desde los años 2002 al 2007 de la base de datos del Oleaje, suministrada por el Banco de Datos Oceanográficos de Puertos del Estado, organismo dependiente del Ministerio de Fomento Español.

Modelo WAM y Puntos de simulación WANA en las islas canarias

El WAM es un modelo de tercera generación que resuelve la ecuación de transporte sin ningún limitante de la forma del espectro de energía; para ello fue necesario una parametrización de la función de transferencia no lineal y la especificación de las funciones de disipación. El WAM está formulado para coordenadas esféricas y usa un método implícito de integración.

Este método tiende a hacer los espectros más anchos que si se utilizaran métodos más rigurosos. Al resolver numéricamente los términos fuente generalmente la solución no es estable por lo que un limitador en el crecimiento de la energía del oleaje es utilizado en función de la frecuencia y del paso de tiempo. *Hersbach y Janssen (1999)* encontraron que el limitador original del WAM no es adecuado para altas resoluciones geográficas por lo que propusieron un limitador que dependía de la velocidad de fricción y de la frecuencia alta de corte.

En el WAM se asume que las olas son generadas en la misma dirección del viento y se utiliza un coeficiente empírico de crecimiento (limitador), práctico para mar abierto, aunque en zona costera estas consideraciones pueden no ser válidas realizan pruebas con el WAM adaptándolo para su utilización en altas resoluciones espaciales principalmente en zonas costeras y en las cuales se han realizado modificaciones de la propagación, inclusión del efecto de corrientes, fricción por fondo y ruptura por fondo. Los autores concluyen que utilizando un paso de tiempo pequeño el WAM es numéricamente estable para casos de crecimiento con *fetch* limitado por lo que los

problemas se vuelven numéricos más que físicos. A pesar de esto el limitador de crecimiento fue también implementado.

Tipos de zonas

Zona Apta: Es la zona que presenta potencial suficiente para implantar sistemas energéticos. Para esta zona se ha considerado una potencia mínima de 15 Kw/m.

Zona Intermedia: Aquella que presenta un potencial intermedio y que sería necesario realizar estudios más minuciosos (como la toma de datos in situ mediante el uso de boyas), para poder aceptar o descartar definitivamente dicha ubicación. Para esta zona se ha considerado un rango que oscila entre los 13-15 Kw/m.

Zona de Exclusión: Son las zonas que no poseen el potencial mínimo (15 Kw/m) necesario para que con los sistemas energéticos actuales sea rentable la explotación del recurso. Estarán dentro de esta zona todos los puntos que presentes potenciales dentro del intervalo 0-13 Kw/m.

Un hecho que corrobora los resultados obtenidos en este estudio, es que los puertos son construidos en los lugares que se encuentran más protegidos de la acción del oleaje y del viento. Teniendo en cuenta la localización de dichos puertos en cada una de las islas del archipiélago y comparándolo con la figura donde se representan las potencias medias, se ve que todos los puertos están ubicados en las zonas de exclusión.

Una de las circunstancias que explica los resultados obtenidos en el presente artículo es la proximidad que hay entre algunas de las islas y la orografía tan escarpada que presentan con grandes montañas y pronunciados acantilados que van a acentuar aún más el conocido "efecto de sombra".

A parte de todo lo expuesto anteriormente, como se puede aprecia en la Figura de los tipos de oleaje, las Islas Canarias están afectadas por un oleaje de componente oeste, por lo que es lógico que los mayores potenciales se localicen en las zonas del oeste-norte de cada una de las islas, mientras que en las aguas que se sitúan al este de cada una de ellas presenten menores potenciales energéticos ya que se encuentran más protegidas a la acción de este tipo de oleaje.

Journal of Maritime Research, Vol. VII. No. 2, pp. 37–48, 2010

ISSN: 1697–4840

INTERNATIONAL SECURITY THROUGH FURTHER MODERNITY: A THEORETICAL APPROACH TO INLAND AND MARITIME SECURITY

L. Kirval[1]

Received 19 January 2010; in revised form 29 January 2010; accepted 15 June 2010

Abstract:

By taking into account, the rising international terrorism, piracy and terror acts in international seas; this paper focuses on the relationship of modernity and international security, utilising a political theory approach. Its main argument is that the international security can be strengthened by further developing the project of modernity. Therefore, it suggests a Habermasian liberal-social synthesis form for global governance, where the idealist International Relations theory is at the heart of the model. To this end, it first analyses the modern nation-state experience as its political institutions has been highly successful in providing security (and also attaining legitimacy) by means of such an understanding; albeit at the national level. Subsequently, it examines the feasibility of a global governance model for the lands and the seas of the world, which follows the footsteps of the nation-states.

Keywords: International and Maritime Security, Political Theory, International Relations, Modernity, Enlightenment.

INTRODUCTION

Historically, the nation-states have been the most successful political constructs that managed to get the masses' consent for the decisions of the central government

[1] Assistant Professor Doctor, Istanbul Technical University Maritime Faculty, lkirval@itu.edu.tr, Tel. +905322068995, Fax. +902163954500, ITU-Maritime Faculty Tuzla, 34940 Istanbul, Turkey.

structures. The nation-states made use of various tools for reaching this goal. Controlling of the education system and taxation, as well as their service providing character has been crucial in their quest for legitimacy. Elites and intelligentsia were also influential in pushing the societies towards convergence within the boundaries of national identities. Yet, besides being a product of modernity and industrialisation, the nation-state has also been an arena of democratisation. Liberty and equality ideas flourished with the French Revolution. Instead of being classified as 'subjects' who have obligations to the monarch, the individuals living within the borders of the nation-states were defined as citizens having basic political and social rights. On the whole, the rights have taken place of the obligations and this has also been crucial in getting the consent of the individuals for the newly developing political model.

Following the demise of the Empires, the newly flourishing model had to include the participation dimension to the decision making mechanisms. Furthermore, its service providing character and developing social policies helped it to attain higher levels of legitimacy. This increasing support of the masses has also been crucial for the development of the security providing character of the model, albeit functioning at the national level.

And today, modernity and the nation-state experiences can still be a guiding light for the policy makers trying to foster security (both inland and maritime security) at the international level. In this context, the following pages will analyse the nation-state experience and the philosophical discussions that accompanied it in the past. Subsequently, the feasibility of an international model which provides inland and maritime security, inspired by these historical experiences, will be commented upon.

MODERNITY AND THE NATION-STATE EXPERIENCE AS AN INSPIRATION FOR INTERNATIONAL INLAND AND MARITIME SECURITY

To fully understand the political experiences of the nation-states, one should focus on the history of the European continent; their geographical and philosophical birthplace.

For centuries the Monarchs have been the most powerful actors in Europe. Yet, the political authority of the monarchs started to be severely questioned with the development of the bourgeoisie. Bourgeoisie, as a financially powerful new class, was capable of fighting against the existing monarchies and especially with a view to create a freer market. To a great extent, an interconnected system started to flourish in Western Europe following the Peace of Westphalia. One can find the first signs of the institutionalisation of the state structures during those years. Institutionalisation of the taxation system, improvement of the transportation routes and infrastructure of the cities, advancements in maritime transportation and increasing levels of communication between the regions of Europe were the first signs of the upcoming centralised state model (Bendix, 1978).

Secularisation and Reformation were also crucial in the development of a critical understanding against the rigid and powerful institutions, most important one being the Church. At the political level, this same questioning started to develop against the kings and lords. As a result, a well institutionalised and participatory state structure started to become an alternative for the majority of the people (Anderson, 1991). Hereditary rulers, metaphysics and God started to be replaced by the secular institutions of state. However, it is difficult to argue that these institutions were considered as legitimate bodies at start. People still had a feeling of belongingness to their local communities and their kings/lords. The national identity would gradually flourish by the backing of the newly emerging state institutions and the service providing character of the model.

The contractual relationship between the King and peasant during the middle ages was not an even one. Peasant had generally a minimal say in his/her relationship with the ruler. Hence, in his/her actions, the ruler did not necessarily take into account whether he/she was regarded as legitimate by the masses. Obviously, the fear from revolts pushed the rulers to take into account the wishes of their subjects; however, this was only creating a minimal responsibility towards the society. On the contrary, the social contract tradition of the subsequent nation-states included democratic participation, and providing of services to the individuals, which were crucial for their legitimization (Hobsbawm, 1992).

One can easily say that, the era between 1600 and 1800 was a period of social, intellectual and cultural transformation for most of the European countries. Whereas the Medieval thinkers assumed that the past knowledge was the most reliable source of wisdom, the greatest thinkers from the seventeenth century onwards rejected the ancient authorities and resolved to rely on their own minds. Eventually, "Have courage to use your own reasoning!" (or Dare to know! - Sapere aude!) became the main motto of the thinkers of the time (Reiss, 1991: 58) who stressed the autonomy of science and the free play of the critical mind.

A new flourishing publishing industry on the other hand helped Europe to diffuse the newly acquired knowledge to all the segments of the society. For the first time reading was available to a wider audience. Books, newspapers and journals could be easily found in the coffee houses and lending libraries. Also, intellectual debates started to take place in the salons of the developing bourgeoisie. Increasing of the trade and the capital accumulation has been crucial in the growth of this class. This wealthy tradesman and merchant class demanded a share of the social and political power that was formally held only by the nobility. Bourgeoisie was also influential in mobilizing the lower segments of the society and would also ignite the following French Revolution.

In time, the debates of the salons have moved to the streets of the cities and this has been crucial in the development of a more demanding and open-society in Europe. Today's parliamentary democracies and civil society monitored political

structures have developed as a result of this historical background. The existing "social contract" tradition of Europe, coming from as early as the feudal times, also helped the development of new political models that brought the individual rights and freedoms to the centre, and reformulated the existing social contracts.

Besides these historical developments in Europe, the philosophical discussions in the continent have also been crucial in the advancement of modernity. Firstly, there have been discussions on the foundations of the individuals' rights. Thinkers like Jean Jacques Rousseau believed that the individuals have basic rights from birth. However, in a society, they were sacrificing some of these in return for political rights. On the contrary, theorists like Durkheim argued that the individuals' rights are solely a result of the society. Hence, Durkheim did not agree with the view that the individuals have basic rights from birth; for him, society was the main element that produced these rights (West, 1998). However, both of these two dimensions of liberalism still agreed on the importance of the basic individual rights for all the political regimes. Whether, coming from birth or flourishing in a society, these rights are considered as extremely important for further freedom of the individuals.

Moreover, the philosophers have also discussed the ways of attaining these rights. Here, a critical human mind was generally given as a main precondition. However, in reaching to this critical attitude which would take individuals to freedom, the philosophers had mainly two diverging opinions. The first camp of scholars that searched for freedom focused on the elimination of the boundaries on the ideas. On the other hand, the second camp of scholars underlined the existing exploitation in the material world as the main reason of the human imprisonment. These two philosophical dimensions have been crucial in the advancement of the political and social rights in the newly developing European political structures; the most important one being the nation-state.

Although the discussions on the freedom of thought is as old as the philosophical inquiry itself, Immanuel Kant can be taken as one of the most important names in this tradition. His underlining of the critical mind and the explanation of the political life as the free arena of conflicting views gives us a chance to reach freedom by discussion. Kant also underlined the importance of the political mechanisms and the legal framework for the healthy functioning of this dialogue model (Guyer, 1992: 1-26). Kant argued that the reason is the means by which the phenomena of experience are translated into understanding and this also marked the beginnings of idealism.

Instead of assuming that our ideas, to be true, must conform to an external reality independent of our knowing, Kant proposed that objective reality is known only insofar as it conforms to the essential structure of the knowing mind. He maintained that objects of experience—phenomena—may be known, but that things lying beyond the realm of possible experience—noumena, or things-in-themselves—are unknowable, although their existence is a necessary presupposition. For Kant, the individuals should have a critical attitude towards all the given truths in the phe-

nomenal world. To this end, Kant suggests the creation of civil and just constitution that permits the different views to take part in the political sphere. However, for him, the human mind is incapable of analyzing the noumena and that's why he does not extent his critical attitude in this realm; instead he offers morals in this dimension, which he considers as crucial for the societal harmony (Keane, 48).

Following Kant's idealism, Hegel also tried to offer a freedom model based on freedom of thought. As another important name in this tradition Hegel suggested a dialectical method where the individual reaches a synthesis by the evaluation of the thesis and the anti-thesis (Miller, 1989). Therefore, Hegel claimed that "the real is the rational and the rational is real". For Hegel human history was the progression from bondage to freedom. Freedom is achieved as the desires of the individual are integrated into the unified system of the state, in which the will of one is replaced by the will of all. This theory is shown in his division of history into three stages, the first of which is in the ancient orient where only the ruler was free, the second in Greece and Rome where some were free, and modern world where all are considered free (Urmson, 1992).

In his 'Philosophy of Right', Hegel opposes the human logic which bases itself on principle of 'non-contradiction'. For Hegel, human mind is set to seek one sort of truth and when it finds that truth it opposes other alternatives. This intrinsic principle of non-contradiction is the main problem of human mind according to Hegel. Instead, he offers a new model in which the reality is regarded as the combination of the subject and its negation. Hence, the reality is the amalgamation of the contradictions and the synthesis of the thesis and the anti-thesis, which Hegel briefly calls as the 'dialectic method'. For Hegel, this whole dialectic process will be over when all the individuals can grasp this type of an understanding and demolish the principle of non-contradiction in their minds. Hegel argues that at this specific moment the 'Geist', an all encompassing spiritual body, will emerge and all the individuals will be a part of this final reality (which can also be taken as the God or the Absolute Idea).

In this whole process, Hegel underlines the importance of three core stages; the Family, the Civil Society and the State. The Family stage is characterised by relationships of love and affection existing among members of the family unit; this is an entity in which all members are freely associated under communal norms-it is a cohesive unit. The family unit generates its own negation in a component called Civil Society. This is characterised by a more intense individualism and competition than the family unit; brother begins to compete with brother, largely in economic realm. The cohesiveness and unity of the Family are lost and replaced by the particular wills of individuals in competition for self-development. These two stages are than mediated by the institution of the State, which takes the unity and general will aspect of the Family and combines it with the best of the Civil Society, that is, the individual appropriation of the environment. We thus have a society that united both particular and general will, the individual and the society, humans with their fellow humans. In concluding his model with the institutionalisation of the State,

Hegel argues that the State would be a neutral agent that would express only the general will of the entire state and hence would be the personification of the will of all the members of the community (Ingersoll, 2001:120).

Considering the state as the final synthesis stage before reaching the 'Geist', 'God' or 'Absolute Idea', Hegel justifies the state control on individuals. Hence, although the individuals are expected to have free minds, the state's authority on society is praised as it is considered as a neutral and mediating agent.

However, one main problem of the 'liberal' thinkers, whose ideas are summarised above, has been their belief in all encompassing morals and ethics, and their never-ending wish to achieve/offer universal explanations. Only a brave soul finally questioned this moral and universal dimension of modernity and this was Friedrich Nietzsche. Nietzsche refused any rational explanation that sought universalism. For Nietzsche, reason was nothing else than power, than will to power, which it so radiantly conceals (Habermas, 1984: 56).

Nietzsche argued that all the political and philosophical suggestions (no matter what their content is) would be limited by the physical desires of the one suggesting the model. Hence, for Nietzsche, the freedom discussions can in fact never be free because of the selfishness of the human mind. That's why; Nietzsche regarded all types of thinking as destined towards the empowerment of the self. As all the ideas were products of the self he also refused the existence of morals and even God. Ideas were always secondary, prior to them; there was always the survival instinct. For this reason, Nietzsche questioned the possibility of a neutral idea and the idealism of all the prior thinkers. He refused all the prior universalistic arguments and accepted the human mind as the cage of the individuals.

However, a problem also existed in Nietzsche's thinking; at the end of the day, his thinking was also limited with his own mind. Indeed, he was aware of this problem, and that's why he said; "All generalisations, including this one, are wrong." and "There are no facts, only interpretations." Yet, following the same logic, one can even say that even these last arguments are the products of a limited mind. Therefore, as the most liberating and emancipating philosopher Nietzsche had to develop the Ubermensch (Superman) concept.

Superman, according to Nietzsche, is a person who reached to a state of being where he is no longer affected by the pity, suffering, tolerance of the weak, the power of the soul over the body, the belief in an afterlife, and the corruption of the modern values. Superman is constantly changing and in a state of rebirth and growth. He determines what is good and what is evil, and does not allow morals/religion/ethics or society to intervene. He uses a reason that is independent of the modern values of society or religion. He determines his own values. Creation of his own values gives him joy, and in order for the Superman to cope with a changing world, the Superman must constantly change. This constant state of change is a constant source of joy, leaving little or no room for suffering. The Superman does not believe in an afterlife or the power of the soul

over the body. Therefore, he makes the most out of this life, not depending on a reward in Heaven or a punishment in Hell for what he has done on Earth (Nietzsche, 1999).

Yet, as Jürgen Habermas argues, in criticising the existent rationalism of modernity, Nietzsche again used the rational model itself and this shows us the elasticity of the modernity in transforming itself. In fact, instead of demolishing the modernity as a project, what Nietzsche did was to try to enlarge its limits to possible extremes. Nietzsche's revolt against the limits of rationalism was surely crucial in extending the limits of the human freedom.

Historically, the nation-state has evolved as a neutral entity providing the rule of law for all the possible and even conflicting discussions of freedom, inclusive towards even the most radical forms of it. Theoretically, the nation-states (and related political institutions of modernity) have been considered as the protectors of freedom of thought, even capable of fulfilling the radical wishes of Friedrich Nietzsche.

Yet, as the nation-states are constructed by means of a clear national identity, they have also been limited in including the 'other'. However, this does not and should not mean that the project of the enlightenment should halt, and it's most important institution the nation-state should be replaced. Indeed today, a transformation can take place at the international level, only by making use of the nation-state experiences (Habermas, 1984). As Habermas argues, the individuals can develop feeling of belongingness to this supra-national political model (or demos as he calls it) due to its legal framework that is permitting all types of ideologies and identities existent in the political life.

Here, the citizenship is defined by the human rights, irrespective of the identities or the political views of the individuals. Surely, even this model will be a result of a limited thinking process, however, it will be able to transform in line with the ideas of its members towards more inclusiveness. As the development of such an understanding would decrease the othering effects of the national identities, it may also lead to internationalism. Besides leading to international inland security, such an understanding may also foster further cooperation between the navy men and merchant mariners sailing in the seven seas of the world. The 'others' of this new formulation will not be different ethnic, cultural or religious (or other) identities, but the political models that do not permit the inclusion of such differences to the political life. However, for the long-run success this model, it will have to be supported by strong social policies, and a welfare regime. Here, one should focus the second camp of philosophical freedom discussions.

GRADUAL DEVELOPMENT OF THE LIBERAL SOCIAL SYNTHESIS: THE 'GREAT TRANSFORMATION' OF THE NATION-STATE MODEL

The second camp of freedom seekers has shifted their focus on the problems of the material world and the clashes between the classes. Unquestionably, Karl Marx was the real revolutionary here as he took the freedom discussion from the world of ideas to the material world. With his well known sentence, "The philosophers have only

interpreted the world in different ways; the point is to change it" (Marx, 1854), Marx underlined the importance of making changes in the material world to reach freedom. For him, even Friedrich Nietzsche's acceptance of the mind as the absolute limit of the universe was not enough. For him, the real freedom could only be achieved with the transformation of the existent material world. Here, the material world was even defining the thinking dimension. Hence, without the solution of the problems at this level, no one could be really free, even though the mind was accepted as their sole guide. For him, there can be no real choice in a matter driven world.

The influence socialist theories on the European continent has been tremendous. At the outset, the struggle for welfare state policies has mostly taken place in the European continent due to the already existent strong trade unions. The middle and working classes were negatively affected by the industrialisation in the continent, and they grew both in numbers and social influence, as did the urban areas in which they worked and lived. The industrialisation was characterised by unique economic growth, the factory system of production and the use of new, artificially powered machines for transportation and mechanical operations. For the first time, human beings had the ability to produce far more than what was needed to sustain a large percentage of the population. However, it was the factory owners that were getting the most of this wealth. Working class bore the burdens of the industrialisation and urban social problems such as low wages, overcrowded cities, poor medical care, insufficient social services, and a host of related problems. Therefore, the working classes started to organise and get united for their rights. Karl Marx's ideas have been crucial in the development of this solidarity. Individuals started to understand the interdependence of men on each other and the negative effects of the uncontrolled capitalism.

However, the European social model has developed in a different way compared with the other parts of the world. In time, European socialists started to have a coalition with the supporters of the market and the democracy. For example, English Fabians' socialism during the 19th century has combined the market and socialism with a view to reach at higher economic development levels for all the society. Instead of following totally individual centric policies, they underlined the importance of society and tried to transform the market model in such a way that it functions for the benefit of all. Therefore, they did not foresee a doomsday for capitalism like the Orthodox Marxists. One can also see a similar trend in the development of the German social democratic alternative. Here, Eduard Bernstein was an important name. Instead of a capitalism that destructs itself due to its inherent inconsistencies, Bernstein suggested a capitalist model that aims to develop societal welfare by means of an organised public (Koray, 2002: 78). These revisionist socialists tried to develop a healthier market model instead of demolishing it. The term of the 'Revision' started to take place of the 'Revolution' for them (Lee and Raban, 1988: 12-33)

Following the Great Depression of 1929, the development of the Keynesian policies that underlined the importance of the state institutions for healthy functioning of

the market was also a result of these new arguments. The development of the social democratic policies in the 1970s (called as the Third Way), which tried to merge the market model and the welfare state policies, have also moved on this type of an understanding. Especially, the Labour Party in England and the German Social Democrats have been supportive of this model in the last decades. In time, the trade unions have also started to act parallel to these ideological transformations. Trade unions have been supportive of the revolution during the early years of tensions with the capital owners. Gradually, they started to fight for the improvement of their working conditions and reformation of the production cycles. Hence, instead of criticising the system, the trade unions started to fight for getting a better share from it (McCarthy, 1972: 128).

As a result of all these developments, the European continent started to experience a liberal-social synthesis. In this model, the capitalists' rights in the market have been guaranteed but in return they have accepted the role of the state to plan and govern for the societal welfare, which also included an intervention to the distribution model. On the other hand, the working classes had to accept the capital accumulation; however, they have been given some basic political/social citizenship rights to have a say in the distribution of the wealth (Przeworski, 1991: 11). In this model, the negative outcomes of the pure market forces are corrected by the governments and these corrections are decided upon by the democratic participation of the individuals (Dahl, 1992).

Therefore, the European experience showed that, besides a radical democratic outlook that is established by critical mind, all the political models also necessitate social and welfare policies for providing the basic mechanisms to the individuals in their freedom expedition. At the end of the day, the main questions and demands of the mankind did not change for centuries. Democratic participation and the solution of the problems arising from the material inequality have always been the major wishes of the masses and the policy goals of the modern political regimes. Similarly, for inland and maritime international security, any international political authority will have to take into account these two main wishes of the individuals. Policies that fulfil these wishes at the international level will be crucial for attaining international inland and maritime security. The increasing living standards and the social protection of the workers both on land and on seas will lead to the fostering of global security.

GENERAL CONCLUSIONS

This paper underlined modernity and the nation-state experience as a major inspiration for supranational/international level governance, having the greatest potential to provide inland and maritime international security. In doing so, it analysed the historical nation-state experience, which broadly institutionalised the liberal-social synthesis model, and provided security and attained legitimacy, albeit at the national level.

Similarly today, as a result of globalisation, a redefinition of politics by means of

a liberal-social synthesis is necessary, but this time this necessity arises at the international level. As Immanuel Wallerstein argued decades ago, if the global politics are left to the hands of the pure market forces today, it will gradually demolish the nationalised powers (whether democratic or not) and thus lead to the Hegemony of a certain group of countries.

Following the 'Great Depression' nation-states has been successful in this endeavour, which is tactfully analysed by Karl Polanyi in his 'Great Transformation'. In Zygmund Bauman's words; 'The project of freedom from fear pursued through the social state was perhaps the boldest endeavour ever consciously undertaken by humanity, along with the resolve it gathered to see it through' (Bauman, 2004: 33).

Today, 'there are valid reasons to suppose that on a globalised planet, where the plight of everyone everywhere determines and is determined by the plights of the others, one can no longer have freedom and democracy in one country, or only in a few select countries, on in international seas. The fate of freedom and democracy decided and settled on the global scale – and only at that stage it can be defended with a realistic chance of lasting success'. What is necessary is then, quoting Habermas again, 'the development of global 'politics' that can catch up with global 'markets'.

Therefore, welfare and social policies are of utmost importance for a secure world. Besides being successful in the democracy-inclusiveness dimension, an international governance model has to also provide social services to the individuals.

Therefore today, the individuals have to further strengthen the welfare state that they once managed to create, which Karl Polanyi once called as the 'Great Transformation'. What is necessary is then global economic governance that helps controlling the destructive forces of global capitalism.

Therefore, for international inland and maritime security, this paper suggests the grasping of the Enlightenment tradition of modernity and its perpetual peace at the international level, which was once tactfully depicted by Immanuel Kant. As Jurgen Habermas observed in one of his recent analyses;

"A nation-state is not going to regains its old strength by retreating into its shell… A politics of self-liquidation (letting the state simply merge into post-national networks) is just as unconvincing. And postmodern neo-liberalism cannot explain how the deficits in steering competences and legitimation that emerge at the national level can be compensated at the supranational level without new forms of political regulation… The artificial conditions in which national consciousness arose argue against the defeatist assumption that a form of civic solidarity among strangers can only be generated within the confines of the nation. If this form of collective identity was due to a highly abstractive leap from the local and dynastic to national and then to democratic consciousness, why shouldn't this learning process be able to continue?" (Habermas, 2001: 81).

Following Habermas, this paper argues that the continuation of this learning process will lead to the development of a global political model; functioning by

means of a political system that is based on communication, democracy, distributive justice and a welfare model; thus, also providing international security on the lands and the seas of the world.

REFERENCES

Anderson, B. (1991) *Imagined Communities: Reflections on the Origin and Spread of Nationalism*, London: Verso.

Bauman, Z. (2004) *Europe: An Unfinished Adventure*, Cambridge: Polity Press.

Bendix, R. (1978) *Kings or People: Power and the Mandate to Rule*, Berkeley: University of California Press.

Dahl, R. A. W (1992) 'Why Free Markets Are Not Enough', *Journal of Democracy*, Volume 3, No 3.

Guyer, P. (Ed.) (1992) *The Cambridge Companion to Kant*, Cambridge: Cambridge University Press.

Habermas, J. (1984) *Theory of Communicative Action*, Boston: Beacon Press.

Habermas, J. (1984) *The Philosophical Discourse of Modernity*, Cambridge: Polity Press.

Habermas, J. (2001) *The Post-National Constellation: Political Essays*, Massachusetts: MIT Press.

Hobsbawm, E. J. (1992) *Nations and Nationalism since 1780: Programme, Myth, Reality*, Cambridge: Cambridge University Press.

Ingersoll, D. E., Matthews, R. K. and Davison, A. (Eds.) (2001) *The Philosophic Roots of Modern Ideology,* New Jersey: Prentice Hall.

Keane, J. (1998) *Civil Society and the State: New European Perspectives,* London: Verso.

Koray, M. (2002) *European Social Model,* Istanbul: TUSES Publications.

Lee, P. and Raban, C. (1988) *Welfare Theory and Social Policy*, London: Sage.

Marx, K. (1854) *Thesis on Feuerbach.*

McCarthy, W. E. J (1972) *Trade Unions*, London: Penguin Books.

Miller, A. V. (1989) *Hegel's Science of Logic*, New York: Prometheus Books.

Nietzsche, F. (1999) *Thus Spoke Zarahustra,* London: Dover Publications.

Przeworski, A. (1991) *Capitalism and Social Democracy*, Cambridge: Cambridge University Press.

Reiss, H. S. (Ed.) (1991) *Kant: Political Writings*, Cambridge: Cambridge University Press.

Urmson, J.O. and Ree, J. (1992) *The Concise Encyclopaedia of Western Philosophy and Philosophers*, London: Routledge.

West, D. (1998) *An Introduction to Continental Philosophy*, Cambridge: Polity Press.

SEGURIDAD INTERNACIONAL CON MODERNIDAD ADICIONAL: UN ACERCAMIENTO TEÓRICO A LA SEGURIDAD INTERIOR Y MARÍTIMA

Por considerar, los actos de levantamiento del terrorismo internacional, de la piratería y del terror en los mares internacionales; este artículo se centra en la relación de la modernidad y de la seguridad internacional, utilizando un acercamiento de la teoría política. Su discusión principal es que la seguridad internacional puede ser consolidada más lejos desarrollando el proyecto de la modernidad. Por lo tanto, sugiere una forma liberal-social de la síntesis de Habermasian para el gobierno global, donde está la teoría de relaciones internacionales idealista en el corazón del modelo. Con este fin, primero analiza la experiencia moderna de la nación estado como sus instituciones políticas han estado altamente - acertada en el abastecimiento de seguridad (y también lograr legitimidad) por medio de tal comprensión; no obstante en el nivel nacional. Posteriormente, examina la viabilidad de un modelo global del gobierno para las tierras y los mares del mundo, que sigue los pasos de las naciones Estado.

JMR

Journal of Maritime Research, Vol. VII. No. 2, pp. 49-62, 2010

ISSN: 1697-4840

ANALYSIS OF THE TURNING CIRCLE MANOEUVRE FROM THE POINT OF VIEW OF AN EFFICIENT MANAGING OF THE MAIN ENGINE

I. Basterretxea[1,2], J. Vila[1,3], I. Lorono[1,4] and L. Martin[1,5]

Received 27 January 2010; in revised form 08 February 2010; accepted 23 June 2010

Abstract

The purpose of this paper is to study the influence of the 360 deg turn in the economy of the voyage and to find out the maximum efficiency by means of the main engine's procedure. Moreover the additional cost of the turning circle manoeuvre out of the whole of sea passage is also studied. The simulation is carried out on two types of vessels: a SUEZMAX of 150,000 dwt and an AFRAMAX of 100,000 dwt.

Keywords: Turning circle manoeuvre (turn of 360 deg). Consumption/speed relationship. Economic speed. Optimum speed. Costs: Percentage of turning circle manoeuvre out of the whole sea passage.

INTRODUCTION

One of the more costly encounter avoidance manoeuvre concerning the economy of the vessel is the turn of 360 deg. This manoeuvre may be carried out when our vessel is to be kept far away from the other vessel or when the other vessel does not steer according to the COLREG and hence force our vessel to alter her heading to starboard up to a complete a turn of 360 deg.

The research intends to find the more economical speed of approach so that the consumption of petrol during the turn of 360 deg be minimum. Moreover the optimum speed of approach to reduce the total cost (consumption of petrol and hire) to a

[1] University of the Basque Country, Maria Diaz De Haro, 68 48920 Portugalete, Espana. [2] Professor, imanol.basterrechea@ehu.es, Tel. 626576323, Fax. 946017700. [3] Professor, jesusangel.vila@ehu.es, Tel. 946014859, Fax. 946017700. [4] Professor, inaki.lorono@ehu.es, Tel. 946012000, Fax. 946017700. [5] Professor, leopoldo.martin@ehu.es, Tel. 946012000, Fax. 946017700.

minimum is calculated. The curves and data representing the economic and optimum speed of approach are calculated by means of interpolation methods (spline and least squares) starting from the real data of the ship sea trials and engine shop trials (Evanas, 1990).

The time spent in tracking the turning circle will depend on the speed of approach, the loading condition or draft, the under keel water, wind, currents and other factors (Clark, 2005). However this research is not to take into account all these parameters. In this way the only variable used in the mathematical calculation is the speed of approach and the vessels are considered in full load condition.

SUEZMAX	AFRAMAX
Type of ship: Tanker	Type of ship: Tanker
150.000 dwt	100.000 dwt
Loaded condition	Loaded condition
Lenght: 274.2 M.	Lenght (O.A.): 246.8 M
Breadth (MLD.): 48.0 M.	Breadth (MLD.): 42.0 M

At the end of this paper a calculation is carried out with regard to the percentage of fuel consumed during the turning circle manoeuvre out of the total fuel consumed during a particular sea passage. In addition the percentage of the turning circle manoeuvre out of the whole sea-passage in respect of fuel consumption and costs will be determined.

TURNING CIRCLE

During the sea trials and especially in the manoeuvring tests, the ship performance is considered with the rudder is deflected and held at a fixed maximum angle, both to starboard and port side. Then it starts a path called turning circle which is divided into three distinct phases (SNAME, 1990):

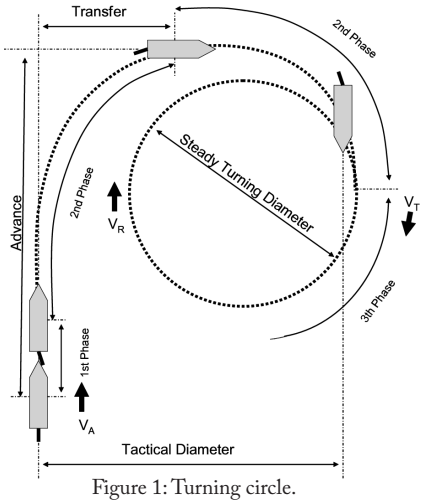

Figure 1: Turning circle.

First phase: Taking into consideration that the vessel is advancing on a straight track, this phase starts when the rudder begins to deflect and is to finish when it has reached a fixed angle (usually the maximum angle). In this any other angle smaller than maximum is not considered since it would be uneconomical according to.

Second phase: During this phase the deflection of the rudder remains unalterable and the forces and resistances affecting the wet surface make the vessel fall to the same side than the deflection of the rudder. The

vessel is also undergoing a progressive loss of velocity. Further the diameter of the turning circle is decreasing.

Third phase: The dynamic equilibrium of turning forces and resistances affecting the vessel is reached. The speed is reduced to around 1/3 of the speed of approach and is kept unalterable from the time worth. The vessel keeps turning in a circle with a steady diameter.

In addition to the different phases, the following information concerning the turning circle should be taken into account:

Advance: It is the distance in the prolongation of original path that vessel moves to alter the heading 90 deg.

Transfer: It is the lateral distance that the vessel moves from the original path whilst tracking the turning circle. In figure 1 it is shown the transfer for altering the heading 90 deg.

Tactical diameter: It is the transfer to alter the heading 180 deg.

Steady turning diameter: After the establishment of the third phase, the ship settles down to a turn of constant diameter as outlined in fig. 1.

Velocity of approach (V_A): It is the speed of the vessel at the beginning of the first phase.

Velocity on steady turn (V_T): It is the speed reached in the third phase.

Speed remainder (V_R): It is the speed of the vessel at any stage of the turning circle. In this research the speed remainder will be the velocity of the ship once her heading is altered 360°.

Before analyzing the economy of the turning circle manoeuvre, it is necessary to know the time elapsed up to the heading alteration of 360° (it will be mentioned as 'manoeuvring time' in this paper). This time is obtained in the ship trials for a velocity of approach similar to the cruise speed. Figure 2 shows the time necessary for the Suezmax and Aframax vessels to alter the heading 90°, 180°, 270° and 360° at a velocity of approach equal to the cruise speed. Logically the Suezmax spent more

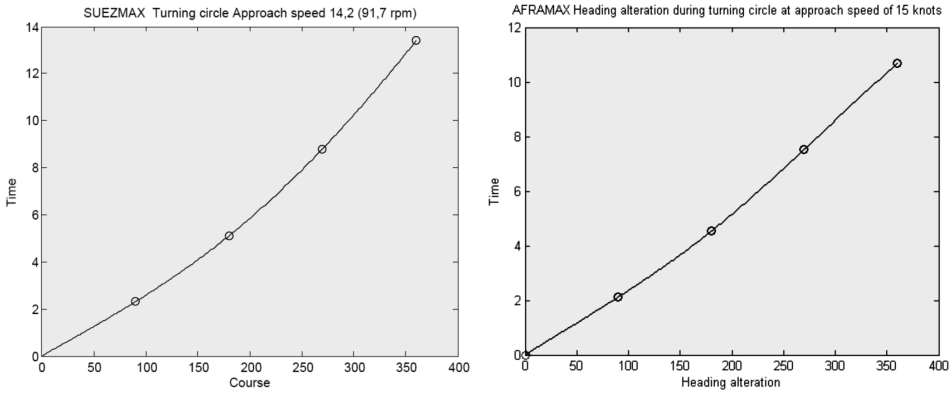

Figure 2: Heading alteration during the turning circle.

time than the Aframax due to the differences between the displacements. The research is carried out without taking into account additional effects such as shallow waters, wind, swell or current.

The following proximate formula is used to know the time elapsed up to the heading alteration of 360° (Crane, 1989):

$$t_B = t_A \cdot \left(\frac{L_B}{L_A} \cdot \frac{V_A}{V_B} \right) \tag{1}$$

Where:

V_A is speed of reference for vessel A
t_A is time spent in effecting the turning circle manoeuvre at velocity of approach of V_A
V_B is speed of reference for vessel B
t_B is time spent in effecting the turning circle manoeuvre at velocity of approach of V_B
L_A is lenght of A
L_B is lenght of B

$$t = t_A \cdot \left(\frac{V_A}{V} \right) \tag{2}$$

Where:

V_A is speed of reference for the vessel A (cruise speed)
t_A is time spent in effecting the turning circle manoeuvre at velocity of approach of V_A
V is any velocity of approach
t is time spent in effecting the turning circle manoeuvre at velocity of approach of V

Table 1 shows the results in the calculation of the manoeuvring time in minutes by means of the application of formulae (2):

Figure 3 shows the approximation of the formula (2) by comparison of the real time spent in altering the heading and the time obtained from the formula:

Velocity Of Approach (KNOTS)	1	2	3	4	5	6	7	8	9	10	11	12	13	14	15	16	17
Suezmax Manoeuvring Time (MIN)	181,5	90,8	60,5	45,4	36,3	30,3	25,9	22,7	20,2	18,1	16,5	15,1	14	13	12,1	11,3	10,7
Aframax Manoeuvring Time (MIN)	160,1	80	53,4	40	32	26,7	22,9	20	17,8	16	14,6	13,3	12,3	11,4	10,7	10,0	9,4

Table 1: Time spent during the turn of 360 deg at different velocity of approach.

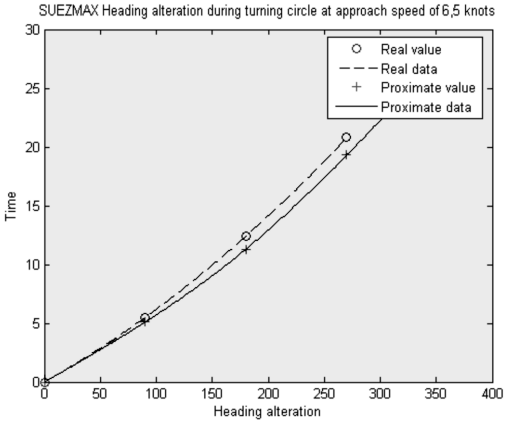

Figure 3: Comparison between real and proximate data of heading alteration during the turning circle.

OPTIMAL SPEED

The ship who sails at economic speed achieves the minimum consumption of petrol per unity of time.

The engine's shop trials provide us with real data on the specific consumption of petrol in gr/kw/h at different BHP. On the other hand, the necessary BHP to provide the vessel with a specific speed whilst sailing may be obtained from the ship's sea trials. Sometimes the speed trials may also show the consumption at different sailing speeds (Watson, 1998).

Hence the relationship between the speed and the consumption is obtained from the real results of engine's shop trials and ship's sea trials by means of interpolation systems as spline and least squares. Nevertheless, the consumption of the main engine is calculated for an output higher than 50% (around 12 knots of speed in the ships tested) and thus the values below this percentage lack the required scientific rigour. In figure 4 and table 2 the approximate results obtained under interpolation are shown.

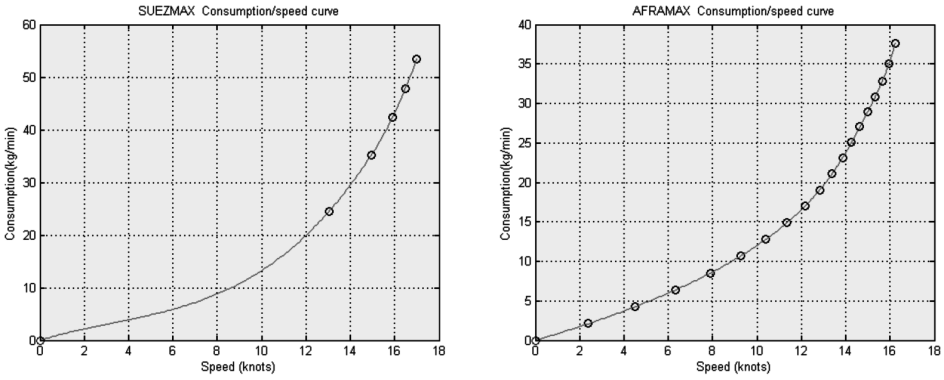

Figure 4: Curves of fuel consumption for vessels tested

Velocity Of Approach (KNOTS)	1	2	3	4	5	6	7	8	9	10	11	12	13	14	15	16	17
Suezmax Consumption (KG/MIN)	1,2	2,2	3	3,9	4,8	5,9	7,2	8,8	10,8	13,2	16,3	19,9	24,3	29,5	35,6	43,3	53,4
Aframax Consumption (KG/MIN)	0,85	1,7	2,7	3,7	4,8	6	7,2	8,6	10,2	12	14,1	16,5	19,6	23,8	29	35,5	49,6

Table 2: Fuel consumption at different speeds.

In figures 5 and 3 the kilos of petrol consumed during the turning circle performance at different speeds of approach are shown.

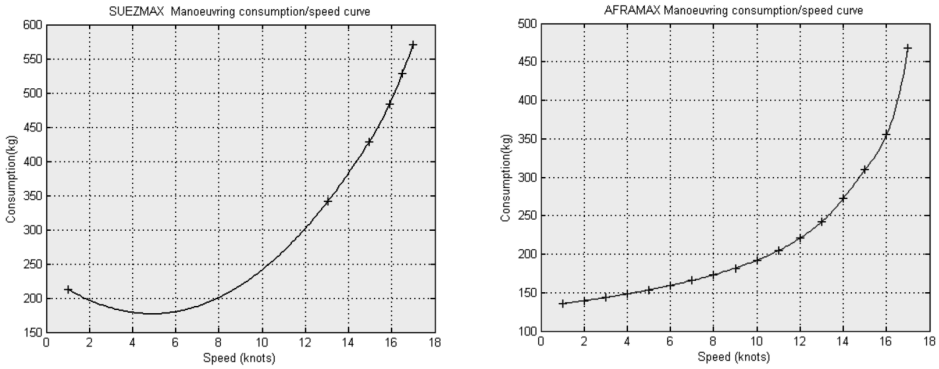

Figure 5: Fuel consumption during turning circle manoeuvre at different velocities of approach.

Speed Of Approach (KNOTS)	1	2	3	4	5	6	7	8	9	10	11	12	13	14	15	16	17
Suezmax Manoeuvring Consumption (KG)	213	196	184	177	175	178	186	199	217	240	269	302	340	383	431	491	570
Aframax Manoeuvring Consumption (KG)	135,8	139,5	143,7	148,3	153,5	159	166	173	182	192	205	221	242	272	310	355	468

Table 3: Fuel consumption during the turning circle manoeuvre at different velocities of approach.

OPTIMUM SPEED

In the computation of the optimum speed the hire of the ship in addition to the petrol consumed and its price is considered. Thus the ship sailing at optimum speed achieves the minimum cost in bunker and hire per time (Laurence, 1984).

The results of the simulation are shown in the following information:

— Graphics of cost, hire and speed of approach for the turning circle manoeuvre taking into account two different prices of fuel-oil (figure 6)

— Data of time and consumption of the turning circle manoeuvre as well as the cost at bunker price of 456 USD per metric tonne for three different daily hires. The estimated optimum speed is marked (tables 4 and 5)

— Graphics of cost, price of bunker and speed of approach for the turning circle manoeuvre taking into account two different hire (figure 7)

— Data of time and consumption of the turning circle manoeuvre as well as the cost at three different bunker prices for four different daily hires. It is marked the estimated optimum speed (tables from 6 to 9)

ZUEZMAX

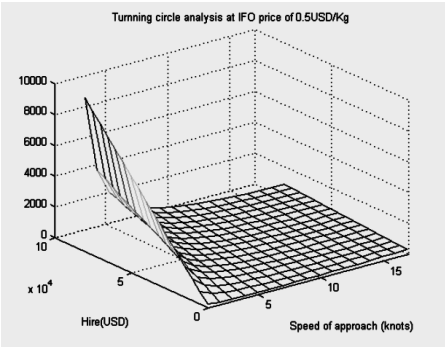

ZUEZMAX

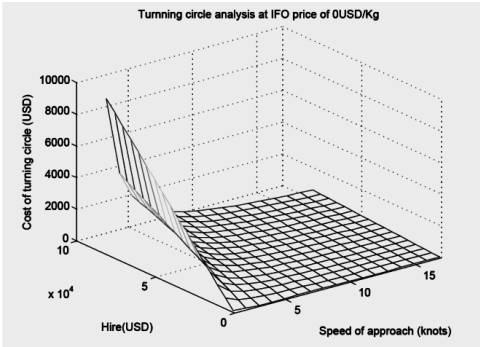

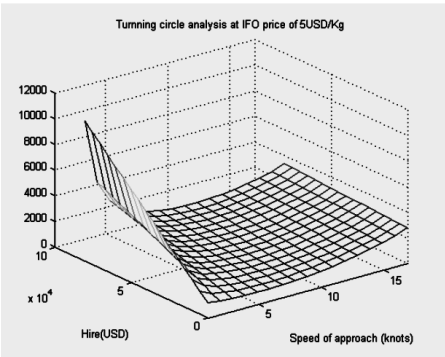

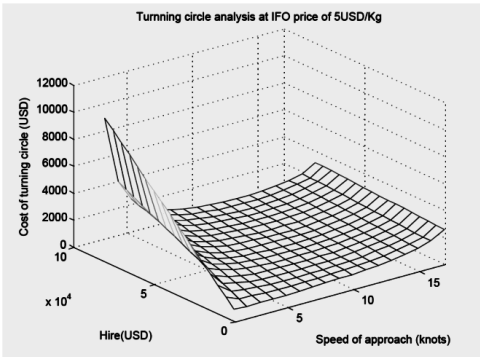

Figure 6: Manoeuvring cost depending on the speed of approach and hire.

Speed Of Approach (Knots)	Manoeuvring Time(Min)	Manoeuvring Consumption (Kg)	Manoeuvring Cost (Usd) Hire: 6,000 Usd	Manoeuvring Cost (Usd) Hire: 30,000 Usd	Manoeuvring Cost (Usd) Hire: 61,000 Usd
1	181,54	212,91	853,50	3879,17	7787,32
2	90,77	195,90	467,54	1980,37	3934,45
3	60,51	183,89	335,99	1344,55	2647,27
4	45,39	176,91	269,78	1026,19	2003,23
5	36,31	174,94	231,06	836,19	1617,82
6	30,26	177,99	207,23	711,51	1362,87
7	25,93	186,06	192,90	625,14	1183,45
8	22,69	199,15	185,36	563,57	1052,09
9	20,17	217,25	183,11	519,30	953,54
10	18,15	240,38	185,25	487,82	878,63
11	16,50	268,51	191,21	466,27	821,55
12	15,13	301,67	200,60	452,73	778,41
13	13,96	339,84	213,15	445,90	746,53
14	12,97	383,04	228,69	444,81	723,97
15	12,10	431,25	247,08	448,79	709,33
16	11,35	491,01	271,18	460,28	704,54
17	10,68	569,82	304,33	482,31	712,21

Table 4: Cost of turning circle manoeuvre for SUEZMAX at IFO price of 0.456 USD/kg.

Speed Of Approach (Knots)	Manoeuvring Time(Min)	Manoeuvring Consumption (Kg)	Manoeuvring Cost (Usd) Hire: 6,000 Usd	Manoeuvring Cost (Usd) Hire: 30,000 Usd	Manoeuvring Cost (Usd) Hire: 61,000 Usd
1	160,17	135,79	729,30	3398,80	6846,90
2	80,09	139,48	397,29	1732,04	3456,09
3	53,39	143,66	287,97	1177,80	2327,17
4	40,04	148,32	234,48	901,85	1763,88
5	32,03	153,47	203,46	737,36	1426,98
6	26,70	159,22	183,83	628,75	1203,44
7	22,88	165,71	170,90	552,26	1044,85
8	20,02	173,14	162,37	496,06	927,07
9	17,80	181,79	157,05	453,66	836,78
10	16,02	192,07	154,32	421,27	766,08
11	14,56	204,66	153,99	396,68	710,14
12	13,35	220,68	156,24	378,70	666,04
13	12,32	242,13	161,75	367,09	632,33
14	11,44	272,18	171,79	362,46	608,76
15	10,68	309,71	185,72	363,69	593,56
16	10,01	354,99	203,59	370,43	585,94
17	9,42	467,63	252,50	409,53	612,36

Table 5: Cost of turning circle manoeuvre for AFRAMAX at IFO price of 0.456 USD/kg.

ZUEZMAX

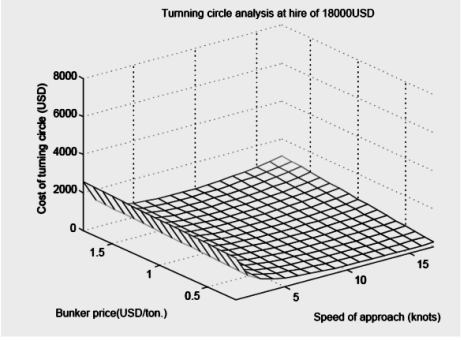

ZUEZMAX

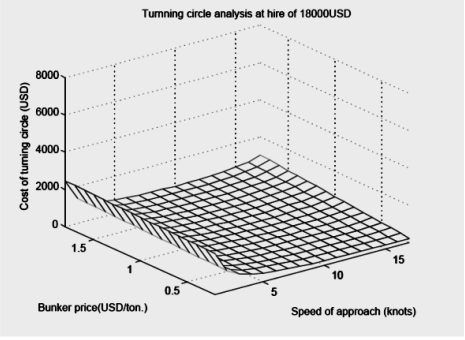

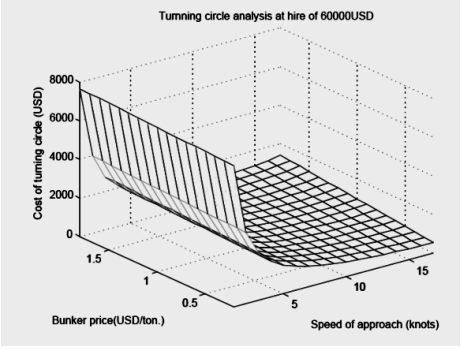

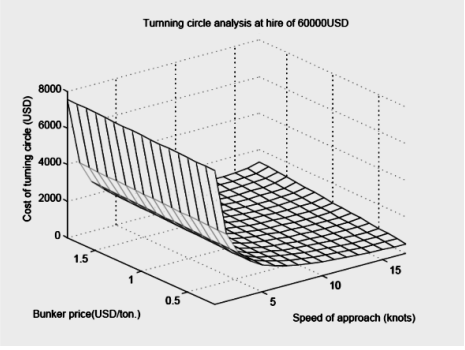

Figure 7: Manoeuvring cost depending on the speed of approach and bunker price.

Velocity Of Approach (Knots)	Manoeuvring Time(Min)	Manoeuvring Consumption (Kg)	Manoeuvring Cost (Usd) At Bunker Price Of 0,3 Usd/Kg	Manoeuvring Cost (Usd) At Bunker Price Of 0,5 Usd/Kg	Manoeuvring Cost (Usd) At Bunker Price Of 1 Usd/Kg
9	20,17	217,25	317,31	360,77	469,39
10	18,15	240,38	299,04	347,11	467,30
11	16,50	268,51	286,85	340,55	474,81
12	15,13	301,67	279,61	339,94	490,77
13	13,96	339,84	276,51	344,48	514,40
14	12,97	383,04	277,00	353,61	545,12
15	12,10	431,25	280,66	366,91	582,53
16	11,35	491,01	289,13	387,33	632,84
17	10,68	569,82	304,43	418,40	703,31

Table 6: Cost of turning circle manoeuvre for SUEZMAX at hire of 18,000 USD daily.

Velocity Of Approach (Knots)	Manoeuvring Time(Min)	Manoeuvring Consumption (Kg)	Manoeuvring Cost (Usd) At Bunker Price Of 0,3 Usd/Kg	Manoeuvring Cost (Usd) At Bunker Price Of 0,5 Usd/Kg	Manoeuvring Cost (Usd) At Bunker Price Of 1 Usd/Kg
12	15,13	301,67	720,85	781,18	932,02
13	13,96	339,84	683,81	751,78	921,70
14	12,97	383,04	655,21	731,82	923,33
15	12,10	431,25	633,65	719,90	935,52
16	11,35	491,01	620,06	718,27	963,77
17	10,68	569,82	615,90	729,86	1014,77

Table 7: Cost of turning circle manoeuvre for SUEZMAX at hire of 60,000 USD daily.

Velocity Of Approach (Knots)	Manoeuvring Time(Min)	Manoeuvring Consumption (Kg)	Manoeuvring Cost (Usd) At Bunker Price Of 0,3 Usd/Kg	Manoeuvring Cost (Usd) At Bunker Price Of 0,5 Usd/Kg	Manoeuvring Cost (Usd) At Bunker Price Of 1 Usd/Kg
12	13,35	220,68	233,05	277,18	387,52
13	12,32	242,13	226,65	275,07	396,14
14	11,44	272,18	224,66	279,10	415,19
15	10,68	309,71	226,39	288,33	443,19
16	10,01	354,99	231,63	302,63	480,12
17	9,42	467,63	258,06	351,59	585,40

Table 8: Cost of turning circle manoeuvre for AFRAMAX at hire of 18,000 USD daily.

Velocity Of Approach (Knots)	Manoeuvring Time(Min)	Manoeuvring Consumption (Kg)	Manoeuvring Cost (Usd) At Bunker Price Of 0,3 Usd/Kg	Manoeuvring Cost (Usd) At Bunker Price Of 0,5 Usd/Kg	Manoeuvring Cost (Usd) At Bunker Price Of 1 Usd/Kg
12	13,35	220,68	622,35	666,49	776,83
13	12,32	242,13	586,00	634,43	755,49
14	11,44	272,18	558,35	612,79	748,88
15	10,68	309,71	537,83	599,77	754,63
16	10,01	354,99	523,61	594,60	772,10
17	9,42	467,63	532,86	626,39	860,20

Table 9: Cost of turning circle manoeuvre for AFRAMAX at hire of 60,000 USD daily.

PREVIOUS DECELERATION AND SUBSEQUENT ACCELERATION

As shown in figure 8 the ship suffers a reduction of the speed from V_C to V_A in an interval of time T_D before the manoeuvre; a loss of speed from V_A to V_R during the manoeuvre and an increase of the speed from V_R to V_C after the manoeuvre. In the simulation the changes of velocity are instantaneous and the time during the deceleration (T_D) and the acceleration (T_A) is not considered.

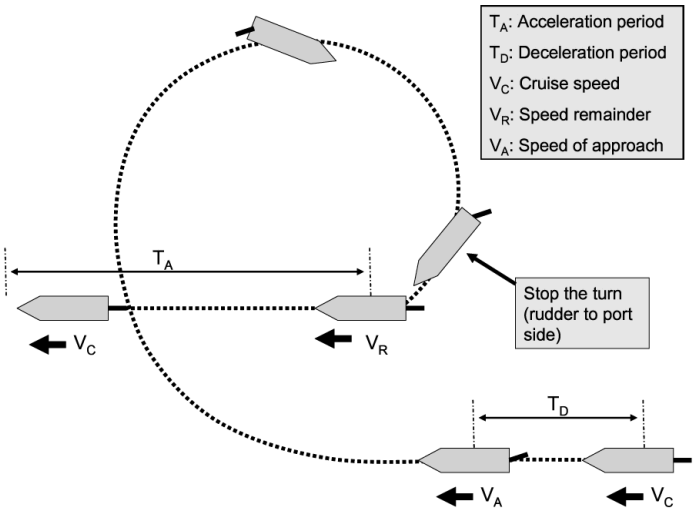

Figure 8: Details of deceleration and acceleration of the ship.

It would be predicted that the ship reaches the steady phase after the turn of 360 deg and, consequently, the speed remainder would be equal to the speed in the steady turn. This speed may be calculated by means of formulae related to the basic ship designs according to Lyster-Knights (Lyster, 1979).

PERCENTAGE OF TURNING CIRCLE MANOEUVRE OUT OF THE WHOLE SEA-PASSAGE WITH REGARD TO PETROL CONSUMPTION AND COSTS

Starting from formulae (1) and (2) a proximate way of calculating the percentage of petrol consumed during the turning circle manoeuvre out of the whole sea passage is obtained:

$$Percentage = 100 \cdot \frac{t_C \cdot V_C \cdot V_A}{60 \cdot D \cdot V_B} \cdot \frac{L}{L_C} \cdot \frac{C_B}{C_A} \tag{3}$$

$$Percentage = 100 \cdot \frac{t_A \cdot V_A^{\,2}}{60 \cdot D \cdot V_B} \cdot \frac{C_B}{C_A} \tag{4}$$

Where:

L is lenght in meters of analyzed ship
L_C is lenght in meters of ship C
t_C is time in minutes for the ship C to turn 360 deg at velocity of approach V_C.
V_B is velocity of approach in knots for analyzed ship
C_B is consumption in kg/min for analyzed ship at speed V_B
V_A is cruise speed in knots of analyzed ship
D is distance of sea passage in miles
C_A is consumption in kg/min for analyzed ship at cruise speed V_A

The results are obtained in formula (3) by using details of a ship other than the analyzed one.

Moreover the cost of turning circle manoeuvre out of the sea passage may be approximately calculated:

$$Percentage = 100 \cdot \frac{t_C \cdot V_C \cdot V_A}{60 \cdot D \cdot V_B} \cdot \frac{L}{L_C} \cdot \left(1 + \frac{C_B}{C_A}\right) \tag{5}$$

$$Percentage = 100 \cdot \frac{t_A \cdot V_A^{\,2}}{60 \cdot D \cdot V_B} \cdot \left(1 + \frac{C_B}{C_A}\right) \tag{6}$$

The following tables (tables 10 to 15) show the extra consumption and extra cost of the turning circle manoeuvre on the whole sea passage. The cost of passage is calculated for different hires, different velocities of approach and a fixed bunker price of 0,456 USD/kg.

Speed Of Approach (Knots)	Manoeuvring Time (Min)	Consumption (Kg/Min)	Fuel Cost (Usd/Kg)	Distance: 500 miles	Distance: 1000 miles	Distance: 2000 miles	Distance: 3000 miles	Distance: 4000 miles
				%	%	%	%	%
8	20,02	8,6478	0,4560	0,381753%	0,190877%	0,095438%	0,063626%	0,047719%
9	17,80	10,2146	0,4560	0,400817%	0,200408%	0,100204%	0,066803%	0,050102%
10	16,02	11,9915	0,4560	0,423488%	0,211744%	0,105872%	0,070581%	0,052936%
11	14,56	14,0553	0,4560	0,451247%	0,225624%	0,112812%	0,075208%	0,056406%
12	13,35	16,5334	0,4560	0,486573%	0,243287%	0,121643%	0,081096%	0,060822%
13	12,32	19,6521	0,4560	0,533867%	0,266933%	0,133467%	0,088978%	0,066733%
14	11,44	23,7908	0,4560	0,600134%	0,300067%	0,150033%	0,100022%	0,075017%
15	10,68	29,0049	0,4560	0,682885%	0,341442%	0,170721%	0,113814%	0,085361%
16	10,01	35,4613	0,4560	0,782712%	0,391356%	0,195678%	0,130452%	0,097839%
17	9,42	49,6331	0,4560	1,031074%	0,515537%	0,257768%	0,171846%	0,128884%

Table 10. AFRAMAX - Percentage of the consumption of turning circle manoeuvre on the total consumption of voyage at cruise speed of 13 knots.

Speed Of Ap. (Knots)	Manoeuvring Time (Min)	Consumption (Kg/Min)	Fuel Cost (Usd/Kg)	Hire (Usd)	Distance: 500 miles	Distance: 1000 miles	Distance: 2000 miles	Distance: 3000 miles	Distance: 4000 miles
					%	%	%	%	%
9	17,80	10,2146	0,456	18000	1,0585983%	0,5292991%	0,2646324%	0,1764254%	0,1323205%
10	16,02	11,9915	0,456	18000	0,9977308%	0,4988654%	0,2494165%	0,1662813%	0,1247123%
11	14,56	14,0553	0,456	18000	0,9545342%	0,4772671%	0,2386180%	0,1590821%	0,1193129%
12	13,35	16,5334	0,456	18000	0,9272790%	0,4636395%	0,2318047%	0,1545398%	0,1159061%
13	12,32	19,6521	0,456	18000	0,9166942%	0,4583471%	0,2291586%	0,1527757%	0,1145830%
14	11,44	23,7908	0,456	18000	0,9260694%	0,4630347%	0,2315023%	0,1543382%	0,1157549%
15	10,68	29,0049	0,456	18000	0,9523478%	0,4761739%	0,2380715%	0,1587178%	0,1190396%
16	10,01	35,4613	0,456	18000	0,9950014%	0,4975007%	0,2487342%	0,1658264%	0,1243711%
17	9,42	49,6331	0,456	18000	1,1475541%	0,5737770%	0,2868699%	0,1912507%	0,1434396%

Table 11. AFRAMAX -Percentage of the cost of turning circle manoeuvre on the total cost of voyage at cruise speed of 13 knots.

Speed Of Ap. (Knots)	Manoeuvring Time (Min)	Consumption (Kg/Min)	Fuel Cost (Usd/Kg)	Hire (Usd)	Distance: 500 miles	Distance: 1000 miles	Distance: 2000 miles	Distance: 3000 miles	Distance: 4000 miles
					%	%	%	%	%
9	17,80	10,2146	0,456	60000	0,8574333%	0,4287166%	0,2143444%	0,1428994%	0,1071757%
10	16,02	11,9915	0,456	60000	0,7851877%	0,3925938%	0,1962842%	0,1308589%	0,0981453%
11	14,56	14,0553	0,456	60000	0,7280588%	0,3640294%	0,1820029%	0,1213379%	0,0910044%
12	13,35	16,5334	0,456	60000	0,6830741%	0,3415370%	0,1707574%	0,1138407%	0,0853815%
13	12,32	19,6521	0,456	60000	0,6487532%	0,3243766%	0,1621778%	0,1081208%	0,0810915%
14	11,44	23,7908	0,456	60000	0,6248697%	0,3124348%	0,1562073%	0,1041404%	0,0781062%
15	10,68	29,0049	0,456	60000	0,6096166%	0,3048083%	0,1523943%	0,1015984%	0,0761996%
16	10,01	35,4613	0,456	60000	0,6021682%	0,3010841%	0,1505323%	0,1003570%	0,0752686%
17	9,42	49,6331	0,456	60000	0,6300712%	0,3150356%	0,1575076%	0,1050073%	0,0787563%

Table 12. AFRAMAX - Percentage of the cost of turning circle manoeuvre on the total cost of voyage at cruise speed of 13 knots.

Speed Of Ap. (Knots)	Manoeuvring Time (Min)	Consumption (Kg/Min)	Fuel Cost (Usd/Kg)	Distance: 500 miles	Distance: 1000 miles	Distance: 2000 miles	Distance: 3000 miles	Distance: 4000 miles
				%	%	%	%	%
9	20,17	10,7705	0,4560	0,386717%	0,19335 8%	0,096679%	0,064453%	0,048340%
10	18,15	13,2409	0,4560	0,427875%	0,213938%	0,106969%	0,071313%	0,053484%
11	16,50	16,2700	0,4560	0,477964%	0,238982%	0,119491%	0,079661%	0,059745%
12	15,13	19,9407	0,4560	0,536981%	0,268491%	0,134245%	0,089497%	0,067123%
13	13,96	24,3361	0,4560	0,604933%	0,302467%	0,151233%	0,100822%	0,075617%
14	12,97	29,5389	0,4560	0,681814%	0,340907%	0,170454%	0,113636%	0,085227%
15	12,10	35,6323	0,4560	0,767631%	0,383815%	0,191908%	0,127938%	0,095954%
16	11,35	43,2751	0,4560	0,874013%	0,437007%	0,218503%	0,145669%	0,109252%
17	10,68	53,3600	0,4560	1,014301%	0,554248%	0,253575%	0,169050%	0,126788%

Table 13. SUEZMAX - Percentage of the consumption of turning circle manoeuvre on the total consumption of voyage at cruise speed of 13 knots.

Speed Of Ap. (Knots)	Manoeuvring Time (Min)	Consumption (Kg/Min)	Fuel Cost (Usd/Kg)	Hire (Usd)	Distance: 500 miles	Distance: 1000 miles	Distance: 2000 miles	Distance: 3000 miles	Distance: 4000 miles
					%	%	%	%	%
9	20,17	10,7705	0,456	18000	1,2174966%	0,6087483%	0,3043544%	0,2029073%	0,1521821%
10	18,15	13,2409	0,456	18000	1,1664482%	0,5832241%	0,2915931%	0,1943996%	0,1458013%
11	16,50	16,2700	0,456	18000	1,1394192%	0,5697096%	0,2848363%	0,1898950%	0,1424228%
12	15,13	19,9407	0,456	18000	1,1326104%	0,5663052%	0,2831342%	0,1887602%	0,1415717%
13	13,96	24,3361	0,456	18000	1,1420273%	0,5710136%	0,2854883%	0,1903296%	0,1427488%
14	12,97	29,5389	0,456	18000	1,1677154%	0,5838577%	0,2919099%	0,1946108%	0,1459597%
15	12,10	35,6323	0,456	18000	1,2059448%	0,6029724%	0,3014666%	0,2009821%	0,1507382%
16	11,35	43,2751	0,456	18000	1,2683294%	0,6341647%	0,3170617%	0,2113791%	0,1585360%
17	10,68	53,3600	0,456	18000	1,3637284%	0,6818642%	0,3409100%	0,2272782%	0,1704605%

Table 14. SUEZMAX - percentage of the cost of turning circle manoeuvre on the total cost of voyage at cruise speed of 13 knots.

Speed Of Ap. (Knots)	Manoeuvring Time (Min)	Consumption (Kg/Min)	Fuel Cost (Usd/Kg)	Hire (Usd)	Distance: 500 miles	Distance: 1000 miles	Distance: 2000 miles	Distance: 3000 miles	Distance: 4000 miles
					%	%	%	%	%
9	20,17	10,7705	0,456	60000	0,9770968%	0,4885484%	0,2442583%	0,1628424%	0,1221331%
10	18,15	13,2409	0,456	60000	0,9005065%	0,4502532%	0,2251120%	0,1500779%	0,1125597%
11	16,50	16,2700	0,456	60000	0,8423458%	0,4211729%	0,2105728%	0,1403849%	0,1052898%
12	15,13	19,9407	0,456	60000	0,7987448%	0,3993724%	0,1996732%	0,1331184%	0,0998399%
13	13,96	24,3361	0,456	60000	0,7660785%	0,3830392%	0,1915072%	0,1276742%	0,0957567%
14	12,97	29,5389	0,456	60000	0,7437537%	0,3718768%	0,1859263%	0,1239536%	0,0929662%
15	12,10	35,6323	0,456	60000	0,7288315%	0,3644157%	0,1821960%	0,1214666%	0,0911010%
16	11,35	43,2751	0,456	60000	0,7247959%	0,3623980%	0,1811872%	0,1207941%	0,0905965%
17	10,68	53,3600	0,456	60000	0,7330915%	0,3665457%	0,1832610%	0,1221766%	0,0916335%

Table 15. SUEZMAX- Percentage of the cost of turning circle manoeuvre on the total cost of voyage at cruise speed of 13 knots.

CONCLUSIONS

— The results for low velocities of approach obtained by interpolation should be considered incorrect and they are shown in this research only for reference purposes.

— The economic speed of the ship for the whole sea passage is close to the velocity of approach to track the more economic manoeuvre of turning 360 deg.

— The optimum speed to perform the manoeuvre of turning 360 deg will depend mainly on the petrol price and hire just as the results shown in table 16.

Table 16.

Hire (USD)	18000			30000			40000			60000		
F.O. price (USD)	0,3	0,5	0,6	0,3	0,5	0,6	0,3	0,5	0,6	0,3	0,5	0,6
SUEZMAX	13	12	10	15	13	11	16	14	12	max.	16	13
AFRAMAX	14	13	11	16	14	12	16	15	13	16	16	14

— The results should not be negligible with regard to the percentage of petrol consumed and costs during the manoeuvre of turn 360 deg out of the whole sea passage. In case of 500 miles sea passages, this percentage would be over one per cent in all cases assumed except one.
— The manoeuvre of turn 360 deg would be reconsidered for the SUEZMAX and AFRAMAX bearing in mind the following reasons:
  – Taking into account the urgency to carry out this manoeuvre by the Officer on watch, it may be unrealistic to reduce the power of main engine to reach the optimum speed of approach.
  – According to the results obtained, the cost of this manoeuvre is high compared to the whole sea passage.
  – Stopping the main engine may be more economic than turning 360 deg however the possibilities of keeping clear the other vessel are not so large. Extending this research to the manoeuvre of stopping the main engine may contribute with further conclusions.
— The research may also be extended to the determination of the costs during the periods of previous deceleration and subsequent acceleration to the turning circle manoeuvre.

REFERENCES

Clark, I.C. (2005). *Ship dynamics for mariners*. London: The Nautical institute.

Crane, C.L.; Eda, H. and Landsburg, A.C. (1989). Controllability. In: Lewis, E.V. ed. *Principles of Naval Architecture Vol. III*. Jersey City, NJ: The Society of naval Architects and marine Engineers, 191-408.

Evans, J.J. and Marlow, P.B. (1990). *Quantitative methods in maritime economics*. London: Fairplay.

Laurence, C.A. (1984). *Vessel operating economies*. London: Fairplay.

Lyster, C.A. and Knights, H.L. (1979). Prediction equations for ship's turning circles. *NECIES transactions*, 23 April.

The Society of Naval Architects and Marine Engineers (1990). *Guide for sea trials*.

Watson, D.G.M. (1998). *Practical ship design*. London: Elsevier.

Journal of Maritime Research, Vol. VII. No. 2, pp. 63-72, 2010

ISSN: 1697-4840

REGIONAL HUBS AND MULTIMODAL LOGISTICS EFFICIENCY IN THE 21ST CENTURY

C. Onyemechi[1]

Received 14 February 2010; in revised form 25 February 2010; accepted 07 July 2010

Abstract

The work assessed the connectivity between hub ports and allied transport networks in the move towards realizing sustainable transport system in the global multi-modal transport supply chain.
The total transport chain connecting the sea, rail and road transport chain or the sea/rail/air chain modifies itself with renewed increasing costs, a good number of which includes additional dredging costs for regional hub ports, infrastructural and super structural costs, for modal and intermodal transfers, dry port construction costs, additional rail infrastructural costs among others.

Keywords: Logistics efficiency, DEA, regional hubs.

New port tariffs have therefore been introduced in such hub ports to absorb the cost effects of introducing hub ports in such regions. The impact of the hub system is not perceived with equal understanding in all water regions of the world. While the south East Asian region, the European water region and the Caribbean region have continued to improve investment in this concept, other water regions are yet to make reasonable investment in this new concept. The hidden issue remains the fact that the rise of hubs, super hubs, and even mega hub ports now constitute a new trend in the multimodal logistics trend of the 21st century. They determine the routes of the multimodal shipping lines in the same way Suez and Panama canal fashion the routes of world shipping trade since the twentieth century.

The technological improvements brought about by improved sea chain transfer demands, efficient intermodal hinterland linkages as well as environmental regulato-

[1] Lecturer, Dept. of Maritime Management Technology, Federal Uniersity of Technology Owerri, conyemechi@yahoo.com, +2348063928094, nil Ihiagwa 01526 Owerri, Nigeria..

ry compliance in the face of a dynamic, fast changing port organizational philosophy. Infrastructural changes, institutional changes and technical advancement are compulsory for both the port complexes; otherwise, the efficiency frontiers will reduce the best industry practices of the organizations to an inefficient level.

This work in realization of the above problem has identified areas in the total transport multimodal logistic chain that require improvement. Furthermore, new methodologies applying data envelopment analysis (DEA) and an ecosystems approach were applied in solving the problems of inefficiency in the total multimodal logistic chain.

INTRODUCTION

The continual growth in containerization in the 21st century has forced shipping lines to evolve new methodologies in the handling of excessive capacity problems associated with such growth. The major innovation brought about as solution to this problem is the emergence of hub ports across the major water regions of the world. Hub ports emanate from the struggle of shipping lines operating in a competitive environment to cut costs through economies of scale. The resulting benefits, when analyzed in terms of cost per TEU, are always smaller for large ships.

One definition of hub port is that which defines it as a container port that provides terminal and marine services that handle and facilitate the transfer or transshipment of containers between feeder and motherships in the shortest possible time. Hub ports or load centers provide for minimum ship calls to few ports within an ocean region. Deposited container freight within these load centers are then feedered down the line across the sub-regional ports, and further down to the hinterlands, via connecting infrastructural facilities and existing corridors.

Campbell (1994) defines hubs as facilities that serve as transshipment or switching points, functioning as connection centers among several origins and destinations. Campell (1994) further exposed five types of discrete problems associated with the location of hub ports, thus:

1. P-hub Median problem (P-HM)
2. Uncapacitated hub location problem (UHLP)
3. Capacitated hub location problem (CHLP)
4. P-hub centre problem (P-HC), and
5. Hub covering problem(HCV) (Aversa *et al*, 2005)

The basic requirements for the location of hub ports have been outlined in Baird (2000). Such a port must have, in addition to a natural deepwater and adequate shelter for motherships, the following features:

a) It must be strategically positioned in a geographically suitable location, sufficiently centrally located to serve a large sub-region with minimum feeding costs.

b) A proximate location to trunk routes where deviation time for ships is kept to a minimum, allowing for minimum short-haul transit time.
c) Lastly, there must be an availability of feeder services to ensure door-to-door movements for various origin/destination cargoes, while remaining cost and time competitive at the same time, with alternative service options.

Transport Networks Adjoining Hub Ports

The search for efficiency across the multimodal transport network requires smooth intermodal interface, efficient transfer of unitized cargoes between the hub port and the feedered port, down through the stacking areas to hinterland dry ports etc. The level of attention given by the government and national port Authorities of nations to the provision of infrastructural facilities, appropriate rail linkages, barge transfer facilities and new freight corridors would go a long way to determining efficient intermodal transfer along the transport & logistics supply chain. Ocean regions with well developed hub and hinterland transfer mechanisms derive cost reduction benefits in the overall logistics transport supply chain. The capital invested in constructing hub ports is a recoverable expense via port dues, though.

Planning an efficient multimodal operation with sustainability is no mean task. Such plan must incorporate environmental issues like the reduction of air and noise pollution from trucks and ships, preservation of the marine ecosystems through ballast water control and efficient garbage, sewage, and oil pollution management, yard management at ports, traffic congestion reduction planning; optimal use of rail & barge services to ensure quick evacuation of several origin/destination containers, the use of dry ports, adoption of logistics theories like the lean port logistics productivity theories, etc.

PROBLEMS DEFINITION

The problem of cost reduction drives logistics organizations towards efficiency. To this end the search for better ways of accomplishing tasks has been a continuous exercise. Rising demands by developing nations and the developed world for international cargo has created new types of problems for the port logistics expert. Such problems are bound to rise infinitely unless adequately checked by new innovations.

These new problems commonly appear along the multimodal linkages across the globes in terms of congested traffic at the port gates, excessive cost of goods in developing African nations brought about by excessive transport costs, blocked stacks at container terminals, delays in cargo delivery time, excessive ship turn round time etc.

The construction of hubs in trade regions across the world's seas will certainly reduce shipping costs as well as produce multiplier effects on cargoes. The logistical benefits of sub-regions adopting the hub concept are also numerous. The chief among them would include the adoption of lean port logistics principles incorporat-

ing the lean port enterprise. The challenges posed for port authorities would then become basically knowledge centered. This would then mean improvements in applied logistics, port environmental policies, and ecosystems management, to mention but a few.

RESEARCH OBJECTIVES

The focus of this work has to do with the assessment of hub infrastructural sufficiency as an element of the total multi-modal transport logistics chain. Special attention will be given to intermodal interface efficiency, optimal distribution of intermodal transport units in a sustainable transport regime, as well as ecosystems preservation under an exclusive economic zone (EEZ) legal regime. An attempt is made to create models that will capture efficient transport requirements in a hub controlled multimodal logistics chain.

JUSTIFICATION

Previous works have focused so far on sectors of the total multimodal supply chain like hub ports, ports logistics, urban transport management etc. Works focusing on the total multimodal logistics chain is rare to find, thus justifying the need for this piece of research. Wherever they appear, however, only limited variables are considered. New legislations affecting the environment of ports thus require the formation of new models of efficiency and cost effectiveness in the world's new multimodal logistic order.

BRIEF LITERATURE REVIEW

The challenge of multimodal logistics efficiency surpasses the application of a single performance measure. For this reason new empirical efficiency measures are being introduced to analyze different efficiency frontiers across the multimodal logistics chain. These measurement devices are not equally effective in measuring efficiency across the multimodal logistics chain (Talley, 1994). A distinction is, thus, often made between technical efficiency, scale efficiency and allocative efficiency in literature. Under technical efficiency, we have output and input oriented technical efficiencies. The producer on the other hand may reduce input (applying improved technology) given the same output. By the term scale efficiency, the divergence between actual and ideal productive size is measured. In contrast to the above two measures, which only address physical quantities, allocative efficiency studies the cost of production given that the information on prices and a behavioral assumption such as cost minimization or profit maximization is properly established (Coelli et al. 1998; Wang & Cullinane 2005).

DATA ENVELOPMENT ANALYSIS APPLIED TO HUB PORTS & THE TRANSPORT SECTOR.

The application of Data Envelopment Analysis (DEA) to efficiency studies in hub and container ports has concentrated mainly on the measurement of technical efficiency (Wang, Song & Cullinane 2005). This is as a result of different currencies being used by different nations, which makes the application of allocative efficiency literally impossible. Frontier models, of which DEA is an example, are said to have been applied to almost all transport modes including the railroad sector (Wang et al 2005, Oum et al. 1999, de Borger et al. 2002).

Many options of DEA models exist. The principal, however, among these options are the DEA – CCR model and the DEA – BCC model. While the first assumes constant return to scale, the later assumes variable return to scale (Fung & Lee, 2007). In analysis with DEA, the best performing ports usually with 100 percent scores occupy the frontier position, thus making themselves the reference ports. The rest of the ports with lower scores are enveloped within the production frontier line.

In most studies hub ports have always occupied frontier positions in productivity and efficiency measurements, making thus them the benchmark ports at the frontier position (Fung & Lee 2007). These authors, in their work with Data Envelopment Analysis computed their inputs based on the following indicators:

1. Berth length and number of quay cranes were used to reflect berth side productivity.
2. Yard side productivity was reflected by container yard area and number of rubber tired gantry cranes and straddle carriers.

In calculating output, they used container throughputs and number of ship calls. The work considered arguments raised by other researchers on the choice of input and output variables before choosing the above variables. Examples include Notteboom et al. (2000), Tongzon (2001), Cullinane and Song (2003) and Wang et al (2005) amongst others.

Multimodal Transport

Der Horst (2008) outlined four main categories of arrangements to improve coordination in hinterland transport chains.

They include:
1. The introduction of incentives
2. The creation of inter-firm alliance
3. Changing the scope of the organization and
4. Collective action

Notteboom (2008) stated that the emergence of global supply chains has placed intense pressures to implement containerization over inland freight distribution sys-

tems. Time, reliability and cost requirements were identified as new problems to which global supply chains must provide an answer.

Among the reasons that necessitated the multimodal transport convention of 1980 includes:

1. The fact that multimodal transport is one means of facilitating orderly expansion of world trade.
2. The need to stimulate the development of smooth, economic and efficient multimodal transport services adequate to the requirements of the trade concerned.
3. The desirability of ensuring the orderly development of international multimodal transport in the interest of all countries and the need to consider the special problems of transit countries, etc UNCTAD (1992).

REPORT OF FINDINGS MODEL FORMULATION

Applied frontier models presently used in determining the efficiency of sea – land intermodal interfaces (ports) ought to be modified to make them suitable for ecosystems efficiency evaluations. Such modification should incorporate at the input side, number of port side environmental processing equipment, MARPOL compliant regulatory enforcement procedures at the port (reflected by port state control agencies), existence of both national and company based port pollution contingency plans and number of existing port security units at the port and within the contiguous zone of the coastal waters.

If we make a distinction between port operational efficiency and port environmental efficiency, then an entirely separate input and output criteria can be applied for environmental efficiency measurement applicable to Data Envelopment Analysis. If we take the variables stated above as the input variables for our DEA environmental efficiency measures, then we are faced with a problem of how to determine the output variables for environmental efficiency.

Unlike the port operational efficiency where cargo throughput is easily available as a measure of output, output variables in environmental efficiency measurements are not easily available. In this paper, we recommend the use of opportunity cost approach. This means that the benefit (output) of port environmental investment is the damage that would have occurred if such investment were not in place. If we choose to limit our measurement at the ecosystems level, we may then represent output as the area of the Exclusive Economic Zone (EEZ) covering the coastal state, along with a value in dollar worth representing the economic richness of the entire zone. This is certainly very reasonable, since the environmental investment is applied as a protective measure to conserve the environment.

Therefore, by applying non parametric frontier measures like the DEA it is now possible to determine operational efficiency and environmental efficiency levels of

sea/land intermodal interfaces (i.e. ports). Hubs ports including superhubs, and megahubs will, thus, qualify for major environmental investments in infrastructures given the multiple hinterlands they serve. Inefficiency at hub ports will certainly affect the global supply chain at the hinterlands served by the hub ports.

Multimodal Effeciency

Efficiency is a desirable property, not only at the hub port but also across the whole multimodal transport chain. Efficiency is required at the regional port, and also at the interface between port-to-rail linkage, inland port infrastructure, as well as the hinterland-to- port road network.

In measuring efficiency, different measures ought to be derived for efficiency assessment of the several sectors of the transport logistics chain. The data envelopment analysis (DEA) offers a means for a quantitative efficiency assessment. A qualitative measure is found in the lean port logistics approach (Paixao & Marlow 2003). The volume of rail activity connecting ports to dry ports should be used as an input factor in measuring port-to-hinterland efficiency using DEA. The other factor should include the level of adoption of short sea shipping in the country's cabotage/coastal transport system. This is because both rail and short sea shipping carry more loads, while they contribute to atmospheric pollution less, provided that they follow an appropriate regulatory regime. They are, thus, a more sustainable means of transport than the road system. They are also more cost effective, and as such more efficient. A DEA measurement obtained using these variables as input factors will thus be a measure of both operational and environmental efficiency in the port-to-hinterland logistics chain.

Hub Ports & Multimodal Logistics Effeciency In World's Ocean Regions

Great developments in world's ocean regions already exist in the South East Asian region, the European and Carribbean water regions. Existing hubs in these regions include: the Port of Singapore, Hong Kong, Shanghai in South East Asia, Rotterdam, Algeciras & Limassol in Europe, and Kingston in the Carribbeans, etc.

However, the search for appropriate location for hub ports in the Indian ocean region, the East Atlantic and the South Atlantic coast of South American water regions have been on the increase. While the public sector alone has been slow in welcoming this innovation, a combination of public-private sector initiatives in the West African sub region has advanced the hub struggle to a point of possible realization in the Lekki region of Lagos (EPZ), Nigeria.

The adoption of hub ports by shipping lines is due to its scale economy advantage, resulting in less cost per ton-mile, as well as cost savings in marine bunkers. The efficiency level will be further increased if coastal shipping and rail connectivity to dry ports is made an issue of national concern in all the port regions of the world.

This will reduce congestion of road vehicles at ports, thus reducing idling of wagons at port gates as well as noise and air pollution at the port gates, a common problem in present day ports, all over the world. The diagram below will illustrate this further.

The Figure may be described as our efficient multimodal logistics model. It proffers a link between hub ports, regional ports, and the port hinterland.

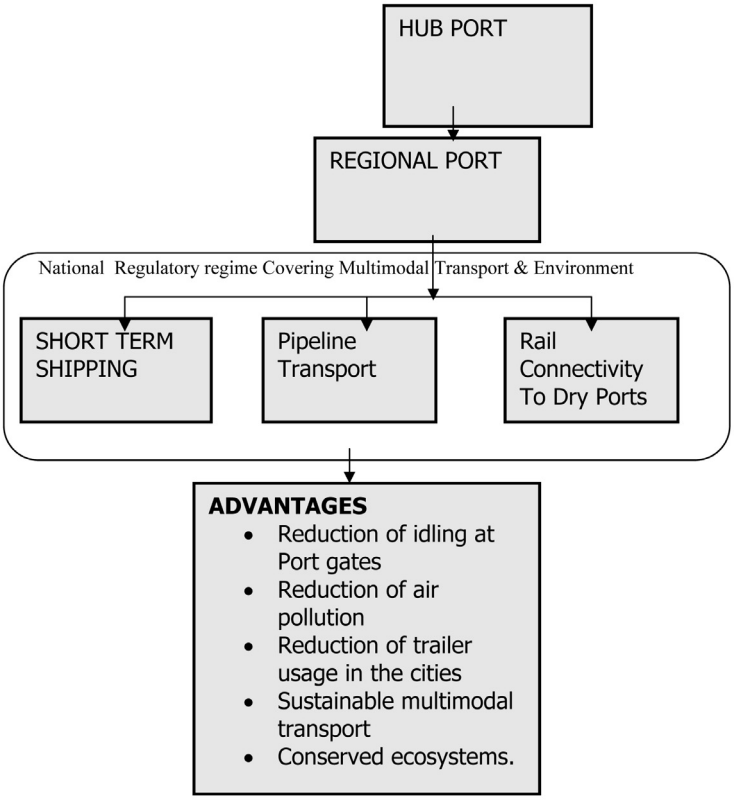

Figure1. Efficient Multimodal Logistics Model.

Further down the line goods are transferred to the hinterland via either the short sea shipping route or the rail lines connected to dry ports. Where this is made a matter of national regulation, the resultant benefits would then include the following:

— reduction of air pollution;
— reduction of idling of trailers at port gates;
— reduction of trailer usage in the cities,
— and overall sustainable multimodal transport and conserved ecosystems.

CONCLUSIONS

The application of frontier efficiency models in evaluating port performance should advance in the direction that will assess environmental efficiency of ports. Thus, variables included in the data envelopment analysis ought to include data that will reflect the number of port side environmental processing equipment.

Furthermore, an efficient multimodal logistics model useful in all the five ocean regions of the world was developed. Reference has been made to its inherent advantages, the most important of which is the development of a sustainable multimodal transport system.

ACKNOWLEDGEMENTS

The Federal University of Technology Owerri is strongly acknowledged for their efforts in ensuring that this work was at least produced.

Further acknowledgements go to the Nigeria Maritime Administration and Safety Agency (NIMASA).

REFERENCES

Aversa R., Botter R.C., Haralambides H.E.and Yoshizaki: HTY (2005): A mixed integer Programming Model on the location of a Hub port in the East Coast of South America

Baird A (2000): Establishment of a container Transshipment Port in Scapa Flow; TRI Marine Transport Research Group/Napier University.

Campbell J.F (1994): Integer programming formulations of discrete hub location problems, European Journal of Operations Research 72.

Coelli et al (1998) An introduction to efficiency and productivity analysis. Kluwer Academic Publishers

Cullinane and Song (2003): A stochastic frontier model of the productive efficiency of Korea container terminals. Applied Economics 35, 251 – 267.

Der Horst M.R.V (2008): Coordination in Hinterland Transport Chains: A Major Challenge for the Seaport Community;

Fung and Lee (2007): Productivity Analysis of container ports in Malaysia: A DEA Approach : Proceedings of the Eastern AsianSociety of Transportation Studies. Vol.6, 2007

Notteboom Theo (2008): Containerization, Box logistics and Global Supply Chains; The Integeration of Ports and Liner Shipping Networks: Maritime Economics and logistics 10, pp. 152-174, palgrave.

Talley (1994): Performance Indicator and Port performance Evaluation Logistics & Transportation Review, 30(4), 339-352

Tongzon (2001): Efficiency measurement of selected Australia and other Intrnational ports using date Envelopment Analysis. Transportation Researcg port A. Policy & practice, 35 (2), 113-128.

Wang, T.F and Cullinane K.P.B (2005): Measuring the Economic Effeciency of Europe's container terminate International Association of maritime Economics, Annual conference, limassol, Cyprus, June 23 - 25

UNCTAD/UNDP (1992): Multimodal Transport Handbook . UNCTAD.

JMR

Journal of Maritime Research, Vol. VII. No. 2, pp. 73-88, 2010

ISSN: 1697-4840

DESIGN ASPECTS AND TWO-DIMENSIONAL CFD SIMULATION OF A MARINE PROPULSOR BASED ON A BIOLOGICALLY-INSPIRED UNDULATING MOVEMENT

M.I. Lamas[1,2], J.D. Rodríguez[1], C. G. Rodríguez[1] and P. B. González[1]

Received 06 May 2010; in revised form 14 May 2010; accepted 30 July 2010

Abstract

Nowadays, it is well known that aquatic animals have higher locomotion performance than man-made marine vehicles. There are a lot of researchers who have built different kinds of machines replicating the movement of animals. The principal problem is that it is very important to fully understand the hydrodynamics of biological swimming to design an optimal mechanism. For this reason, the CFD (Computational Fluid Dynamics) has become a very powerful technique because it solves the governing equations of conservation of mass and momentum so as to obtain the fluid flow characteristics.

This paper presents the development of a marine propulsor based on an undulating fin which emulates fish movement. Furthermore, an extensively CFD investigation of the fluid flow around the propulsor is presented. As experimental tests were performed on a scaled model rather on a real ship, a non dimensional analysis was done. Particularly, the non-dimensional governing groups analyzed were the Reynolds, Froude and Strouhal numbers. The CFD results compared reasonably well with the experimental ones obtained on the lab prototype.

Keywords: CFD, biomimetic, undulating fin, marine propulsion.

INTRODUCTION

Throughout history, the implementation of rotating propulsion mechanisms has been highly used because they are relatively easy to design. On the contrary, undulat-

[1] Escola Universitaria Politécnica, Universidade da Coruña, Avda. 19 de Febrero s/n, 15405, Ferrol, Spain. Tlf.: 981337400. Fax.: 981337416. [2] E-mail: isabellamas@udc.es.

ing mechanisms, which are very common in nature, have been poorly considered. Nowadays, engineering of marine vehicles and machines is changing and new propulsion methods are being studied, specially the biologically-inspired ones.

Biomimetic is an emerging field which employs the principles of living organisms to derive man-made mechanisms which are capable of emulating the efficient movement of animals. Given that most vertebrates are aquatic and have had hundreds of millions of years to adapt to that environment, it is reasonable to suppose that natural selection has optimally developed the kinematics of these animals. For this reason, it is expected that mechanisms which emulates fish movement are more efficient, versatile and maneuverable than classical rotating propellers. In the field of marine propulsion, there are a lot of researchers who applied the biomimetic to make ship propulsors, for example Barret *et al.* (1999) constructed a fish-like mechanism and studied it on a laboratory in order to compare the undulating fish movement with a rigid wall movement. They concluded that the power required to propel an actively swimming fish-like body is significantly smaller than the power needed to tow the body straight and rigid and they obtained drag reductions up to 70% for the undulating fish movement.

Zhang (2007) investigated the bionic neutral network control method for fish-robots.

Young-hua *et al.* (2007) designed an environment-friendly propulsion system mimicking undulating fins and developed a two-dimensional CFD method to study the unsteady flow around the fin. They focused its study on studying the amplitude configuration.

Bozkurtass *et al.* (2008) constructed a propulsor for an autonomous underwater vehicle based on the mechanical design and performance of a sunfish pectoral fin, and developed a three-dimensional numerical model.

Low (2008) constructed an underwater vehicle using a fin-like mechanism based on a series of connecting linkages which produce undulations similar to those produced by the fin rays.

The main problem is that there are many aspects about the undulating propulsion which are not well understood yet. An important technique which helps to answer a lot of decisive questions is the CFD (Computational Fluid Dynamics). The CFD is used to solve the governing equations so as to obtain the hydrodynamics of the fluid flow. In the field of numerical simulation, there are several researchers who applied the CFD to study the laminar and turbulent flow over a sinusoidally shaped solid surface. Bordner (1978) studied the laminar flow over a periodic wavy wall. Markatos (1978) used the k–ε model to study the heat, mass and momentum transfer at a wavy boundary. Caponi *et al.* (1982) developed a two-dimensional, laminar model. McLean (1983) developed a two-dimensional simple algebraic eddy-viscosity model to study the flow for small and larger amplitude waves. Patel *et al.* simulated the laminar (Patel *et al.,* 1991) and turbulent (Patel *et al.,* 1991) flow in a channel with a wavy wall.

This paper presents a design of a marine vehicle mimicking the undulating fin

fish. In addition, a two-dimensional CFD model was developed to analyze the laminar flow over the propulsor. It is organized as follows. Firstly, details of the model and prescribed kinematics are presented. Secondly, the numerical method is briefly described. Thirdly, the hydrodynamic forces and other aspects are discussed and compared with experimental results. Finally, the conclusions of this work and an outline of areas for future research are presented.

NOMENCLATURE

L	[m]	Fin length	*Greek symbols*		
t	[s]	Time	τ	[N/m^2]	Viscous stress tensor
F	[N]	Force	ρ	[kg/m^3]	Density
C	[ ]	Force coefficient	ν	[m^2/s]	Kinematic viscosity
A	[m^2]	Area			
n	[ ]	Unit normal vector	*Subscripts*		
V	[m/s]	Velocity	x		X direction
T	[1/s]	Period	F		Force
f	[Hz]	Frequency of oscillation	p		Pressure
P	[Pa]	Pressure	v		Viscosity
g	[m/s^2]	Gravity	∞		Free stream
Re	[ ]	Reynolds number			
Fr	[ ]	Froude number	*Superscripts*		
St	[ ]	Strouhal number	*		Non-dimensional

PROBLEM DEFINITION

Design and kinematics

"Innovacións Mariñas" Research Group (Coruña University-Spain) built a marine undulating propulsor. The prototype is shown in Fig. 1a and a detail of the undulating fin is shown in Fig. 1b. The fin was 0.52 m length and 0.1 m width.

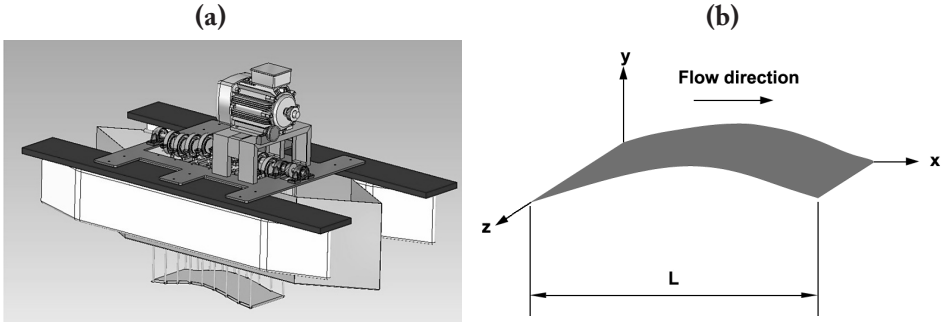

Figure 1. (a) Experimental prototype. (b) Detail of the fin.

The undulating motion is created by means of rods and connecting parts moved by an electric motor. Details of the mechanism were presented elsewhere (Rodríguez *et al.*, 2008).

An important advantage of this system is that it is reversible, *i.e.,* it has the same efficiency either operating forward or backward, which makes it ideal for vehicles that require high maneuverability.

CFD analysis

The flow around a travelling waving wavy wall is quite different from the flow around a rigid wall. As the fluid moves along the surface, the undulations from the anterior to the posterior fin produce thrust. Under the same conditions, a fish consumes much less energy to displace than a rigid body because the motion of the fish reduces turbulence effects. For this reason, the design of the wave is very important, and several CFD studies with different wave configurations were carried out before making the experimental prototype.

Governing equations

The flow motion is governed by the mass conservation equation and the Navier-Stokes equation, which for a laminar, Newtonian and constant properties fluid are given by Eqs. (1) and (2), respectively.

$$\nabla \cdot \vec{V} = 0 \tag{1}$$

$$\frac{\delta \vec{V}}{\delta t} + \nabla \cdot (\vec{V}\,\vec{V}) = -\frac{\nabla p}{\rho} + \nu \nabla^2 \vec{V} + \vec{g} \tag{2}$$

As mentioned above, tests were performed on a scaled model rather on a real ship, so a non-dimensional analysis was carried out. All the variables were converted to dimensionless quantities by introducing the reference parameters given in Table 1. The dimensionless variables, quoted with *, are also shown in this table.

Dimension	Reference parameter	Dimensionless parameter
Length	$L_{ref} = L$	$x^* = x / L_{ref}\ ;\ y^* = y / L_{ref}$
Velocity	$V_{ref} = U_\infty$	$\vec{V}^* = \vec{V} / V_{ref}$
Pressure	$P_{ref} = \rho V_{ref}^2$	$P^* = P / P_{ref}$
Time	$t_{ref} = L_{ref} / V_{ref} = L / U_\infty$	$t^* = t / t_{ref}$
Gravity	$\vec{g}_{ref} = \vec{g}$	$\vec{g}_{ref} = \vec{g} / \vec{g}_{ref}$

Table 1. Reference and dimensionless parameters.

The resulting field equations in dimensionless form are shown as follows:

$$\nabla^* \cdot \vec{V}^* = 0 \tag{3}$$

$$\frac{\delta \vec{V}^*}{\delta t^*} + \nabla^* \cdot (\vec{V}^* \vec{V}^*) = -\nabla p^* + \frac{1}{\mathrm{Re}} \nabla^{*2} \vec{V}^* + \frac{1}{Fr^2} \vec{g}^* \tag{4}$$

where Re is the Reynolds number, defined by Eq. (5). It represents the relation between inertial and viscous effects.

$$\mathrm{Re} = \frac{U_\infty L}{\nu} \tag{5}$$

Fr is the Froude number, defined by Eq. (6). It represents the relation between inertial and gravity effects.

$$Fr = \frac{U_\infty}{\sqrt{Lg}} \tag{6}$$

In the equations above, U_∞ represents the free stream velocity.

NUMERICAL IMPLEMENTATION

Computational mesh

In order to implement the fin movement in the CFD code, it was necessary to use a dynamic mesh. The computational domain, as shown in Fig. 2a, was 3L height and 5L length (L is the fin length), and was discretized with 27000 nodes. The elements were triangular, and the size mesh was refined in the zone near the fin because this is the most critical area in terms of velocity and pressure gradients. A detail of the mesh in the zone closed to the fin is shown in Fig. 2b.

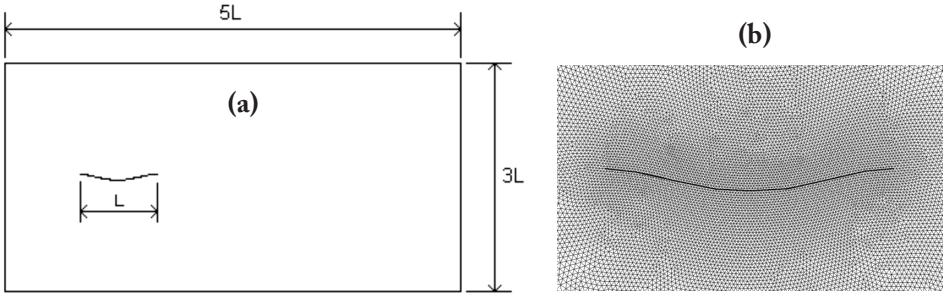

Figure 2. (a) Computational domain. (b) Detail of the grid around the fin.

The fluid flow was simulated using the commercial software Ansys Fluent 6.3. The numerical algorithm implemented in this code automatically updates the mesh after each time step in order to minimize convergence problems if a cell becomes too large, too small or excessively stretched.

Calculation Parameters

A first-order differencing scheme in time and second-order upwind differencing scheme in space was used and an implicit method was employed. Pressure velocity coupling of the continuity equation was achieved using the SIMPLE algorithm.

The period T was divided in 100 parts, *i.e.*, the time step was $\Delta t=T/100$. The grid size and the time step sensibility were studied and it was verified that both of them were adequate to obtain accurate enough results.

Boundary Conditions

Upstream the velocity components were fixed to be uniform, i.e., $u=U_\infty$ and $v=0$, while the gauge pressure was set to zero. Downstream, a zero gradient condition was taken for both velocity and pressure. On the fin surface, the no slip condition was used for the velocity components and finally, on the top and bottom surfaces the slip condition was imposed.

Calculation of the Hydrodynamic Forces

As the fin moves through the water, a force along the x and y directions is produced. The components of the force, F_x and F_y, can be evaluated by integrating the projection of the pressure and the shear stress in the x and y directions respectively. The total thrust component along the x direction was computed by adding the pressure and viscous forces contributions, Eq. (7):

$$F_x = F_{px} + F_{vx} \tag{7}$$

where F_p is the pressure force and F_v is the viscous force.

The pressure force along the x axis is given by:

$$F_{px} = -\int_A p n_x dA \tag{8}$$

where n_x is the x component of the unit normal vector on dA.

The viscous force along the x axis is given by:

$$F_{vx} = \int_A \tau_{xj} n_j dA \tag{9}$$

where τ_{xj} is the viscous stress tensor.

For the present non dimensional analysis, the force coefficients, defined by Eq. (10), were obtained.

$$C_F = \frac{F}{\rho U_\infty^2 L^2} \tag{10}$$

RESULTS AND DISCUSSION

In order to reach the steady state it has been necessary to consider a large time. It was verified that after approximately thirty wave periods the time is large enough to reach the steady state. For this reason, all the results given in the present paper correspond to the 30th period of time.

For almost all results presented in the present paper, the amplitude was taken as 0.02 m, the electrical motor frequency as 10 Hz, the free-stream velocity as 1 m/s and the fluid properties the corresponding ones to water at 25°C. For these conditions the Reynolds number is 52000, the Froude number is 0.44 and the non-dimensional frequency, defined by means of the Strouhal number, Eq. (11), is 1.2.

$$St = \frac{fA}{U_\infty} \tag{11}$$

Velocity field

The non dimensional velocity field for the instant 0.1t/T is shown in Fig. 3.

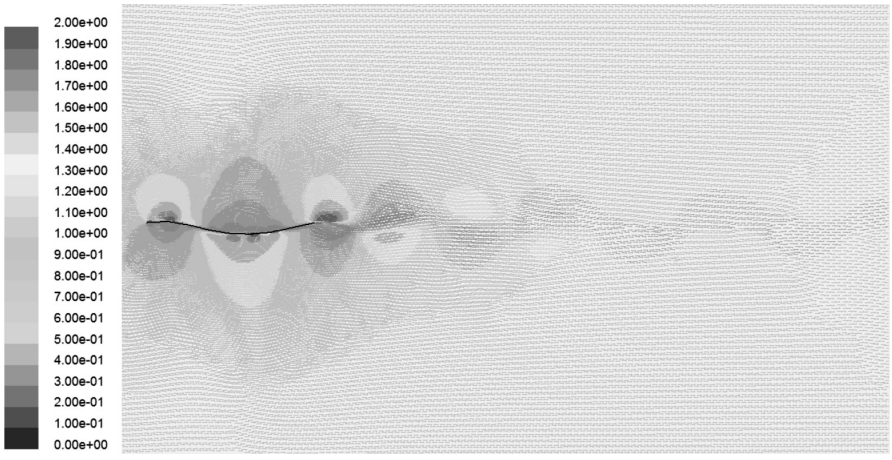

Figure 3. Velocity field for 0.1t/T, St = 1.2, Re = 52000 and Fr = 0.44.

From Fig. 4, it can be seen that a jet is formed at the right side of the fin. This jet is the source of the thrust because it creates a force which tends to move the fin from

the right to the left. As the jet separates from the fin, its intensity decreases due to viscous dissipation.

Pressure field

Fig. 4 shows the non dimensional dynamic pressure field for the instant 0.1t/T, corresponding to Fig. 3. The effect of the undulating movement on the flow field can be clearly seen and confirms the of the velocity field tendency. The high and low pressure regions are greatly developed by the influence of the undulating fin motion and the free stream velocity.

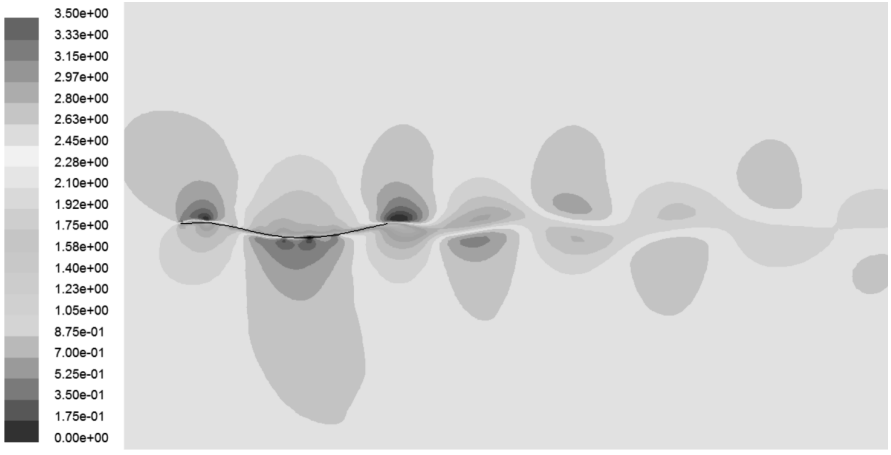

Figure 4. Dynamic pressure field for 0.1t/T, St = 1.2, Re = 52000 and Fr = 0.44.

From Fig. 4, it can be seen that the fin generates two spanwise vortices per oscillation which are arranged into a staggered array resembling a Karman vortex, but with the signs of the vorticity reversed. Some authors refer to this pattern as a reverse Karman vortex street (Triantafillou et al, 1993; Yong-hua Zhan, 2007).

Hydrodynamic forces

In order to systematically quantify the forces, Fig. 5 was created. This figure represents the time history of the instantaneous pressure force coefficient, the viscous force coefficient and the average total force coefficient.

The magnitude of the instantaneous force is dependent on the flapping frequency, flow velocity and amplitude, but in general it reaches its maximum value twice in each cycle because of the symmetrical undulating movement. The pressure force coefficient in Fig. 5 depicts two peaks of acceleration.

From Fig. 5, it can also be observed that the mechanism is accelerating for these conditions because the net thrust force is positive.

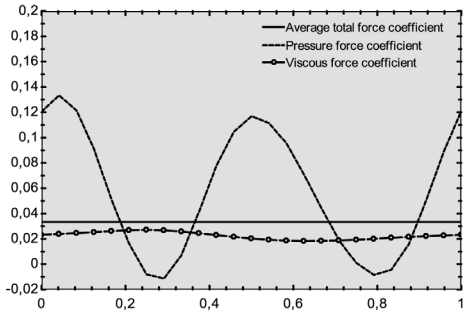

Figure 5. Time history of the pressure force, viscous force and average total force for St = 1.2, Re = 52000 and Fr = 0.44.

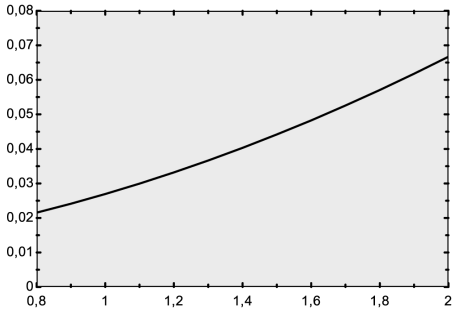

Figure 6. Variation of the total force coefficient with Strouhal number for Re=2000 and Fr=0.44.

The influence of the frequency on the force was studied. As expected, thrust increases when the frequency increases. This phenomenon is shown in Fig.6, which shows the total average force coefficient by means of the St number for values between 0.8 and 2, which corresponds to frequencies of 6.67 and 16.67 Hz respectively.

Experimental results

In order to compare the numerical results with experimental ones, the frequency was incremented from 6 to 15 Hz and numerical and experimental results were compared. Experimental results were based on the "fixed pull point" method, which consists on fixing the prototype to a bollard by means of a rope, Fig. 7, and measuring the force produced.

Numerically, this experiment was simulated imposing a zero free stream velocity. Numerical and experimental results of the average thrust force against the frequency are compared in Fig. 8.

Figure 7. Bollard pull trial under real conditions (fixed pull point).

From Fig. 8, it can be seen that thrust varies with the frequency following an exponential function. Numerical results are higher than experimental ones because first do not consider three-dimensional losses. In the experimental prototype it was observed that, apart from the longitudinal force, a small but not neglecting transversal force is produced. This force was zero for the numerical model because it was two-

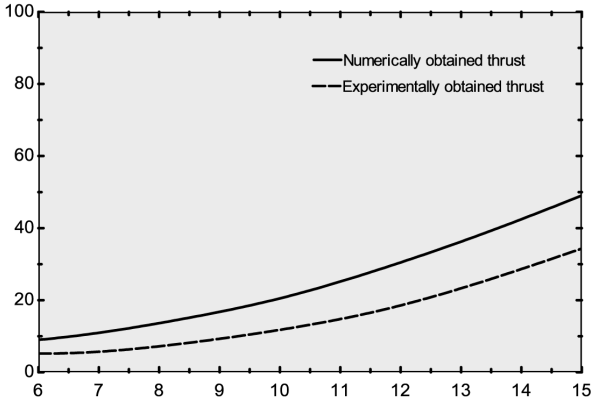

Figure 8. Variation of the average thrust with frequency for numerical and experimental results.

dimensional. Unfortunately, a three-dimensional model is quite computationally consuming and was not carried out in the present work.

CONCLUSIONS

This paper proposes an undulating marine propulsor based on the fin fish movement. The system consists of a flexible fin moved by an electric motor. It was implemented in a small ship built in our lab.

Although fish movement is very efficient because it has the advantage of optimization via natural selection, a CFD model was developed to improve fish movement and optimize the design of the mechanism. CFD was very useful to answer several important questions, for example the influence of the oscillation frequency, amplitude, wave length and other design parameters. For this reason, the propulsor is very efficient and maneuverable. Details of the velocity and pressure field provided by the CFD model were presented in the present paper. Pressure, viscous and total forces were presented too. Numerical results agreed well with experimentally obtained ones.

It was found that a more thorough study should be done in order to investigate tri-dimensional effects. Future works including turbulence modeling shall also be needed because it was found that the flow becomes turbulent for higher frequencies than the ones studied in the present paper. Adding turbulence and creating a three-dimensional simulation would provide a more accurate and realiscit numerical simulation. Nevertheless, the present work is an important step to study and design biologically-inspired mechanisms.

REFERENCES

Barret, D.S.; Triantafyllou, M.S.; Yue, D.K.P.; Grosenbaugh, M.A. and Wolfgang, M.J. (1999). Drag reduction in fish-like locomotion. *Journal of Fluid Mechanics* 392, 183-212.

Bordner, G.L. (1978). Non linear analysis of laminar boundary layer flow over a periodic wavy wall, *Physics of Fluids* 21, 1471.

Bozkurttas, M.; Tangorra, J.; Lauder, G. and Mittal, R. (2008). Understanding the hydrodynamics of swimming: from fish fins to flexible propulsors for autonomous underwater vehicles. *Advances in Science and Technology* 58, 193-202.

Caponi, E.A.; Fornberg, B.; Knight, D.D.; McLean, J.W.; Saffman, P.G. and Yuen, H.C. (1982). Calculations of laminar viscous flow over a moving wavy surface. *Journal of Fluid Mechanics* 124, 347-362.

Low, K.H. (2008). Locomotion simulation and system integration of robotic fish with modular undulating fin. *International Journal of Simulation* 7 (8), 64-77.

Markatos, N.C.G. (1978). Heat mass and momentum transfer across a wavy boundary. *Computer Methods in Applied Mechanics and Engineering* 14, 323-376.

McLean, J.W. (1983). Computations of turbulent flow over a moving wavy boundary. *Physics of Fluids* 26, 2065-2073.

Patel, V.C.; Chon, J.T. and Yoon, J.Y. (1991). Laminar flow over wavy walls. *Journal of Fluids Engineering* 113, 574.

Patel, V.C.; Chon, J.T. and Yoon, J.Y. (1991). Turbulent flow in a channel with a wavy wall. *Journal of Fluids Engineering* 113, 579.

Rodríguez, J.; González, P.; Couce, A.; González, G. (2009). Diseño de sistema de propulsión ondulante. *Proceedings of XIII International Congress on Project Engineering, June, Badajoz, Spain, pp. 1961-1972.*

Triantafyllou, M.; Triantafyllou, M.S.; Grosenbaugh, M.A. (1993). Optimal thrust development in oscillating foils with appliction to fish propulsion. *Journal of Fluid Struct.* 7, 205-224.

Yong-hua Zhang, Lai-bing Jia, Shi-wu Zhang, Jie Yang and Low, K.H. (2007). Computational research on modular undulating fin for biorobotic underwater propulsor. *Journal of Bionic Engineering* 4, 25-32.

Zhang, D.; Hu, D.; Shen, L.; Xie, H. (2007). Design of an artificial bionic neural network to control fish-robot's locomotion. *Neurocomputing,* 71, 648-654.

ASPECTOS DE DISEÑO Y SIMULACIÓN CFD BIDIMENSIONAL DE UN PROPULSOR MARINO BASADO EN UN MOVIMIENTO ONDULATORIO DE INSPIRACIÓN BIOLÓGICA

Resumen

Actualmente, es bien sabido que los animales acuáticos son más eficaces que los vehículos marinos. Existen un gran número de investigadores que han construido diferentes tipos de maquinas replicando el movimiento de los animales. El principal problema es que es muy importante entender completamente la hidrodinámica del movimiento si se quiere diseñar un mecanismo de manera óptima. Por este motivo, la dinámica de fluidos computacional (CFD) se ha convertido en una herramienta muy poderosa porque resuelve las ecuaciones gobernantes de conservación de la masa y cantidad de movimiento para obtener las características del flujo de fluido.

Este artículo presenta las características de un propulsor marino basado en una aleta ondulante que imita el movimiento de los peces. Además, se presenta una extensa investigación CFD del flujo de fluido alrededor del propulsor. Como las pruebas experimentales fueron hechas en un modelo a escala en lugar de un barco real, se hizo un análisis adimensional. Particularmente, los grupos adimensionales analizados fueron el número de Reynolds, el de Froude y el de Strouhal.

DEFINICIÓN DEL PROBLEMA

Diseño y cinemática

El grupo de investigación "Innovaciones Marinas" (Universidad de la Coruña – España) desarrolló un propulsor ondulante marino. Los aspectos fundamentales se muestran en la Fig. 1a, en la que aparece el prototipo, y la figura 1b, que muestra un detalle de la aleta ondulante de 0,52 m de longitud.

El movimiento ondulante es creado por medio de un sistema de bielas y cigüeñales que producen una forma de onda. Los detalles fueron presentados previamente (Rodríguez *et al.*, 2009). El movimiento es producido por un motor eléctrico y la frecuencia de oscilación es regulada por un controlador de frecuencia.

Una ventaja muy importante de este sistema es que es reversible, es decir, tiene la misma eficiencia operando marcha adelante o atrás. Esto lo hace ideal para vehículos que requieren alta maniobrabilidad.

Análisis CFD

El flujo alrededor de una pared ondulante es distinto al del flujo alrededor de una pared rígida. A medida que el fluido se mueve a lo largo de la superficie, se produce

empuje debido a las ondulaciones desde la parte anterior a la parte posterior de la aleta. Para las mismas condiciones, un pez consume mucha menos energía para desplazarse que un cuerpo rígido debido a que el movimiento del pez reduce los efectos de turbulencia. Por este motivo, el diseño de la forma de la onda es muy importante. Se han realizado varios estudios CFD para varias configuraciones de onda antes de construir el prototipo experimental.

Ecuaciones gobernantes

El movimiento de flujo es gobernado por las ecuaciones de conservación de la masa y de Navier-Stokes, que para un fluido incomprensible, newtoniano y de propiedades constantes vienen dadas por las Ecs. (1) y (2) respectivamente.

$$\nabla \cdot \vec{V} = 0 \tag{1}$$

$$\frac{\delta \vec{V}}{\delta t} + \nabla \cdot (\vec{V}\vec{V}) = -\frac{\nabla p}{\rho} + \nu \nabla^2 \vec{V} + \vec{g} \tag{2}$$

Todas las variables fueron convertidas en adimensionales introduciendo los parámetros de referencia dados en la Tabla 1. Las variables adimensionales, denotadas con *, también se muestran en esta tabla.

Las ecuaciones gobernantes en forma adimensional resultan como sigue:

$$\nabla^* \cdot \vec{V}^* = 0 \tag{3}$$

$$\frac{\delta \vec{V}^*}{\delta t^*} + \nabla^* \cdot (\vec{V}^* \vec{V}^*) = -\nabla p^* + \frac{1}{\mathrm{Re}} \nabla^{*2} \vec{V}^* + \frac{1}{Fr^2} \vec{g}^* \tag{4}$$

donde Re es el número de Reynolds, definido por la Ec. (5). Representa la relación entre los efectos de inercia y los viscosos.

$$\mathrm{Re} = \frac{U_\infty L}{\nu} \tag{5}$$

Fr es el número de Froude, definido por la Ec. (6). Representa la relación entre efectos de inercia y de gravitatorios.

$$Fr = \frac{U_\infty}{\sqrt{Lg}} \tag{6}$$

IMPLEMENTACIÓN NUMÉRICA

Malla computacional

Para simular el movimiento de la aleta, fue necesario emplear una malla dinámica. El dominio computacional, que se muestra en la Fig. 2a, fue de 3L por 5L (siendo L la longitud de la aleta), y fue discretizado en 27000 nodos. Los elementos fueron triangulares y el tamaño de malla fue refinado en la zona cercana a la aleta. Un detalle de la malla en la zona cercana a la aleta se muestra en la Fig. 2b.

El software utilizado ha sido Ansys Fluent 6.3. El algoritmo numérico implementado en este software actualiza automáticamente la malla tras cada paso de tiempo con el fin de minimizar problemas de convergencia si una celda resulta demasiado grande, pequeña o deformada.

Parámetros de cálculo

Se ha utilizado un esquema de discretización de primer orden en tiempo y segundo reden en espacio, y se ha acudido a un método implícito. El acoplamiento entre presión y velocidad se ha tratado mediante el algoritmo SIMPLE.

El periodo T fue dividido en 100 partes, es decir, el paso de tiempo fue $\Delta t=T/100$. Tanto el tamaño de malla como el paso de tiempo fueron estudiados y se verificó que el tamaño de malla y de paso de tiempo empleados son insensibles ante refinamiento de los parámetros

Condiciones de contorno

Aguas arriba, las componentes de velocidad fueron fijadas como uniformes, es decir, $u=U_\infty$ and $v=0$, mientras que la presión manométrica se fijó como cero. Aguas abajo, se impuso una condición de gradiente nulo tanto para la presión como para la velocidad. En la superficie de la aleta, se impuso una condición de no deslizamiento y finalmente, en las superficies superior e inferior del dominio, se impuso la condición de deslizamiento libre.

Cálculo de las fuerzas hidrodinámicas

A medida que la aleta se mueve en el agua, se produce una fuerza en las direcciones x e y. Las componentes de la fuerza, F_x y F_y, fueron evaluadas integrando la proyección de la presión y de la tensión cortante en las direcciones x e y respectivamente. La componente de empuje a lo largo del eje x fue calculada sumando la contribución de la presión y de la viscosidad, Ec. (7):

$$F_x = F_{px} + F_{vx} \tag{7}$$

donde F_p es la fuerza de presión y F_v es la fuerza de viscosidad.

A su vez, la fuerza de presión a lo largo del eje x está dada por:

$$F_{px} = -\int_A p n_x dA \tag{8}$$

donde n_x es la componente x del vector unitario normal en dA.

La fuerza viscosa a lo largo del eje x viene dada por:

$$F_{vx} = \int_A \tau_{xj} n_j dA \tag{9}$$

donde τ_{xj} es el tensor de tensiones viscosas.

Para el presente análisis adimensional, se calcularon los coeficientes de fuerza, definidos por la Ec. (10).

$$C_F = \frac{F}{\rho U_\infty^2 L^2} \tag{10}$$

CONCLUSIONES

Este artículo propone un propulsor marino basado en el movimiento de las aletas de los peces. El sistema cosiste en una membrana flexible movida por un motor eléctrico. Fue implementada en un pequeño barco construido en un laboratorio.

A pesar de que el movimiento de los peces es muy eficaz porque es el resultado de la optimización de la selección natural, se ha desarrollado un modelo de CFD para mejorar el movimiento de los peces y así optimizar el diseño del mecanismo. El CFD ha sido de utilidad para contestar algunas preguntas importantes, como la influencia de la frecuencia de oscilación, amplitud, longitud de onda y otros parámetros de diseño. Por este motivo, el propulsor diseñado es muy eficiente. Los detalles del campo de presiones y de velocidades proporcionados por el modelo CFD se han mostrado en este artículo. Las fuerzas resultantes de presión, viscosidad también han sido presentadas. Los resultados obtenidos numéricamente mostraron buena concordancia con los obtenidos experimentalmente en el prototipo.

Se encontró que es necesario un estudio de la influencia de los efectos tri-dimensionales. Trabajos futuros incluyendo modelos de turbulencia también se ha visto que son necesarios porque para frecuencias mayores que las estudiadas el flujo se vuelve turbulento. Sin embargo, el presente trabajo es un importante paso para entender y diseñar mecanismos de inspiración biológica.

INSTRUCTIONS FOR AUTHORS

http://www.jmr.unican.es

Description

Journal of Maritime Research (JMR) publishes original research papers in English analysing the maritime sector international, national, regional or local. JMR is published quarterly and the issues—whether ordinary or monographic—include both theoretical and empirical approaches to topics of current interest in line with the editorial aims and scope of the journal.

The objective of JMR is to contribute to the progress, development and diffusion of research on the maritime sector. The aim is to provide a multidisciplinary forum for studies of the sector from the perspective of all four of the following broad areas of scientific knowledge: experimental sciences, nautical sciences, engineering and social sciences.

The manuscripts presented must be unpublished works which have not been approved for publication in other journals. They must also fulfil all the requirements indicated in the 'Technical specifications' section. The quality of the papers is guaranteed by means of a process of blind review by two scientific referees and one linguistic reviewer. Although the journal is published in print format, the processes of submission and reception of manuscripts, as well as revision and correction of proofs are all done electronically.

The publication process

Submission and acceptance of manuscripts

Papers should be sent via the journal's web site at http://www.jmr.unican.es, following the guidelines indicated for the submission of manuscripts by authors. Submitting the manuscript involves sending electronically via the web site three different types of information: general information about the article and the authors, an abstract and the complete paper.

The general information about the article and the authors, as well as the acknowledgements, is to be introduced by means of an electronic form, in which the following data are requested:

- Title of the paper. Subtitle.
- Field of the manuscript presented (Experimental Sciences, Engineering, Nautical Sciences or Social Sciences) and sub-field.
- E-mail of the author to whom correspondence should be addressed.
- Personal data of each author including name, professional category or position, institution or organisation, postal address and e-mail.
- Acknowledgements, if included, should be no longer than 150 words without spaces between paragraphs.

The manuscripts submitted which are in line with the aims and scope of JMR will be submitted to a blind review process. The objective is to assess the scientific quality (two referees) and ensure that the text is linguistically acceptable (one reviewer). Only those works which are considered adequate from a scientific point of view will be reviewed linguistically. Manuscripts which do not pass the linguistic filter will be admitted with the condition that the author make linguistic and stylistic modifications as indicated.

Authors will be informed of the acceptance, rejection and/or modifications required no later than four months after the receipt of the manuscript. Once the paper has been accepted, authors can check on the status of their article via the web site. Any doubts or questions should be addressed to the Editor at jmr@unican.es

Copyright

After manuscripts have been definitively accepted, the authors must complete the copyright agreement assigning the copyright to JMR so that it can be published.

Proofs

Once the copyright transfer agreement has been completed, the Editors will assign the paper to an upcoming issue of JMR and proofs will be sent as a PDF file to the author who has corresponded with JMR throughout the reviewing process. The corrected proofs must be returned by e-mail to the Editor of JMR within 96 hours of receipt.

Reprints

Once the paper has been published, the authors will be sent a total of 12 free reprints, which will be sent the postal address of the corresponding author. Authors may also request, via the JMR web site http://www.jmr.unican.es, a maximum of 10 complete journals at 50% of the cover price.

Style and technical specifications

Manuscripts should be sent to JMR's web site in a format that is recognisable to Microsoft Word (.doc) in any of its versions for Windows. The maximum length of manuscripts is 23 double-spaced pages (approximately 7000 words) including the abstract, references and appendices. Manuscripts will be submitted using a specific application of the electronic form used to send personal data. The page layout should follow these guidelines:

- Size: DIN A4 (29 cm by 21 cm)
- Margins, 3 cm: top, bottom, left, and right.
- Font: Times New Roman, normal style, 12-point type.
- Double spacing should be used for all the paper except for the references which are to be single-spaced.
- Notes, when necessary, are to be placed at the end of the paper and numbered in their order of appearance in the text. Mathematical derivations should not be included in these endnotes.

The abstract is to be presented on one page and should include the following information:

- Title and subtitle of the paper
- Field and sub-field of the work presented.
- Abstract, which is to be no longer than 200 words, and should have no spaces between paragraphs.